SNOW COMPACTION AS A MITIGATION TECHNIQUE TO REDUCE PERMAFROST THAW ALONG HIGHWAYS IN THE CANADIAN ARCTIC

LE COMPACTAGE DE LA NEIGE COMME TECHNIQUE D'ATTÉNUATION POUR RÉDUIRE LE DÉGEL DU PERGÉLISOL LE LONG DES ROUTES DANS L'ARCTIQUE CANADIEN

A Thesis Submitted to the Division of Graduate Studies
of the Royal Military College of Canada
by

Jay Cumming

In Partial Fulfillment of the Requirements for the Degree of
Master of Applied Science

January, 2023

Dedication

For my friends, and my family

Acknowledgements

I would like to thank my wonderful thesis supervisors Dr. Greg Siemens and Dr. Ryley Beddoe for their mentorship, encouragement, and expertise in helping me to complete this research. Their willingness to allow me to relocate home was invaluable to me for maintaining my motivation and sanity after frequent lockdowns. I am incredibly grateful for everything I have learnt from them and look forward to our future encounters.

This research would not have been possible without Alice Wilson at the Government of the Northwest Territories. I am deeply grateful for her willingness to collaborate and share data from her research sites along the Inuvik-Tuktoyaktuk Highway.

Finally, I would like to thank my friends and family for their support and encouragement of which was invaluable to me during these past few years of my life.

Abstract

The serviceability of Highways in northern climates is best maintained when permafrost thaw under the road structure is kept at a minimum. In current practice, roads are designed to keep the original ground surface under the road frozen year-round. However, in reality this is a highly complex problem with significant challenges including (but not limited to) poor drainage and ponding water, warming air temperatures increasing thaw, and the impact of snow depth accumulating on the embankment. The impacts of these challenges on a road include lateral spreading of the embankment, differential and irrecoverable settlement and thaw. One mitigation technique being investigated to prevent the excessive thaw of permafrost under road embankments is snow compaction. Snow acts as a thermal insulator which leads to a reduced cooling of the ground during the winter months. Through snow compaction, the thermal insulation is reduced facilitating a greater flow of heat from the ground to the air during the winter months. Field studies currently investigating snow compaction are developing databases of ground temperatures under different snow conditions, however they are limited by the snow conditions that actually occur each year and by the time required to study long-term effects. Currently, a field study is being conducted along the Inuvik-Tuktoyaktuk Highway in the Northwest Territories measuring the effects of snow compaction on ground temperature. The objective of this thesis is to study the influence of snow compaction as a mitigation technique for the maintenance of the Inuvik-Tuktoyaktuk Highway through numerical ground temperature modelling. Using numerical models calibrated to the field site thermal data records allows for a rapid assessment of this permafrost technique under a wide range of snow conditions.

This research first focuses on the calibration of a numerical model for the Inuvik-Tuktoyaktuk Highway site and discusses model development with limited measured soil properties. Using climate, snow depth and density measurements from two sites, one undisturbed and one compacted, the numerical model was developed through an iterative approach. The model was developed by iterating soil properties until model temperature outputs matched the recorded temperatures recorded at the two sites. With the exception of one model output, the model temperature outputs after the final iteration for the minimum, maximum, and average annual ground temperatures were within 1 °C of the thermistor recordings.

Furthermore, this research presents a parametric study, exploring what most influences the thermal regime of the sites. This included evaluating the impact of snow depth, snow compaction cycles (both annually and monthly), lateral heat flow under different compactions, and the effect of an embankment snow accumulation. The snow scenarios included snow compaction applied to historically low, high, and average snow depth and an investigation into the efficacy of the time and frequency of when snow compaction occurs using 18 years of snow depth data (2003-21) from Inuvik. In the 1D model and 2D model with embankment it was found that snow compaction works best with a historically average snow depth and had little effect on when applied to high or low snow depths. It was also found that snow compaction works best when applied multiple years in a row, as changes in ground temperature will eventually revert to non-compacted conditions when snow is left undisturbed. Investigations into the time during which snow compaction is applied in a winter revealed that it is most effective to apply snow compaction early during the winter in December. Using the 2D model to investigate lateral heat flow changes in thaw depths are seen up to 2 m into an area of uncompacted snow area with that has undergone snow compaction. The 2D model also revealed that long term snow compaction can greatly reduce the time the active layer is present, with a 37-to-45-day reduction after 10 years of snow compaction.

The final section of the thesis summarizes the findings obtained from the numerical models, limitations in the research, and presents further areas for future research. Potential areas of future research include developing models for different sites with different ground conditions along the Inuvik-Tuktoyaktuk Highway, using greenhouse gas emission scenarios to test the viability of snow compaction with rising temperatures, and to incorporate a geothermal flux function into the model.

Resume

Les infrastructures linéaires dans les climats nordiques ont le défi unique de maintenir leur état de fonctionnement tout en étant construites sur le pergélisol. Dans la pratique actuelle, les routes sont conçues pour maintenir la surface du sol d'origine sous la route pour qu'elle soit gelée toute l'année. Cependant, en réalité, il s'agit d'un problème très complexe avec des défis importants, notamment (mais sans s'y limiter) un mauvais drainage et des flaques d'eau, le réchauffement des températures de l'air augmentant le dégel et l'impact de l'épaisseur de la neige qui s'accumule sur le remblai. Les impacts de ces défis sur une route comprennent l'étalement latéral du remblai, le tassement différentiel et irrécupérable et le dégel. Une technique d'atténuation à l'étude pour empêcher le dégel excessif du pergélisol sous les remblais routiers est le compactage de la neige. La neige agit comme un isolant thermique, ce qui réduit le refroidissement du sol pendant les mois d'hiver. Grâce au compactage de la neige, l'isolation thermique est réduite facilitant un plus grand flux de chaleur du sol vers l'air pendant les mois d'hiver. Les études sur le terrain portant actuellement sur le compactage de la neige développent des bases de données sur les températures du sol dans différentes conditions de neige, mais elles sont limitées à la fois par le temps et les conditions de neige se produisent réellement chaque année et par le temps nécessaire pour étudier les effets à long terme. Actuellement, une étude sur le terrain est menée le long de la route Inuvik-Tuktoyaktuk dans les Territoires du Nord-Ouest pour mesurer les effets du compactage de la neige sur la température du sol. L'objectif de cette thèse est d'étudier l'influence du compactage de la neige comme technique d'atténuation pour l'entretien de l'autoroute Inuvik-Tuktoyaktuk grâce à la modélisation numérique de la température du sol. L'utilisation de modèles numériques calibrés sur les enregistrements de données thermiques du site sur le terrain permet une évaluation rapide de cette technique de pergélisol dans une large gamme de conditions de neige.

Cette recherche se concentre d'abord sur l'étalonnage d'un modèle numérique pour le site de l'autoroute Inuvik-Tuktoyaktuk et discute du développement d'un modèle avec des propriétés de sol mesurées limitées. À l'aide de mesures du climat, de l'épaisseur et de la densité de la neige sur deux sites, l'un non perturbé et l'autre compacté, le modèle numérique a été développé selon une approche itérative. Le modèle a été développé en itérant les propriétés du sol jusqu'à ce que les sorties de température du modèle correspondent aux températures enregistrées sur les deux sites. À l'exception d'une sortie de modèle, les sorties de température du modèle après l'itération finale pour les températures annuelles minimales, maximales et moyennes du sol se situaient à moins de 1 °C des enregistrements de la thermistance.

Le chapitre 3 est une étude paramétrique, explorant ce qui influence le plus le régime thermique des sites. Cela comprenait l'évaluation de l'impact de l'épaisseur de la neige, des cycles de compactage de la neige (annuels et mensuels), du flux de chaleur latéral sous différents compactages et de l'effet d'une accumulation de neige sur un remblai. Les scénarios de neige comprenaient le compactage de la neige appliqué à une épaisseur de neige historiquement faible,

élevée et moyenne et une enquête sur l'efficacité du moment et de la fréquence du compactage de la neige à l'aide de 18 années de données sur l'épaisseur de la neige (2003-21) d'Inuvik. Dans le modèle 1D et le modèle 2D avec remblai, il a été constaté que le compactage de la neige fonctionne mieux avec une épaisseur de neige historiquement moyenne et a peu d'effet lorsqu'il est appliqué à des épaisseurs de neige élevées ou faibles. Il a également été constaté que le compactage de la neige fonctionne mieux lorsqu'il est appliqué plusieurs années de suite, car les changements de température du sol reviendront éventuellement à des conditions non manipulées lorsque la neige n'est pas perturbée. Des enquêtes sur le moment auquel le compactage de la neige est appliqué en hiver ont révélé qu'il est plus efficace d'appliquer le compactage de la neige au début de l'hiver en décembre. En utilisant le modèle 2D pour étudier les changements de flux de chaleur latéraux dans les profondeurs de dégel, on peut voir jusqu'à 2 m dans une zone de neige non compactée et une zone avec qui a subi un compactage de la neige. Le modèle 2D a également révélé que le compactage de la neige à long terme peut réduire considérablement la durée de présence de la couche active, avec une réduction de 37 à 45 jours après 10 ans de compactage de la neige.

Le chapitre 4 résume les résultats obtenus à partir des modèles numériques, les limites de la recherche et présente d'autres domaines de recherche future. Les domaines potentiels de recherche future comprennent le développement de modèles pour différents sites avec différentes conditions de sol le long de l'autoroute Inuvik-Tuktoyaktuk, l'utilisation de scénarios d'émissions de gaz à effet de serre pour tester la viabilité du compactage de la neige avec la hausse des températures et l'intégration d'une fonction de flux géothermique dans le modèle.

Co-Authorship Statement

This thesis document is written in the manuscript-based format as laid out in the Royal Military College of Canada Thesis Preparation Guidelines, dated May 2015. The author of this thesis document, Jay Cumming, was the main author for both articles contained within this document; the listed co-authors R. Beddoe, G.A Siemens provided guidance, advice, and feedback throughout all steps of article writing. As the author plans to submit both articles contained in this document for publication in peer-reviewed journals, each individual article will have both supervisors noted as co-authors.

Table of Contents

List of Figures

List of Tables

List of Symbols and abbreviations

Abbreviations	Definition
c	Volumetric Heat Capacity
cm	Centimeters
d	Day
g/cm^3	Bulk Density
k	Thermal Conductivity
km	Kilometers
m	Meters
t	Time
w	Volumetric Water Content
w_u	Unfrozen Volumetric Water Content
1D	1-Dimensional
2D	2-Dimensional
ECC	Environment and Climate Change Canada
HBR	Hudson Bay Rail
ITH	Inuvik to Tuktoyaktuk Highway
K	Kelvin
KJ	Kilojoules
L	Latent Heat of Water
MAGT	Mean Annual Ground Temperature
NWT	Northwest Territories
Q	Applied Boundary Flux
R	Resistivity

RMC	Royal Military College
T	Temperature
W_u	Unfrozen Water Content
λ	Heat Storage Capacity
δ	Thermal Conductivity at a Given Time
ΔH	Snow Depth
'	Minutes
"	Seconds
°C	Degrees Celsius

Chapter 1
Introduction

1.1 Introduction

1.1.1 Background

Permafrost is ground that has existed at sub-zero temperatures for a minimum of two consecutive years (Brown, 1973). In Canada, it is estimated that 50% of the landmass is comprised of permafrost, mostly located in the northern part of the country (Figure 1). In an engineering context, the stability of infrastructure depends on the stability of the permafrost. Due to this, maintaining the integrity of permafrost that supports infrastructure is an important factor in ensuring the continued serviceability of structures such as building foundation, railways, and roads. With rising global temperatures because of climate change, permafrost is at risk of experiencing significant degradation in the coming century. Thawing permafrost leads to ground instability, which in turn can impact foundations. For shallow foundations this is often seen as differential settlement, resulting in cracking and leaning infrastructure. For pile foundations, thawing permafrost will increase the depth of thaw in the ground, which can have negative impacts on structure stability as it exceeds the pile design thaw depth. In the case of roads and railways, thawing permafrost quickly causes embankment instability and differential settlement (e.g., ITH closing in the day at the start, Hudson's Bay Railway being shut for a few years). These in turn impact the communities they serve, to the extreme of isolating communities and cutting off their only available ground transportation.

A typical thermal profile of permafrost, also known as a trumpet curve, plots temperature vs depth. An example of a trumpet curve is shown in Figure 2, which includes the minimum, average, and maximum ground temperatures (for a set period of time) plotted versus depth. An upper layer that freezes and thaws annually (i.e., maximum annual temperature rises above 0 °C) is called the active layer. Below the active layer is the permafrost layer where the maximum annual temperature does not go above 0 °C. At a certain depth, the minimum and maximum temperatures will meet at what is called the zero annual amplitude where there is no variation in temperature over the year at those depths. Below the zero annual amplitude, the temperature will increase with depth from heat from the Earth's core and will at some point rise above 0 °C, signifying the lower boundary of the permafrost. Permafrost layers can exist from a few meters to hundreds of meters in depth (Andersland & Ladanyi, 2004).

Currently, general practice when constructing linear infrastructure on permafrost is to maintain the underlying permafrost with minimal disturbance. This means that roads are constructed using a fill technique using an intermediary geotextile layer between the fill and ground as opposed to the traditional cut and fill technique (Government of the NWT, 2017). The height of the embankment is designed such that the ground below the road is maintained as permafrost with the active layer remaining within the fill. While these construction techniques exist to ensure continued serviceability of linear infrastructure, evidence of serviceability issues due to thawing permafrost have occurred. For example, observations have been made on the access road to the Umiujaq Airport in Nunavik where differential subsidence is occurring as high as 0.85 m (Fortier, et al.,

2011). If any degradation occurs under embankments, lateral spreading of the fill material can occur. In the Northwest Territories, the department of infrastructure expects that spring closures are to be a regular occurrence due to the difficulty in maintaining the roads structural integrity in such an extreme environment. Following road closure, repairs are conducted to the damaged areas, which involve reforming the embankments with more fill material. Road closures have been known to occur with little notice, so a road can be open during the morning and closed during the afternoon, stranding any travellers who required the road to be open for travel (Bowling, 2020).

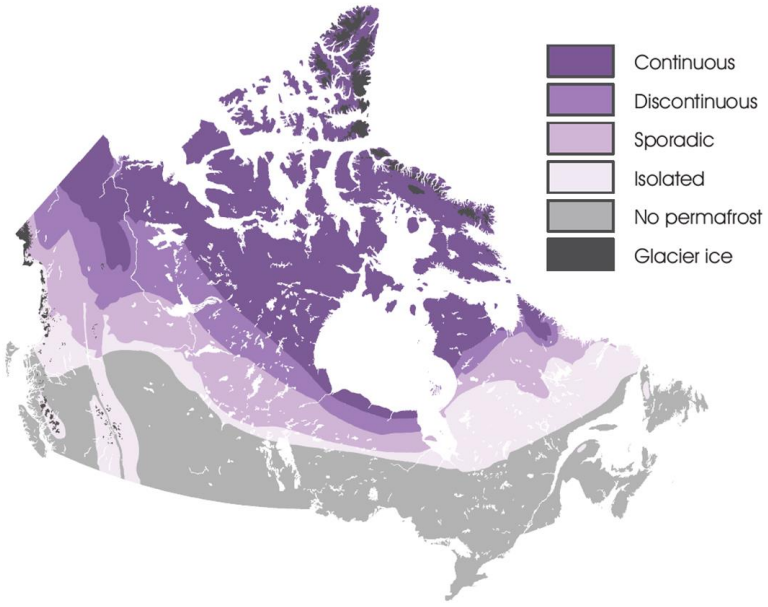

Figure 1: Permafrost map of Canada (O'Neill, et al., 2022).

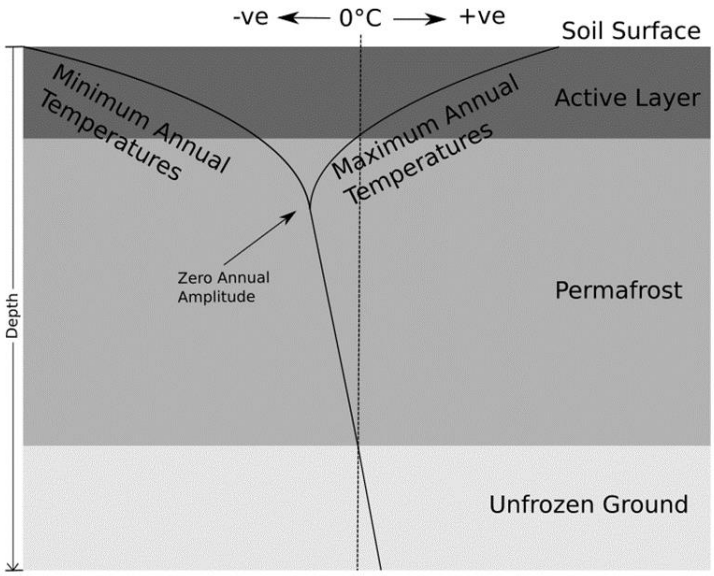

Figure 2: Typical ground temperature profile of permafrost.

Furthermore, the mechanical properties of permafrost change significantly with rising temperatures. An increase of temperature in permafrost from -4 °C to -1 °C, leads to a decrease in bearing capacity by 30 %. With occurrences of engineering failure on linear infrastructure, maintenance cost is estimated to increase. In the Yukon, Canada, an additional $22,000 CAD per year per kilometer is estimated to be required to maintain the road network. Further estimates put the cost of repairs needed due to permafrost thaw rising above $3 million CAD per year by 2055 in the Northwest Territories, Canada (Kong, et al., 2019).

While permafrost thaw on roads is increasing rapidly due to climate change, another contributor to permafrost thaw is the presence and buildup of snow on the embankments. For example, on the access road to Umiujaq Airport in Nunavik, the extreme thaw observed was attributed to the access road embankment accumulating excess snow. Snow is a thermal insulator and with a heavy build up of snow on an embankment, heat in the ground does not easily transfer to the surrounding cold air in the winter as it would have with no excess snow build up on an embankment (Fortier, et al., 2011). Flynn et al., (2016) performed an in-depth study, monitoring temperatures beneath the toe, midslope, shoulder, and centreline of an embankment north of Thompson, Manitoba. There they found that the differences in ground temperature between the embankment and the centre of the road were from different snow depth conditions. In the winter snow was cleared from the road but allowed to accumulate on the road embankment. With the embankment having greater insulation during the winter than the centre of the road, the temperature was kept warm during the winter months when snow was on the ground.

1.1.2 Snow compaction as a mitigation technique to warming permafrost

In order to combat permafrost thaw under linear infrastructure, multiple mitigation techniques have been developed to facilitate either the prevention of heat intake into the permafrost, or to promote the extraction of heat from the permafrost. Methods that seek to prevent heat intake include applying a high albedo surface material to paved roads, increasing the embankment depth to increase insulation, and by applying sun-sheds to block direct sunlight on sensitive areas of linear infrastructure. Some heat extraction methods include the use of air convection embankments, air ducts, heat drains, and thermosyphons (Dore, et al., 2016). Recent investigation has begun to investigate snow compaction as a permafrost thaw mitigation technique to facilitate heat extraction from the ground.

O'Neill and Burn (2017) investigated the effects of long-term snow compaction and/or snow removal on road embankments using numerical models on the thermal ground regime. This study calibrated models utilizing sites along the Dempster Highway in the Northwest Territories and applied different snow depth scenarios to the model. It found that snow compaction applied over multiple years can cool near-surface ground temperatures and prevent ice-rich permafrost at an embankment toe and in long-term application permafrost can cool to significant depths.

A relativity new road the Inuvik-Tuktoyaktuk Highway, an extension of the Dempster Highway, that links Inuvik to Tuktoyaktuk situated on the coast of the Arctic Ocean offers opportunity to further investigate snow compaction as a mitigation technique. Construction of the highway, begun in 2014 and competed in November 2017, covers 138 km between Inuvik and Tuktoyaktuk in the Northwest Territories. Before the construction of the highway, Tuktoyaktuk was accessible on land only by an ice-road, which was only available in the winter months when conditions permitted.

The construction of such a road has been discussed for decades, but approval did not come until 2013 and had a cost of $300 million CAD (Government of the NWT, 2017). While still only less than a decade old, the ITH requires frequent repairs and road closures occur when damage becomes extensive. Without the application of effective permafrost thaw mitigation techniques, the ITH is at risk of becoming financially unsustainable, which would cut off Tuktoyaktuk from the rest of the transportation network in Canada.

In order to understand the applicability of snow compaction as a permafrost thaw mitigation technique a long-term snow compaction study, starting in late 2019, is being conducted at six locations along the ITH. These sites, instrumented with ground thermistor strings, provide useful information. Information that can be used to validate and calibrate ground temperature numerical models. Such models would allow for long-term simulations of ground temperatures under varying snow compaction conditions, assessing the viability of snow compaction as a long-term permafrost thaw mitigation technique. Evaluating anything longer than seasonal impacts of snow compaction through onsite observations and compaction would take years and is dependent on the unpredictability of the annual snow fall. Using numerical models to simulate the impact of snow compaction under a wide range of snow conditions would allow for a rapid assessment of this permafrost thaw mitigation technique.

However, good thermal modelling requires one to start with a well calibrated and validated model domain and boundary conditions. Developing a calibrated model requires the input of significant data and values, ranging from soil properties, site conditions, moisture contents, climate data, current thermal profile, etc. In northern and remote communities, this type of data availability and access is often scarce. This study investigates the ability to develop accurate numerical models for snow compaction studies from inputs and data sourced at variable distances from the study location. Following the development of these models, different snow compaction scenarios will be examined to help determine the feasibility of this mitigation technique for the ongoing maintenance and sustainability of the ITH.

1.1.3 Permafrost Modelling

Permafrost models are idealized mathematical representations that simulate the thermal state of the ground based on heat transfer theory. Previously, many models adopted the use of N factors, which relate ground surface temperature to air temperature (Riseborough et al., 2008). Specifically, N-factors are calculated as the ratio of freezing or thawing indices to the indices in the air. (Vincent et al., 2017). However, past limitations related to an inability to express various processes influencing soil thermal behaviour have seen the development of transient numerical models in spatial applications. Numerical modeling is capable of accounting for variable soil materials and energy balance boundary conditions, whereas previous models could not.

These geothermal models simulate vertical ground temperature in one- or two-dimensions using finite-element analysis. Set up of numerical models begins by defining the model space, the starting point in time, and the boundary conditions. The space is divided into a grid of finite nodes and the time is divided into finite time steps. Model depths should be deep enough to capture the annual temperature fluctuations that occur in the near-surface depths of the permafrost. However, the deeper depth of permafrost overtime influences the near-surface temperatures necessitating deeper model profiles to limit errors at the near-surface (Riseborough et al., 2008).

The soil material needs to be specified, which involves defining the thermal conductivity, specific heat capacity, and volumetric water content. Thermal conductivity and specific heat capacity are further divided into frozen and unfrozen properties, because the phase of water affects how it will transfer heat (Côté, and Konrad, 2005). A soils thermal conductivity is defined as its ability to transmit heat through a unit area of a of unit thickness in unit time under a unit temperature gradient. Furthermore, the quarts content of a soil will influence the thermal conductivity of a soil. Soils with higher percentage of quartz content have larger thermal conductivity values. A soils specific heat capacity is the quantity of heat needed to increase the temperature by a unit degree (GEO-SLOPE, 2014). The model begins with every node in the profile being defined by a starting temperature. As the model moves forward in time a new temperature is calculated for every time step based on the thermal properties, boundary conditions, and previous temperature value using equation 1:

$$\frac{\partial}{\partial y}\left(k_y \frac{\partial T}{\partial y}\right) + Q = \left(c + L\frac{\partial W_u}{\partial T}\right)\frac{\partial T}{\partial t} \quad [1]$$

Where c is volumetric heat capacity (KJ/m^3 °C), k_y is the thermal conductivity in the y-direction (1D model), Q (KJ/day m^2) is the applied boundary flux, L (KJ/m^3 °C) is the latent heat of water, w_u (m^3) is the unfrozen volumetric water content, T (°C) is the temperature, t (days) is time (Harlon & Nixon, 1978).

The upper boundary condition, the surface energy balance, is determined by the seasonal snow cover, overlying vegetation, solar radiation, and air temperature (Zhang et al., 2003; Mittaz et al., 2003). The air temperature is further influenced by wind speed (Ling and Zhang, 2004). The lower boundary condition is a constant geothermal flux value and represents the heat flowing from the Earth's core (Blackwell and Richards, 2004).

In the upper boundary condition, the seasonal snow cover plays an important role in insulating the underlying ground in ground temperature profiles. Both the snow covers' depth and density influence heat conduction (Zhang et al., 2003). The snow acts as a barrier between the ground and the air that restricts energy moving from the ground to the air. Snows insulation come from its low thermal conductivity, which prevents thermal movement. Also, snow has a high albedo, greater than 0.8 for freshly fallen snow, that reflects solar energy back towards the atmosphere. In comparison, bare ground has an albedo of around 0.2 (Vincent et al., 2017).

Initial soil temperatures can be provided from observations or through more sophisticated analysis, such as a spin-up analysis. A spin-up analysis provides initials conditions by running the model using repeated climate conditions and typically needs hundreds of cycles to reach an equilibrium. The conditions at the equilibrium provide for the initial conditions of the model. For deep model domains, spin-up analysis provides a practical method of establishing initial thermal conditions. Real world site locations that are being modelled are unlikely to have temperature recordings at depths below 20 m, therefore a spin-up analysis can provide for initial conditions at deeper depths (Riseborough et al., 2008).

1.2 Scope of Research

1.2.1 Definition of research project and objectives

This thesis presents a study in the influence of snow compaction as a mitigation technique for the maintenance of the ITH through numerical ground temperature modelling. The first objective is to show that model calibration can be successfully done when there is lack of site-specific data. To do this, a ground temperature model will be developed and calibrated based on a current snow compaction along the ITH. The site is located 49 km from the nearest source of weather data, an Environment Canada climate monitoring station based in Inuvik, NWT. This will show the validity of developing ground temperature models with a lack of direct on-site weather data, as well provide the basis of a model that will be used to study the effect of snow compaction on ground temperatures. The second objective is to conduct the study of snow compaction on the ITH model with varying snow conditions to assess its effectiveness in mitigating permafrost thaw. The snow compaction scenarios include looking at the assessment of frequency of snow compaction year to year, as well as within a year. These will be done under real snow conditions, as well as under minimum, average, and maximum snow depth years based on historical snow data from the region. Subsequent modelling in two-dimensions will explore the effect of lateral heat flow from snow compaction. Lastly, snow compaction is assessed on a two-dimensional model with an embankment structure to determine the effectiveness of such the application in mitigating permafrost thaw and maintaining the thermal integrity of the embankment.

1.2.2 Scope of thesis within current body of research

Current studies have shown that snow compaction models under simplified scenarios can influence ground temperatures and decrease the thaw depth of the active layer. No ground temperature models for snow compaction have been developed on sites along the ITH. This study provides the first investigation using numerical modelling into the applicability of snow compaction as a mitigation technique to prevent the thaw of permafrost along the ITH. Furthermore, no 2D models have been completed of snow compaction investigating the effect of compacting snow on lateral heat flow. This study fills this gap in the literature determine the lateral extent of the effect of snow compaction has on undisturbed adjacent ground, along with the first 2D modelling of snow compaction on a simulated embankment structure.

1.2.3 Thesis Content

This thesis is organized following the article-based format. Chapter 2 of the thesis presents a case study for the calibration of ground temperature models on the ITH in the Northwest Territories. First the site conditions and data available from each site will be described, followed by the development and calibration of models for each site. The calibration of the model of ITH site is then presented which is developed with input data sourced from 49 km away.

Chapters 3 will describe the snow compaction scenarios developed from measured weather data to assess the use of snow compaction as a mitigation technique to prevent the thaw of permafrost along linear infrastructure. The snow compaction scenarios will be applied to a 1D model of the site, then to a 2D model of the site to investigate lateral heat flow, then finally applied to a 2D

model with an embankment structure to investigate the ability of snow compaction on preventing permafrost thaw under the structure.

Chapter 4 will review the results of the research and discuss avenues of further investigation to further the understanding of snow compaction as a mitigation method for permafrost thaw along linear infrastructure.

Chapter 2
Ground Temperature Model Calibration

2.1 Introduction

The effects of climate change are increasingly becoming an issue of concern for northern communities. Since 1948, the average air temperature in northern Canada has risen by 2.3 °C. A further increase between 1.8 °C and 6.3 °C is predicted by the end of the 21st century as reported in 2019 by Environment and Climate Change Canada, (ECCC). In fact, observations from the eastern Canadian Arctic show that the ground is warming at a rate of 0.3 °C to 0.5 °C per decade. These northern communities are built on permafrost, which is ground that has temperature remaining at or below 0 °C for at least two consecutive years. With rising air temperatures, permafrost is increasingly thawing, which has led to ground instability affecting the integrity of existing infrastructure (Bell & Brown, 2018). Many structures have their foundations built deep into the permafrost and thawing permafrost can shift foundations leading to structural issues. Structures with a long operating life or those that have high consequences of failure, such as waste containment facilities, are especially susceptible to thawing permafrost (Ednie & Smith, 2011). To predict future ground conditions, numerical ground temperature models are typically used.

Ground temperature models use the basis of heat transfer theory to simulate the thermal state of the ground (Risenborough, et al., 2008). More advanced models, such as transient numerical modelling for ground temperatures is capable of variable soil materials and energy balance boundary conditions (Cote & Conrad, 2005). The upper boundary conditions, typically a surface energy balance, requires meteorological data as inputs from climate monitoring stations. The localized meteorological data required include air temperature, solar radiation, seasonal snow depth, wind speed, and relative humidity. The locations of climate monitoring stations in Canada are shown Figure 3. As seen in the figure, in the more northern regions of the country the climate monitoring stations become more sparsely located. This sparsity is challenging for transient numerical ground temperature models, as the input data may be required to come from a station at a distance of possibly over 100 km from the site of interest with uncertain consequences.

One example of transportation infrastructure that must deal with the challenges of degrading permafrost is the Inuvik-Tuktoyaktuk Highway. This all-season 138 km highway from Inuvik to Tuktoyaktuk in the Northwest Territories was completed in November 2017 and now provides year-round road access to Tuktoyaktuk. Previously, Tuktoyaktuk was only accessible by an ice-road in the winter and by air in summer. With year-round road access to Tuktoyaktuk, residents' benefit from reduced cost of living, and improved access to health care, education, and economic opportunities (Government of the NWT, 2017). Therefore, maintenance of the ITH is of great importance to the residents of Tuktoyaktuk to have a better quality of living.

Figure 3: Location of ECCC climate monitoring stations in Canada (2010). Climate monitoring stations used in this study (Inuvik) are coloured red (ECCC 2019).

In Canada, approximately 50 % of the landmass is permafrost. Permafrost can extend down to hundreds of meters and be thousands of years old. In addition to depth, permafrost varies in its spatial extent and diminishes as one travels south. Where permafrost comprises greater than 90 % of the land, it is considered continuous, between 50-90 % it is discontinuous, 10-50 % it is sporadic, and less than 10 % it is considered isolated patches. Based on yearly air temperature and snow depth, the southern limit of permafrost is approximated to determine where the distribution ends (Vincent, et al., 2017). Currently, the ITH runs through continuous permafrost. In profile, there are several layers of permafrost that impact infrastructure design. The first layer, the buffer layer is comprised of overlying vegetation, or could be any kind of infrastructure built on the ground. Conditions in the buffer layer affect heat transfer and influence the lower soil layers in the permafrost (Vincent, et al., 2017). The next layer is the active layer, which thaws in the warm summer months and refreezes in the winter. Then it is permafrost, the frozen layer, which stays frozen year-round and extends downwards until heat from the earths core causes the ground temperature to rise above 0 °C (Brown, 1973).

When constructing on permafrost, it is general practice to construct the foundations on the frozen layer. For roads like the ITH, permafrost is preserved by designing the road to be thick enough so that the summer thaw does not extend down to the road-ground interface (Government of the NWT, 2017). While the ground under the road is meant to stay frozen, the ground interface with the embankment can experience thaw, especially near the embankment toe. Thawing of ground under embankments can lead to lateral spreading of the embankment, differential settlement, and instability which would require repairs. If the damage is extensive enough, then road closures are possible (Parent, et al., 2019).

While the ITH only just opened in November of 2017, some observations suggest that the state of the road is deteriorating with gravel fill having been spread out onto the surrounding landscape (Bowling, 2020). Furthermore, during the thaw period muddy conditions can lead to frequent road

closures and even when alleviated can still require travel restrictions based on vehicle weight (Bowling, 2020). The Northwest Territories department of infrastructure expects that spring closures are to be a regular occurrence due to the difficulty in maintaining the roads structural integrity when the active layer is thawing. Road closures can be particularly debilitating for community members because they can occur with little notice with open conditions in the morning and closed conditions in the afternoon leaving potential travellers stranded.

As such, there are several ongoing mitigation and adaptation studies along the ITH. One such study is a snow compaction study currently being conducted at six sites along the ITH. This study is evaluating the efficacy of compacting snow in the winter as a method to mitigate permafrost thaw by comparing ground temperatures recorded from thermistor strings to a control site. However, the limitation of this study is that data is only collected on an annual basis, and long-term studies will take decades to conduct. However, a thermal numerical model calibrated with the recorded ground temperatures and onsite snow data could be used to study the thermal regime of a site on the ITH under different snow compaction scenarios and predict future ground thermal behaviour to applied compaction techniques. To do this with confidence would require local climate data from climate monitoring stations, and the closet climate monitoring station to the site of interest along the ITH is located in Inuvik, 49 km away.

This chapter presents the results of a ground temperature model that is developed from meteorological data sourced away from the site of interest. The site only measured limited snow data at a control and compacted site, while the rest of the weather data was sourced from Inuvik. The ground profile of the area was limited, and an iterative approach was adopted to modify soil properties until model results agreed with the onsite thermistor recordings. Using both the control and compacted snow measurements this paper shows how well the model could be calibrated using this iterative approach under the different snow conditions. The numerical models were developed from the GeoStudio TEMP/W (version 11.1.1.22085) module developed by GEOSLOPE INC.

2.2 Background

2.2.1 Heat transfer Theory

Heat transfer in soils occurs mainly through conduction, which is defined as the "amount of heat passing in unit time through a unit cross-sectional area of the soil under a unit temperature gradient applied in the direction of the heat flow" (Harlon & Nixon, 1978). The differential equation for time-dependent heat transfer, where the difference between heat energy entering and leaving an elemental volume of soil is equal to the change in energy stored within the element at that point in time is seen in Equation 2.

$$\frac{\partial}{\partial y}\left(k_y \frac{\partial T}{\partial y}\right) + Q = \lambda \frac{\partial T}{\partial t} \quad [2]$$

k_y is the thermal conductivity in the y-direction (1D model), Q (KJ/day m^2) is the applied boundary flux, λ (KJ/m^3 °C) is the heat storage capacity, and t (days) is time.

Both the volumetric heat capacity of the soil and the energy needed for a phase change in water in the soil make up the heat storage of the soil. Latent heat is the energy required to change the phase of water, where the volumetric heat capacity is the energy stored in water and soil without phase change. Heat storage capacity is expressed as shown in Equation 3.

$$\lambda = c + L\frac{\partial w_u}{\partial T} \quad [3]$$

where c is the volumetric heat capacity (KJ/m^3 °C), L (KJ/m^3 °C) is the latent heat of water, w_u (m^3) is the unfrozen volumetric water content, T (°C) is the temperature, and λ (KJ/m^3 °C) is the total capacity for heat storage.

The moisture content in soils going through a phase change require a large amount of latent heat for phase change to occur. This results in slowing down the phase change due to more heat being required to affect the phase change. During phase change, the thawing/freezing of the phase of water does not occur at a single temperature. Particles of water will undergo phase change before others. In Geostudio the unfrozen water content varies between 0 and 1.0 and is expressed as shown in Equation 4.

$$w_u = W_u w \quad [4]$$

Where W_u is the unfrozen water content and w (m^3) is the volumetric water content within the soil.

An equation for determining the temperature of an element of soil is made by substituting Equations 3 and 4 into Equation 5, shown below.

$$\frac{\partial}{\partial y}\left(k_y \frac{\partial T}{\partial y}\right) + Q = \left(c + L\frac{\partial W_u}{\partial T}\right)\frac{\partial T}{\partial t} \quad [5]$$

2.2.2 Site Background

The field site in this study is the Trail Valley Hill site, located 49 km North of Inuvik. Figure 4 shows the location of the site along the ITH along with the climate monitoring located in Inuvik used for input data in the development of the model.

The nearest climate monitoring station to the site is located in Inuvik 49 km away with another climate monitoring station located in Tuktoyaktuk 89 km away. Air temperature recordings from both Inuvik and Tuktoyaktuk are shown in Figure 5 from September 1st, 2019, to September 1st, 2020. Based on the graph there is not a large difference between the two recordings indicating a relatively homogeneous air temperature profile between the two communities.

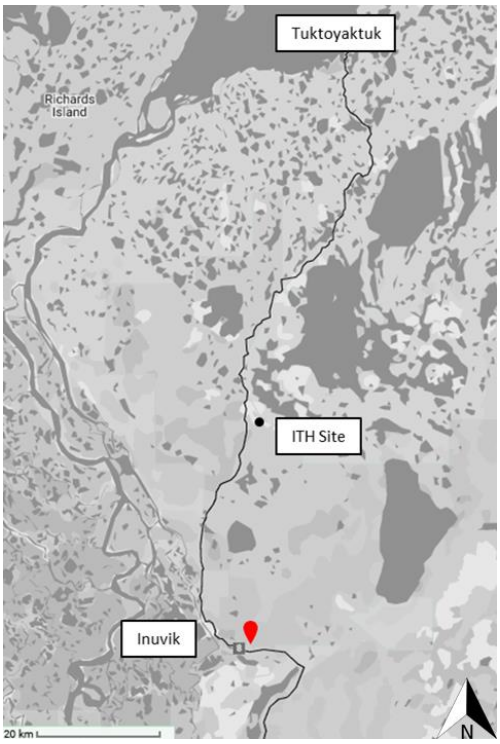

Figure 4: Location of site and weather stations on the ITH. The ITH is located approximately at the 49 km mark of the highway traveling from Inuvik to Tuktoyaktuk. The ECCC climate monitoring station is located at the red marker in the town of Inuvik.

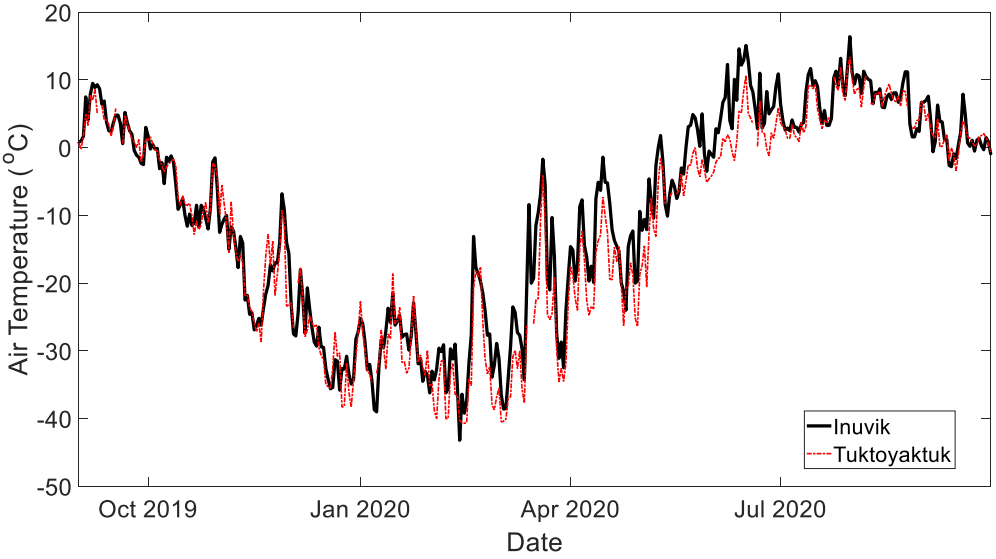

Figure 5: Air temperature recordings from ECCC climate monitoring stations located in both Inuvik and Tuktoyaktuk from September 1st, 2019, to September 1st, 2020 (ECCC 2019).

The site was comprised of two 50 m x 50 m plots with one site undergoing snow compaction and the other site being left undisturbed during the winters between 2019 to 2021. At the control site was a thermistor cable embedded into the ground that measured ground temperature every two hours at 1.0 m, 2.0 m, 4.0 m, 8.0 m, 16.0 m, and 20.0 m starting July 31st, 2017, until August 20th, 2020. At the compacted site was three thermistor cables that measured ground temperatures every one hour at 0.5 m, 1.0 m, 1.5 m, 2.0 m, and 3.0 m starting August 19th, 2019, until August 27th, 2021. The thermistor strings were Geoprecision loggers with TNode EX sensors that had a resolution of 0.001 °C and an accuracy of ±0.1 °C at -20 to +25 °C, ±0.2 °C at -30 to +40 °C, and ±0.5 °C at -40 to -85 °C. Sensors were manufactured in the same year of installation.

Starting in 2019 each plot was subdivided into 10 m x 10 m grids and snow measurements were taken at each grid point for a total of 36 points in each plot. At six grid points for each plot snow density measurements were taken. One site was established as a control and left undisturbed, and the other site underwent snow compaction at multiple times during the winter. Snow compaction was conducted by driving a Sno-Cat over the study plot. For the control site, measurements for both snow depth and snow density were taken three times during the winter of 2019-2020. The measurements were taken on December 1st, 2019, January 17th, 2020, and March 12th, 2020. Snow depth and snow density measurements at the site that underwent snow compaction were taken six times during the winter of 2019-2020. Measurements would be taken then the site would be compacted and follow up measurements were taken a few days later for a total of three compactions per winter. The measurements were taken December 1st, 2019, December 5th, 2019, January 17th, 2020, January 21st, 2020, March 13th, 2020, and March 19th, 2020. Figure 6 shows bulk density data from both the control and compacted site and the snow depth measurements taken on the three dates where recordings were done for the control site. Figure 7 shows a picture from the compacted site.

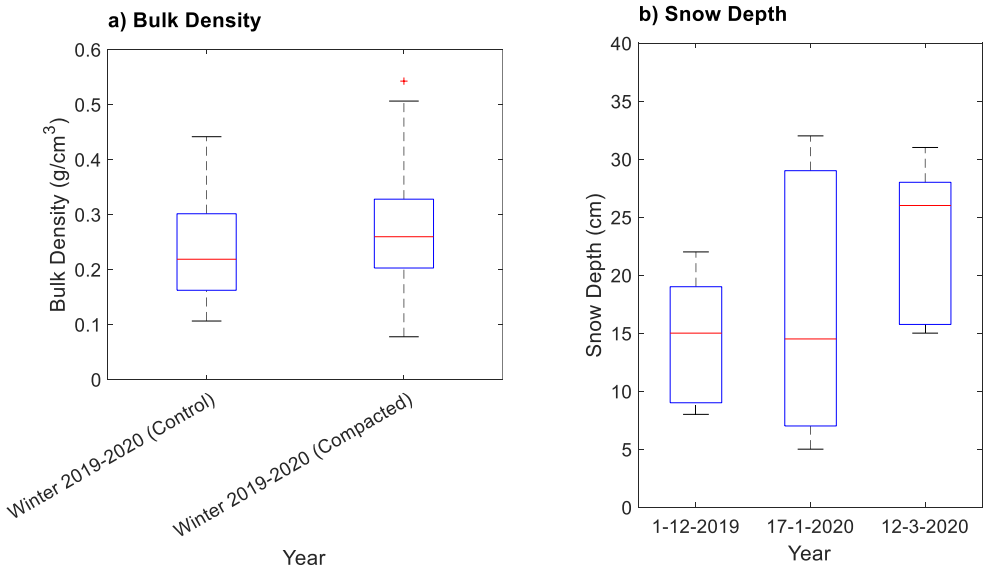

Figure 6: Measured a) bulk density and b) snow depth at both the control and measured site for the two winters measurements were taken. The red lines in the figure are the median values of the data, the blue box limits are the 25th and 75th percentiles, the whiskers are the outer limits of the data sets that are not outliers, and outliers are represented by red crosses (Wilson, 2021).

Figure 7: A picture of the field site undergoing snow compaction by driving a Sno-Cat over the site (Photo Credit: Alice Wilson & the Northwest Territories Geological Survey).

2.2.3 Model Development

The ground temperature model developed for calibration and validation for the ITH site was a one-dimensional thermal model. The program used to develop the model was the Geostudio TEMP/W (version 11.1.1.22085) module developed by GEOSLOPE INC. The model was calibrated using the ground temperature recordings from the thermistor data on site from the control and compacted site.

Soil Properties

The model was developed to be 50 m deep and comprised of 2 layers, a sand soil top layer from 0 to 20 m depth and bedrock from 20 to 50 m depth. The 50 m model depth was selected because deep permafrost affects ground temperatures at shallower depths and needs to be accounted for (Ross et al., 2022).

The initial ground profile was developed from borehole data from a site located approximately 800 m from the site (ITH Winter 2017 Geotechnical Drilling Program, 2017). Using the Johansen 1975 method (GEO-SLOPE, 2014; Andersland & Ladanyi, 2004), the unfrozen & frozen volumetric heat capacity and the unfrozen & frozen thermal conductivity were calculated from the initial soil porosity and degree of saturation estimated from the borehole data. Initial porosity was selected from the theoretical range of porosity for the soil type as described in the borehole data. Initially, this included layers of sand & gravel, silt and sand, and gravel. In the end, the final ground profile was developed to consist of a single layer of clayey sand on top of a bedrock layer. The range of possible values for the material properties and the final values established from the calibration are shown in Table 1.

Table 1: Range of possible values for material properties and final values used in ITH ground temperature model (Andersland & Ladanyi, 2004).

	Clayey Sand		Bedrock	
Properties	Range	Final	Range	Final
Unfrozen thermal conductivity (KJ/d m °C)	43.2 - 345.6	65		260
Frozen thermal conductivity (KJ/d m °C)	86.4 - 259.2	100		260
Unfrozen volumetric heat capacity (KJ/m^3 °C)	1090 - 3040	2806		2,100
Frozen heat capacity (KJ/m^3 °C)	1090 - 3040	2100		2,100
Water Content (%)	N/A	25		0

Boundary Conditions

The upper boundary condition was established as a Land-Climate Interaction boundary and was created from historical weather data from the Inuvik airport (68°19’00.000” N, 7133°31’00.000” W) and snow measurements taken on site. Historical weather data for the site was provided from Environment Canada. Weather data included daily average temperature, wind, speed, and snow depth. Because the snow data obtained onsite only contained measurements from three different times during the winter it was assumed that snow increased or decreased linearly from one data snow measurement to the next. Furthermore, no records were taken for when snow cover first occurred and for when snow completely melted in the spring. It was assumed that the snow appeared and disappeared on the same days as snow appeared and disappeared in Inuvik based on the climate monitoring station data, which were October 5, 2019, and May 25th, 2020, respectively. The model input data was set up to increase from or decreased to 0 m snow depth from those dates from the first and last snow measurements. Solar radiation was estimated using a built-in function in Geostudio with the Latitude of the snow compaction study site (69° N). Albedo was designated a value of 0.2 when there was no snow and 0.8 when there was snow on the ground (National Snow and Ice Data Center, 2020).

The lower boundary condition was designated as a heat flux boundary with a constant value of 4.32 kJ/d m^2, which represents heat flow from the earths core (Blackwell and Richards, 2004).

Snow Properties

Onsite snow measurements show that the snow density changes over the course of the winter, however TEMP/W does not include a function to allow for change in snow density overtime, instead just allowing a singe input. The thermal conductivity values used were calculated from the recorded snow density measurements from the Trail Valley Hill site. Density was converted into thermal conductivity using the Sturm (1997) equation:

$$K = 10^{(2.65*d-1.652)} \quad [6]$$

Where K is thermal conductivity (W/m/k) and d is snow density (g/cm^3). In TEMP/W, the snow depth and snow density values are used to calculate a single thermal resistivity value for the land-climate interaction boundary. The equation used to calculate the thermal resistivity value is as follows:

$$R = \frac{\Delta H}{\delta} \quad [7]$$

Where ΔH is the snow depth and δ is thermal conductivity at a given time. Using this equation, the thermal resistivity value can be calculated using the snow depth and snow density measurements, which can then be used to calculate a new snow depth value to give the same thermal resistivity value if the snow conductivity value must stay constant in the model input. This was used to modify the snow depth so that the model incorporates the changing snow density over time and better reflects the onsite conditions. The snow thermal conductivity input in to the model was the initial thermal conductivity, which was 5 kJ/d/m/°C. Figure 8 shows the snow data from the winter of 2019-2020 from the Inuvik airport, the values of the recorded snow depth from the ITH site, the linear increase and decreased between the measured snow depth vales, and the snow depth from the site modified to account for the change in snow density over the winter for the model input. As shown in the figure, the snow depth measurements from Inuvik and the ITH site are significantly different, which indicates that unlike air temperature snow depth cannot be assumed to be homogenous between the communities of Inuvik and Tuktoyaktuk.

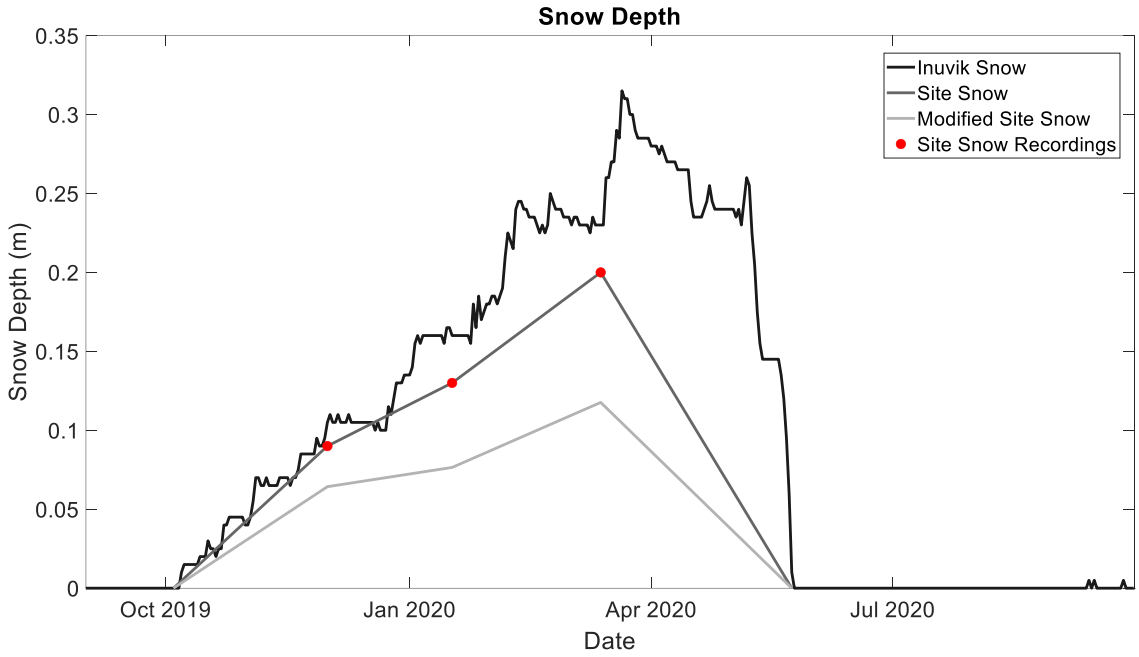

Figure 8: Graph showing snow depth data retrieved from the Inuvik climate monitoring station, snow depth measurements from the ITH site (Wilson, 2021), and the modified ITH snow depth that was used in the model.

Model Domain and Spinup

Shown in Figure 9 is the final model profile. The mesh size was finer (0.01 m) in the upper layer (0.0-1.6 m) and increased in size at lower depths: 0.1 m (1.6-10.0 m), 1 m (10.0-20.0 m), and 2 m (20.0-50.0 m). This was done to minimize model runtimes as the lower depths due not fluctuate in temperature during the model runtime and does not need as many calculations to occur to produce accurate results. The timestep length was 0.5 days. The convergence criteria for a solution at each timestep a difference of less than 0.1 °C between iterations at two significant digits with a maximum of 500 iterations.

The model's initial ground temperatures were established through a spin-up analysis (Ross, et al., 2021). In the spin-up analysis, the top boundary condition was established using weather data from Environment Canada from the Inuvik Airport between July 31, 2016, and July 31, 2017. The initial ground temperature throughout the model was set to -6.6°C, the MAGT as determined from the recorded thermistor data. The model was set-up to run for 500 years repeating the weather data from the site over the 500 years. The ground temperature profile was deemed to reach equilibrium when the ground temperatures after each cycle were the same values. The model was set-up to run for 500 years repeating the weather data from the site over the 500 years. The ground temperature profile was deemed to reach equilibrium when the ground temperatures after each cycle were less than 0.01 °C. If the equilibrium condition were not satisfied in the 500 years, the years would have been increased until equilibrium occurred.

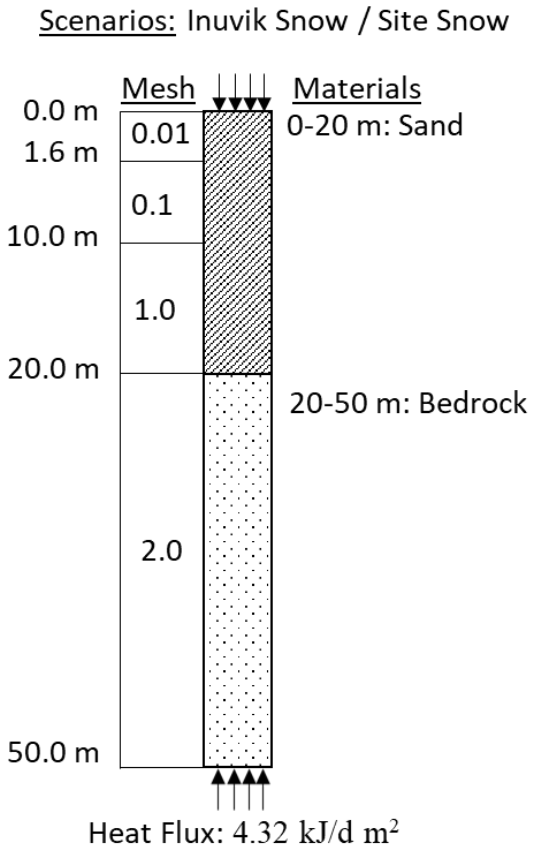

Figure 9: Model profile of the Trail Valley Hill site along the ITH.

2.3 Results and Discussion

2.3.1 Results

The numerical ground temperature model for the Trail Valley Hill site along the ITH was calibrated using the measured ground temperature data from August 1, 2019, to August 20, 2020. Figure 10 shows the daily ground temperature of both the recorded and modelled ground temperatures at 1 m, 2 m, 4 m, and 8 m. Calibration was further visualized by comparing the minimum, mean, and maximum annual ground temperatures for the time period of August 1st to July 31st for and 2019-2020 for the control site (Figure 11). The model had continuous temperature data along the depth of the model, from 0-50 m overlaid by the temperature recordings at the depths of 1 m, 2 m, 4 m, 8 m, 16 m, and 20 m. The model in its final iteration had all minimum, mean, and maximum ground temperatures within 1 °C of the corresponding recorded ground temperatures.

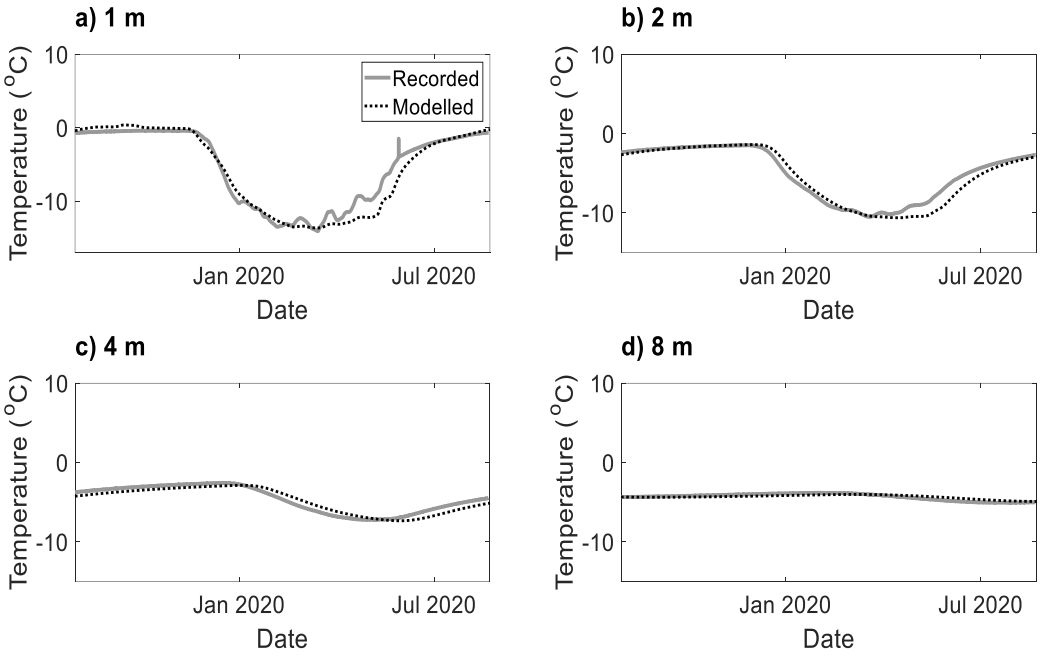

Figure 10: Ground temperature vs time of recorded and modelled ground temperatures at a) 1 m, b) 2 m, c) 4 m, and d) 8 m from August 1st, 2019, to August 20th, 2020. Recorded temperatures from Wilson & Rudy (2021)

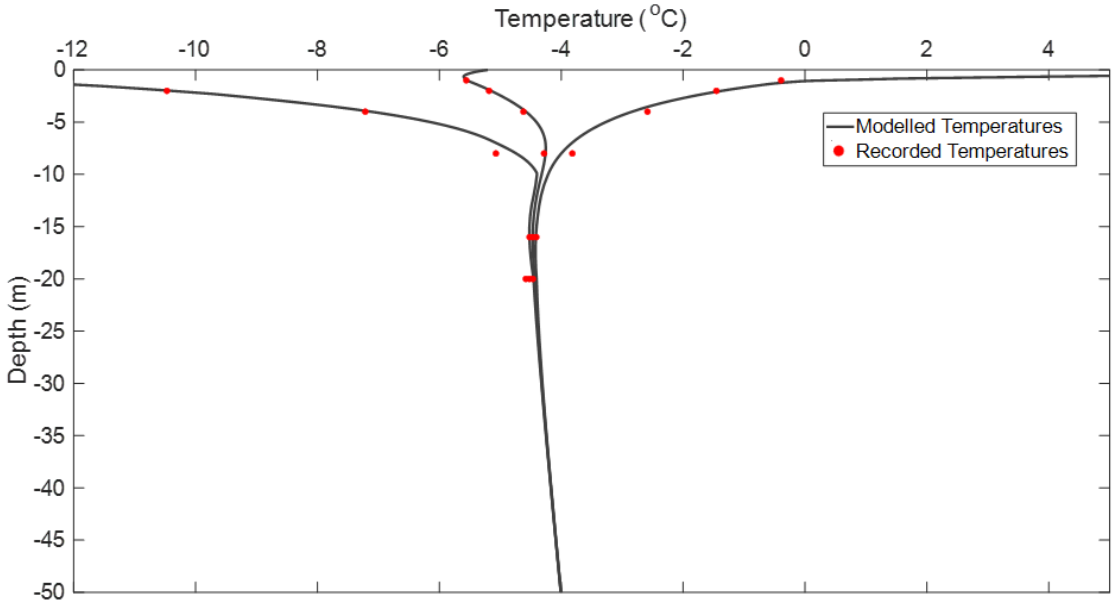

Figure 11: Trumpet Curve showing calibration of the Trail Valley Hill control site using ground temperature recordings from August 1st, 2019, to July 31st, 2020.

Adjacent to the undisturbed snow plot was the disturbed snow plot that underwent snow compaction three times during the winter that contained three shallow multibeaded thermistor strings recording temperatures at 0.5 m, 1.0 m, 1.5 m, 2.0 m, and 3.0 m. With the two plots located next to each other it was possible to validate the material properties calibrated for the ground temperature model using the new snow depth data. A model was produced where this new snow data was used modelling ground temperatures from January 1st, 2020, to December 31st, 2020. Figure 12 shows the daily ground temperature of both the recorded and modelled ground temperatures at 0.5 m, 1.0 m, 1.5 m, and 2.0 m. The model results were further visualized by comparing the minimum, mean, and maximum annual ground temperatures for the time period of January 1st, 2020, to December 31st, 2020 (Figure 13). The model had continuous temperature data along the depth of the model, from 0-50 m overlaid by the temperature recordings at the depths of 0.5 m, 1.0 m, 1.5 m, 2.0 m, and 3.0 m. The model had most minimum, mean, and maximum ground temperatures within 1 °C of the corresponding recorded ground temperatures. The only exception was the maximum annual ground temperature at 0.5 m, which had a difference between the modelled results and the recorded results of 3.2°C. Overall, it was determined that the material properties of the model was validated with the new snow depth inputs, since most the annual ground temperatures modelled were within 1 °C of the recorded temperatures.

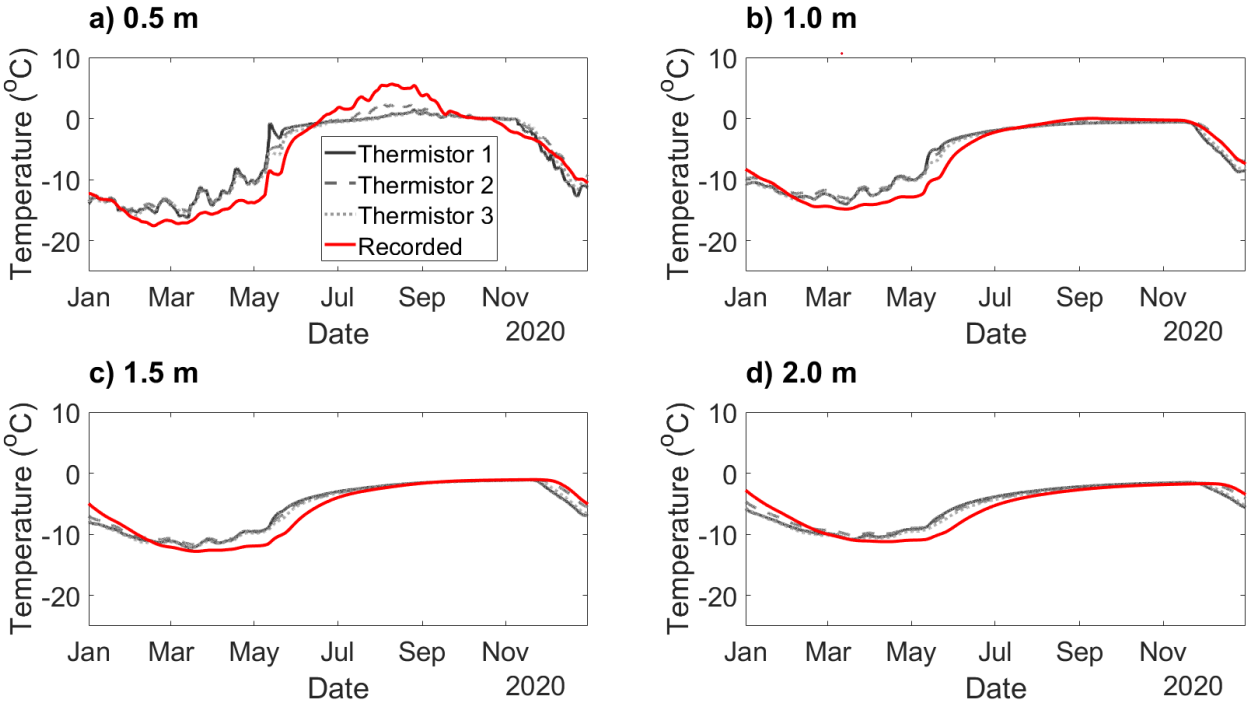

Figure 12: Ground temperature vs time of recorded and modelled ground temperatures using the snow depth data from the compacted snow site at a) 0.5 m, b) 1.0 m, c) 1.5 m, and d) 2.0 m from January 1st, 2020, to December 31st, 2020.

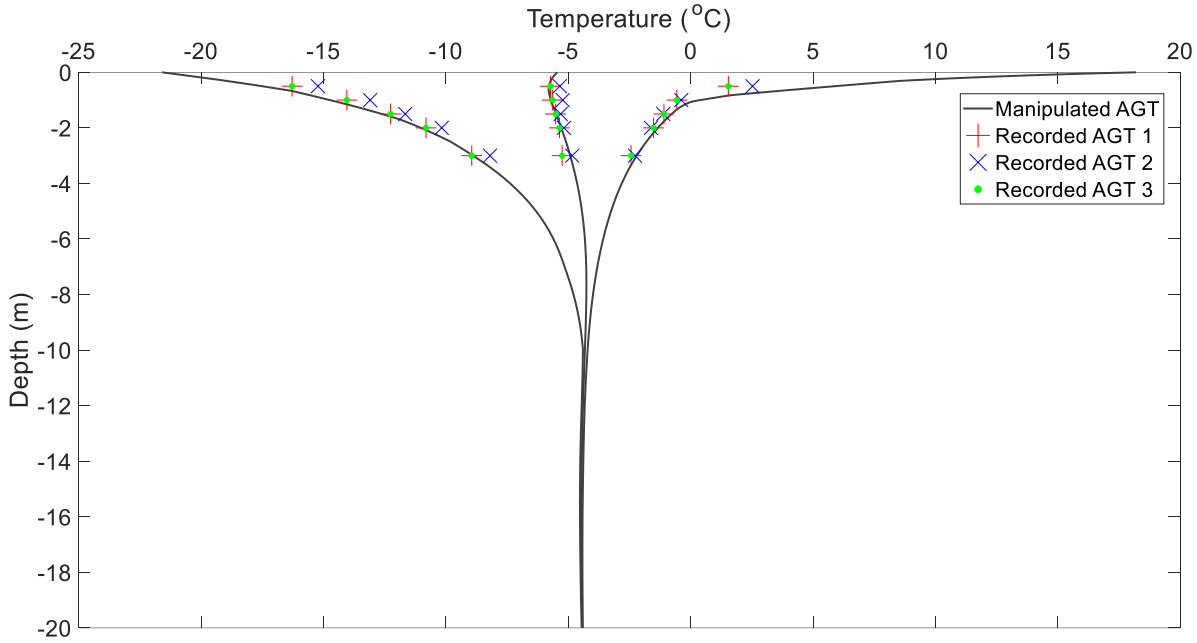

Figure 13: Trumpet Curve showing validation of the final material properties of the Trail Valley Hill site using ground temperature recordings from the compacted snow site from January 1st, 2020, to December 31st, 2020.

2.3.2 Discussion

In developing the numerical model representing the site at Trail Valley Hill along the ITH, the 49 km distance from the nearest climate monitoring station raised concern over the accuracy of a model developed using climate inputs from such a distance. Based on the results from the Trail Valley hill site, it is possible to develop an accurate model, as defined by having modelled annual ground temperatures within 0 °C of recorded annual temperatures, at a distance 49 km from a source of climate input data. However, challenges still arose in the development of the model. When setting up the model domain, it was necessary to first establish a starting point for the ground materials. The closest borehole that could be sourced to provide a ground profile was 800 m away and in a different geographic feature than the site of the model. The borehole was located next to a shallow stream and was characterized by a coarse top layer of gravel and the presence of ground ice, whereas the Trail Valley hill site is located away from the stream in a more elevated position.

When developing the model, it was found that this ground profile was not able to produce a model that was able to accurately simulate the ground temperatures that were recorded by the thermistor string. In order to develop a better model, a more iterative estimate and check approach was taken which resulted in the final model profile of a top layer of clayey sand over a bedrock layer. While ideally, an onsite ground profile would be available with measured soil properties, it is possible to apply this iterative design approach as shown by the accuracy of the Trail Valley Hill model to the recorded ground temperatures at the site. However, such a method can be time intensive as it requires the model to be ran multiple times where each time a soil property is changed to better align the model outputs with the recorded ground temperature data. Because of the amount of time

an iterative approach to the development of the ground profile can take it is recommended that while not necessary, soil measurements to identify thermal properties should be taken from a site when developing a model.

Another issue that arose in the calibration of the model was the use of the snow data starting in the second half of 2019 from the Trail Valley Hill site. Snow was measured at 36 points in the 50 m x 50 m site with five measurements at each site. Over the entirety of the site the snow measurements at a given time could be highly variable with differences in measurements getting as high as between 10-20 cm snow depth. With such high variance in snow measurements, it can be difficult to select a snow depth value at a given time to be used in the land-climate interaction boundary condition. Such different snow depths will greatly affect the thermal regime of the near-surface ground temperatures being modelled. When calibrating the model, it may then be necessary to modify the snow depth within the range of observed snow depth measurements in order to identify the measurement that best simulates the ground temperatures recorded by the thermistor string.

While it was shown that the air temperature in the region was relatively homogenous between Inuvik and Tuktoyaktuk, the same cannot be said for snow. By applying the Inuvik snow depth data to the model inputs in lieu of the ITH site snow depth data, a different thermal profile is produced at the near surface depths. Figure 14 shows the ground temperatures vs time at 1.0 m, 2.0 m, 4.0 m, and 8.0 m of the results from the calibrated model and the model with Inuvik snow depth inputs.

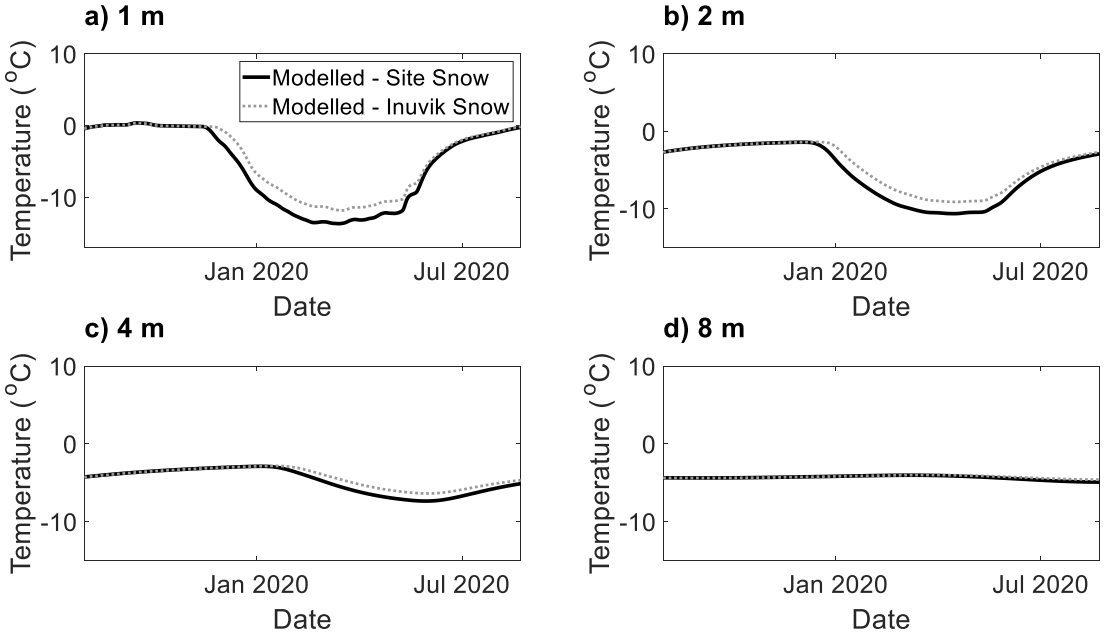

Figure 14: Ground temperature vs time of modelled ground temperatures with site snow and Inuvik snow at a) 1 m, b) 2 m, c) 4 m, and d) 8 m from August 1st, 2019, to August 20th, 2020.

As shown in the results, the ground temperature results from the model with Inuvik snow is approximately 2 °C warmer during the winter at 1.0 m depth. This is due to the higher snow depth recorded in Inuvik than what was measured on site. Deeper snow depth would increase the insulation between the air and the ground, resulting in less heat flow from the ground to the air during the winter months. The ground temperatures between the two models at the deeper depths do not differ. This is due to deeper depths being less responsive to changes in surface conditions, but given enough time is possible that the lower depths would also start to diverge. This was further visualized by comparing the minimum, mean, and maximum annual ground temperatures for the time period of August 1st to July 31st for and 2019-2020 for between the two snow depth inputs (Figure 15).

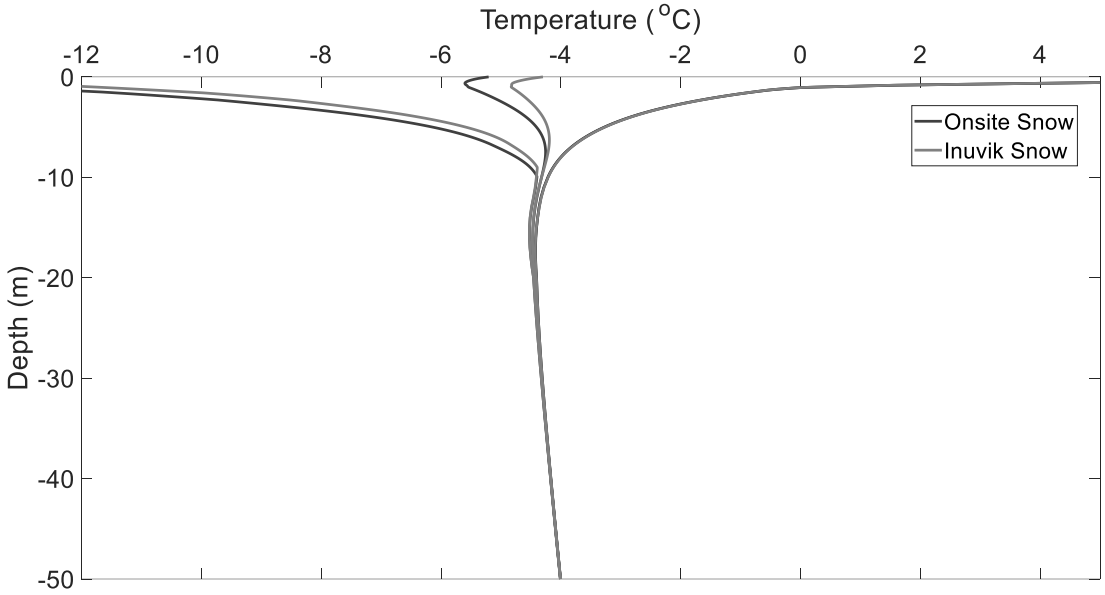

Figure 15: Trumpet Curve showing ground temperatures from model results with onsite snow and Inuvik snow from August 1st, 2019, to July 31st, 2020.

Shown in the results between the two models, ideally field sites developed as ground temperatures models of a will have onsite snow depth recordings that would provide for a more accurate model. However, snow depth data source from a different area is still useful if less accurate results are adequate, there just may be certain time periods where there is enough of a difference in the snow depth between the sites to affect the accuracy of the model. A detailed model development case study where there is no onsite snow depth data available is presented in Appendix A - Kingston Case Study. Furthermore, shown in the results of the compacted snow depth model, there was a difference in the results of the compacted snow depth and non-compacted snow depth for the year of 2020. This further illustrates the importance of having onsite snow measurements to develop a more accurate model, as differences in snow depth between two areas will provide different results. The compacted results also show the accuracy of the model domain. By representing ground temperatures at different snow depths, the model is shown to be accurate to the sites ground soil composition and can be used to model the ground temperature under different

conditions to predict how the ground thermal regime will respond. Since the model results show differences in ground temperature when snow conditions changed, snow depth has a clear effect on ground temperatures. The calibrated model can be used to investigate snow compaction as a method to mitigate permafrost thaw that is affecting northern infrastructure.

2.4 Conclusion

With rising air temperatures due to climate change permafrost is thawing leaving northern infrastructure, such as the Inuvik-Tuktoyaktuk Highway vulnerable to damage. Different mitigations methods are being tested to slow or stop the thawing of permafrost underlying critical infrastructure. One method is snow compaction where snow is compacted to reduce its depth and increase its density, which reduce its overall insulative properties.

Investigating the impact of snow compaction in the field relies on variability of seasonal snow and temperature conditions. Numerical models provide an effective method of testing snow compaction under varying conditions and can be site specific when calibrated to field data. A snow compaction study occurring along the ITH provided valuable site information for model calibration but had limited information on the ground profile and onsite weather data. This study measured snow depth and density along with ground temperature at two adjacent sites where one was left undisturbed, and the other was compacted resulting in two different thermal regimes. However, because the study did not engage in a ground investigation, soil properties are unknown and developing a calibrated model required an iterative approach.

Since the control and compacted snow sites were next to each other it was possible to develop a single model through iteration that was calibrated with different snow depths by comparing the model outputs to ground temperature recordings. The model results show that the temperatures agree with measured data from September 1st, 2019, to August 31st, 2020. When looking at the minimum, maximum, and average annual ground temperatures from the thermistor recordings, all control recordings were within 1 °C of the final model outputs, whereas compacted recordings had all but one of the results within 1 °C. Additionally, results showed that snow data is best received from onsite due to the high variability that can occur in snow properties in a geographic area, unlike other weather properties such as air temperature.

Based on the different model outputs from the control and compacted snow depth, different snow properties can affect a thermal regime. Because snow compaction studies are subject to the variability of seasonal weather and can require years to understand long term effects, the calibrated ITH model offers a useful tool to study snow compaction under varying scenarios. Chapter 3 uses this model under various seasonal and annual snow compaction configurations to assess its ability to slow or stop the thawing of permafrost under linear infrastructure.

Chapter 3
Snow Compaction Scenario Analysis

3.1 Introduction

The Inuvik-Tuktoyaktuk Highway is an important piece of Canada's northern infrastructure that gives Tuktoyaktuk year-round access to Canada's ground transportation network. Constructed in 2017, the ITH replaced the previous seasonal ice-road that was only traversable in the winter months when ice conditions permitted. With the construction of the ITH, Tuktoyaktuk has seen improvements to its cost of living, access to health care, and now has greater economic opportunities (Government of the Northwest Territories, 2017). The ITH was designed for the original ground surface to stay frozen year-round. However, this did not consider the ground surface interface with the embankment, which when thawed can lead to lateral spreading of the embankment, differential settlement, and instability which could require repairs (Parent, et al., 2019). Since its opening, the ITH has had serviceability challenges during the spring thaw period where muddy and rutted conditions have led to road closures and travel restrictions based on vehicle weight. Road closures are particularly troublesome for community members travelling between Inuvik and Tuktoyaktuk where the road can be drivable in the morning but deteriorate by the afternoon potentially leaving people stranded (Bowling, 2020).

With difficulties in maintaining the structural integrity of the ITH, mitigation methods that will reduce the thawing of the permafrost and help maintain access to the road are being investigated. One such mitigation method is snow management. Snow acts as a thermal insulator, which reduces ground during winter months. If the transfer of heat from the ground to the air is reduced, then when it is summer, the ground can increase in temperature quicker due to more heat being added to the system year after year. Snow compaction is one example of snow management, combining a decrease in snow thickness and increase in density, both which improve heat transfer. Snow compaction has been used in the arctic with varying success (Lepage et al., 2012; O'Neill & Burn, 2017). Performance of snow compaction in these studies and trials can be attributed to several factors, some which can be controlled (e.g. timing and frequency of snow compaction) and those that cannot (e.g. cumulative annual snow depth). There are ongoing field studies, which are monitoring the thermal regime under snow compaction investigations to try and improve its efficacy as a technique (Wilson, 2021). However, field investigations are confined to climate conditions on site, including the annual snow distribution and accumulation. The current field datasets present an opportunity to use numerical modelling techniques to investigate snow compaction for broader application scenarios.

The objectives in this chapter are to (1) characterize the effect of snow compaction for the expected range of snow depths along the ITH, (2) examine the effect of compaction frequency and timing within an individual year on the ground thermal regime, (3) examine carryover effects on thermal regimes from snow compaction in subsequent years, (4) characterize the lateral thermal impact of snow compaction, and (5) examine the effect of snow compaction on the thermal regime of a simulated embankment structure. These objectives are met using the ground temperature model developed in Chapter 2, coupled with the site calibration and validation from the field site data.

3.1.1 Site Details

The field site in this study is a snow compaction site on the ITH located 49 km north of Inuvik. The field investigation is being performed by the Northwest Territories Geological Survey and the Aurora Research Institute, (Rudy, et al., 2020). The site contains two side-by-side 50 m x 50 m plots with one side undergoing snow compaction and the other side left undisturbed. The location of the site can be seen in Figure 4 in Chapter 2. A thermistor cable at the control site measures ground temperature at 1.0 m, 2.0 m, 4.0 m, 8.0 m, 16.0 m, and 20.0 m depths, every two hours. In this study, thermistor data was used from July 31st, 2017, until August 20th, 2020 (Wilson, 2021). At the compacted site, there are three thermistor cables measuring ground temperatures every hour at depths of 0.5 m, 1.0 m, 1.5 m, 2.0 m, and 3.0 m from August 19th, 2019, until August 27th, 2021. On each plot site, snow density measurements were taken at 6 points and snow depth was measured at 36 points based on a 10 m x 10 m grid. Measurements were taken in December, January, and March of each year.

3.2 Methods

The impact different snow compaction scenarios have on the short- and long-term permafrost protection is explored using one- and two-dimensional numerical models. First, the efficacy of snow compaction is evaluated for different snow depths (i.e., high, low, avg. annual snow fall) with a 1D model. This is followed with an evaluation of the thermal 'memory' snow compaction has on the ground thermal regime, to determine if snow compaction needs to be applied yearly for best results. Then, snow compaction frequency and temporal timing during winter season is evaluated to understand when and how often snow compaction should be applied for the best thermal results. Finally, using a 2D model lateral heat flow from snow compaction was investigated, followed by the impact of snow compaction on the thermal regime of an embankment. The numerical models were developed using the Geostudio TEMP/W module (version 11.3.1.23726) developed by GEOSLOPE INC.

3.2.1 Model Development

Three distinct model domains were used in this chapter. The first is the one-dimensional model developed in the previous chapter for the ITH snow compaction site (Figure 16a). The second model is a 2D model used to analyze the effect of snow compaction has on lateral heat flow (Figure 16b), and the third is a 2D model further developed to include the structure of an embankment (Figure 16c). Soil properties are listed in Table 2 and were selected through an iterative approach as outlined in Chapter 2. The equation for heat transfer used in the 1D model is outlined in Chapter and the equation for the 2D models is shown in Equation 8.

$$\frac{\partial^2 T}{\partial y^2} + \frac{\partial^2 T}{\partial x^2} + \frac{Q}{k} = \frac{\left(c + L\frac{\partial W_u}{\partial T}\right)}{k}\frac{\partial T}{\partial t} \quad [8]$$

where k is the thermal conductivity (same for both x and y direction), Q (KJ/day m^2) is the applied boundary flux, t (days) is time, c is the volumetric heat capacity (KJ/m^3 °C), L (KJ/m^3 °C) is the latent heat of water, w_u (m^3) is the unfrozen volumetric water content, T (°C) is the temperature.

The upper boundary condition for all models was a Land-Climate Interaction boundary, which was used to establish the different snow conditions for the snow compaction scenarios. The solar radiation was obtained from the built-in function in Geostudio using a latitude of 69°N. Albedo was designated a value of 0.2 when there was no snow and 0.8 when there was snow on the ground (National Snow and Ice Data Center, 2020). Timestep length was 0.5 days. The lower boundary condition was designated as a heat flux boundary with a constant value of 4.32 kJ/d m^2, which represents heat flow from the earths core (Blackwell and Richards, 2004).

The mesh sizes were finer in the upper layers of the model domains and increased in size at lower depths (Figure 16). This was done to minimize model runtimes as the lower depths due not fluctuate in temperature during the model runtime and does not need as many calculations to occur to produce accurate results. The timestep length was 0.5 days. The convergence criteria for a solution at each timestep a difference of less than 0.1 °C between iterations at two significant digits with a maximum of 500 iterations. For the 2D models the mesh was generated automatically as an unstructured mesh of quads and triangles by the TEMP/W software. The automatic meshing ensures compatibility across different regions in the model domain (GEO-SLOPE, 2014). Mesh structures for the 2D models are shown in Appendix B - 2D Model Mesh Structure.

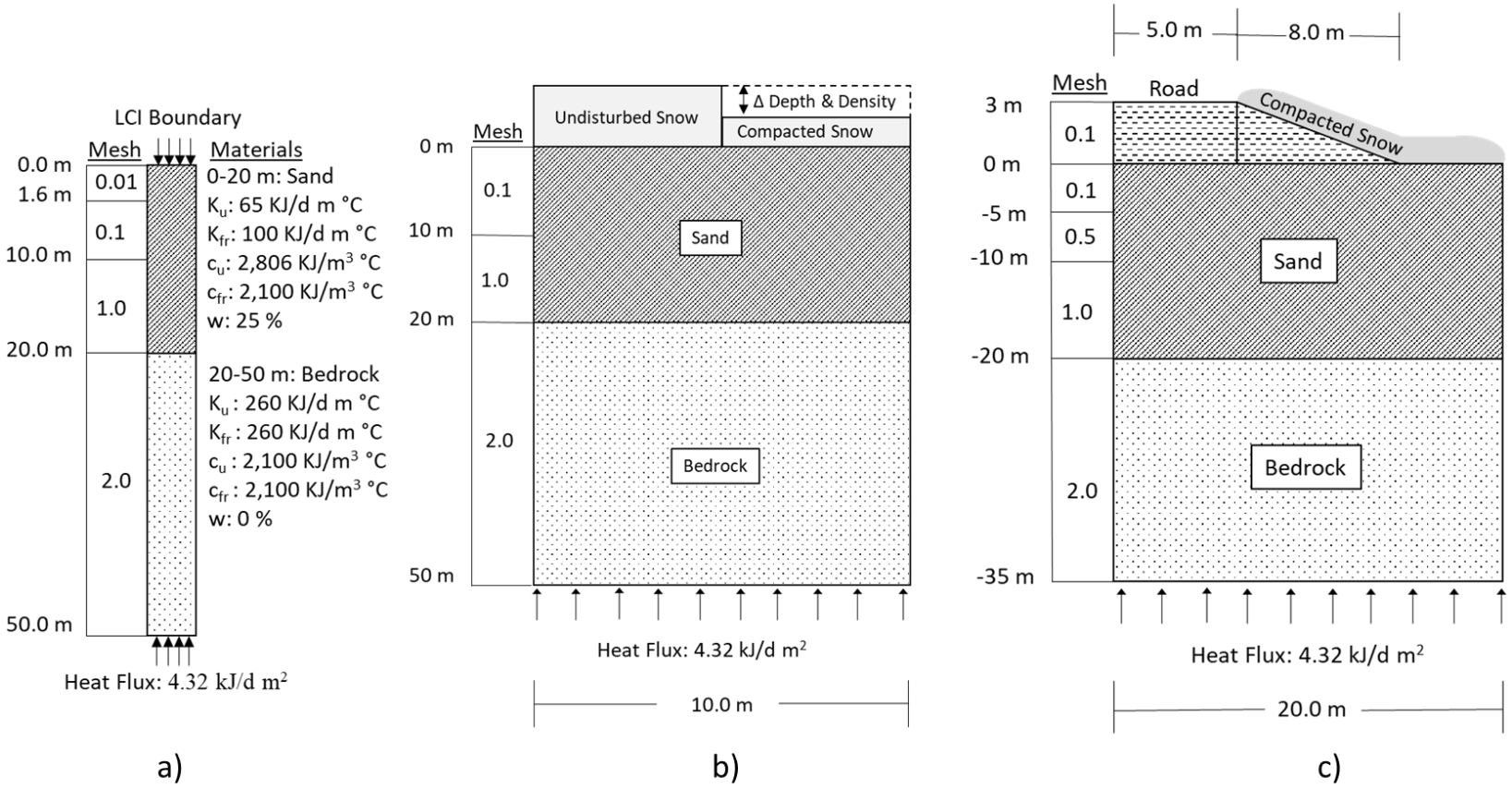

Figure 16: a) Model profile for the 1D ITH site, b) Model profile for the ITH site in 2D. The left 5 m of the model is composed of undisturbed snow where the right side of the model is either undisturbed snow or compacted snow, c) Model profile of ITH site with a road and embankment.

The model's initial ground temperatures were established through a spin-up analysis (Ross, et al., 2021). In the spin-up analysis, the top boundary condition was weather data at Inuvik Airport from Environment Canada between September 1st, 2003, and August 31st, 2004. This was chosen because some of the model scenarios, which are presented below, modelled Inuvik snow depth data from 2003-21. All model scenarios were decided to start from the same initial ground temperatures. The initial ground temperature throughout the spin-up model was set to the MAGT, -6.6 °C, as determined from the recorded thermistor data. The model was set-up to run for 500 years repeating the weather data from the site over the 500 years. The ground temperature profile was deemed to reach equilibrium when the ground temperatures after each cycle were less than 0.01 °C.

Table 2: Material properties for embankment model.

Material	Unfrozen thermal conductivity (KJ/d m °C)	Frozen thermal conductivity (KJ/d m °C)	Unfrozen volumetric heat capacity (KJ/m^3 °C)	Frozen heat capacity (KJ/m^3 °C)	Water Content (%)
Backfill	204	157	2,326	1,853	23
Clayey Sand	65	100	2,806	1,883	25
Bedrock	260	260	2,100	2,100	0

3.2.2 Snow and climate data for the model scenarios

Multiple snow scenarios were developed for this investigation. The first set of snow scenarios were scenarios of high, low, and average cumulative snow covers, and the second set of snow cover scenarios included different snow compaction conditions.

The cumulative snow cover scenarios were based off historical data from the Inuvik climate monitoring station. Figure 17a shows the daily snow depth obtained from the Inuvik climate monitoring station from 2003-2021. As seen in Figure 17a, the region can experience a wide rage of snow depths in a given year with some years having recorded snow depths over 70 cm and other years where there was 30 cm of snow. Furthermore, there is a large range of dates for the first snowfall and final snow melt across the two decades. From 2003-2021 the day of first snow fall ranges from September 9th to October 9th and the first day snow free ranges from April 30th to May 29th.

From this large range of snow conditions, three representative snow cover scenarios were established and plotted in Figure 17b. The minimum snow year was taken from the 2019-2020 depths recorded at ITH snow compaction site (plotted in Figure 17). The maximum snow cover year was taken from September 1st, 2005, to August 31st, 2006, and came for the ECCC Inuvik climate monitoring station. The average snow cover scenario was not a specific year, but rather was built by averaging the daily snow from the data set. It should be noted that the average year calculations did not include the field data as it was not collected on a daily basis. The three scenarios are highlighted in Figure 17a and shown accompanied with the compacted snow scenarios in Figure 17b.

Air and wind speed data for the minimum and maximum snow cover scenarios were taken from the ECCC Inuvik station, from the corresponding years. The air temperature and wind speed data for the average scenario were calculated by averaging the daily recordings at the ECCC Inuvik station between 2003 – 2021.

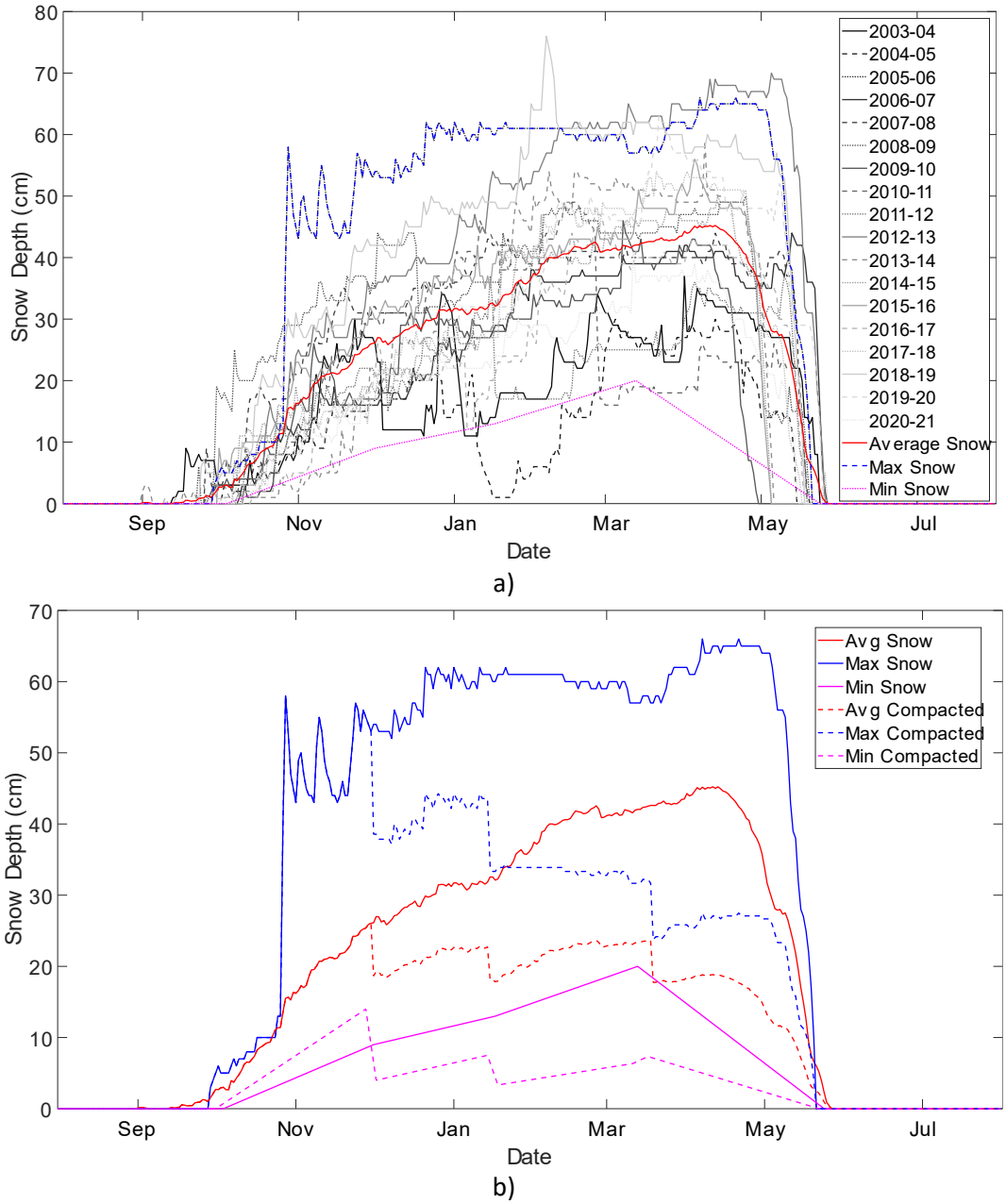

Figure 17: a) Yearly snow depth measurements obtained from the Inuvik climate monitoring station (2003-2021) showing the maximum, avg., and minimum snow depths in relation to the historical data. b) Snow depth measurements showing uncompacted and compacted maximum, avg., and minimum snow depths used in the model scenarios.

3.2.1 Modelling Snow Compaction

In the field, snow compaction reduces the thickness of the snow and increases the density. The numerical modelling software in this study, TEMP/W, uses snow depth and snow density (by way of thermal conductivity) to calculate a single thermal resistivity value for the land-climate interaction boundary. The equation used to calculate the thermal resistivity value is as follows:

$$R = \frac{\Delta H}{\delta} \quad [9]$$

Where ΔH is the snow depth and δ is thermal conductivity at a given time. TEMP/W requires the input of a single thermal conductivity value, which was 10 kJ/d/m/ °C based off the ITH field data. To apply snow compaction in the model, the daily snow recordings were multiplied by a modified thermal conductivity value (representing snow compaction), then divided by 10 kJ/d/m/ °C. This produces an equivalent R-value as the combined reduction in height and increase in density. Based on the field data, snow compaction was designated to occur on December 1st, January 15th, and March 19th. To represent the combined effects, snow height was modified to increase thermal conductivity by 2 kJ/d/m/ °C. Thus, in addition to the snow height reduction, the first compaction increases the thermal conductivity to 12 kJ/d/m/ °C, the second to 14 kJ/d/m/ °C, and the third to 16 kJ/d/m/ °C.

3.3 Model Results & Discussion

Lines of investigation for the models are divided into 1D and 2D models. There were also two 2D models, ones which investigated lateral heat flow from a compacted zone to non-compacted zone. And the second which was a 2D model including a road embankment. Table 3 summarizes the different snow scenarios and the models of which they were applied to:

1. 1D models
    a. Effect of repeating same average, minimum, or maximum snow cover for 20 years.
    b. Evaluate ground thermal memory with four different annual frequencies applied to the average, minimum, and maximum snow.
    c. Evaluate optimal frequency and timing for snow compaction.
2. 2D models
    a. Impact of snow compaction on lateral heat flow
    b. Impact of snow compaction on embankment

Table 3: Snow scenarios applied to the three model domains.

	Model Domains		
Snow Scenarios Analysis	1D	2D	2D w/ Embankment
Control (no compaction) - Avg/Max/Min	x	x	x
Compacted - Avg/Max/Min	x	x	x
Annual Freq - Avg/Max/Min	x		
Seasonal Freq. – Control	x	x	x
Seasonal Freq. - 3x Compaction (Dec, January, & March)	x	x	x
Seasonal Freq. - 2x Compaction (December & January)	x	x	x
Seasonal Freq. - 2x Compaction (December & March)	x	x	x
Seasonal Freq. - 2x Compaction (January & March)	x	x	x
Seasonal Freq. - 1x Compaction (December)	x	x	x
Seasonal Freq. - 1x Compaction (January)	x	x	x
Seasonal Freq. - 1x Compaction (March)	x	x	x

3.3.1 1D Models - Effect of control and compacted snow cover repeated for 20 years

To provide a baseline for future models, the first analysis investigated the impact of maximum, average, and minimum snow cover for both control and compacted cases when repeated for 20 years. Six 1D models were completed in this analysis, where the only difference was the snow cover function plotted in Figure 17b (Compacted snow scenarios are presented in Appendix C - Compacted Snow Data). Each of these six snow scenarios is repeated for 20 years.

Control and compacted MAGT at 5 m depth (approximate ZAA) for the average, minimum, and maximum snow is shown in Figure 18. Evident in Figure 18 is that after 20 years a difference of 5 °C has developed between the snow cover depth scenarios. In contrast, the variability between each set of compacted snow vs control is a maximum of -0.82 °C. Both MAGT values for maximum and average snow depths increase from the initial MAGT -3.80 °C. This is driven by the specificity of the snow depth scenario applied which had no interspersed years with low snow fall. For the maximum snow depth, the final MAGT for the control scenario +0.09 °C and the compacted scenario is -0.09 °C (-0.18 °C difference highlighted on Figure 18). While for average snow depth the final MAGT for the control scenario is -0.52 °C whereas the final MAGT for the compacted snow depth is -0.77 °C (-0.25 °C difference). The ground temperature under these snow conditions increases and compaction of the snow cover has little relative effect to mitigate the insulation from significant snow cover on ground thermal regime. For the minimum snow depth, the ground the final MAGT for the control and compacted scenario are -3.50 °C and -4.30 °C respectively. The minimum snow depth scenario shows the smallest increase from the initial MAGT of approximately -4.70 °C. These models illustrate extreme cases for repeated snow cover situations.

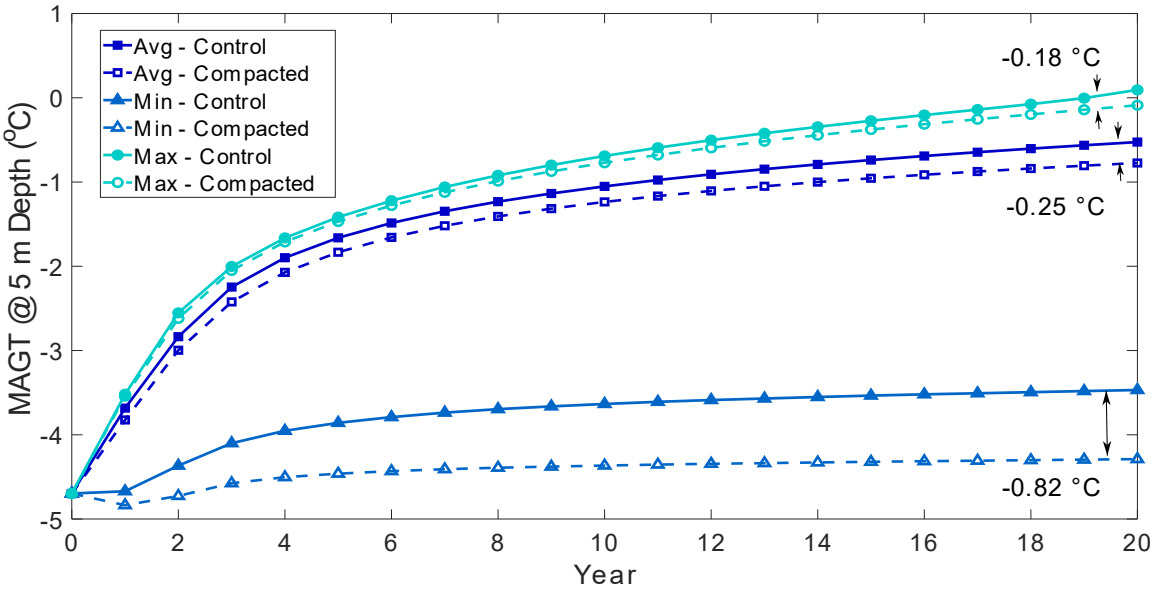

Figure 18: MAGT at 5 m depth each year for the control and compacted snow depth scenarios with a minimum snow depth year, a maximum snow depth year, and an average snow depth year.

The same models are compared in terms of active layer depth for the twenty years of repeated snow conditions and plotted in Figure 19. All six models start at a common active layer depth of -1.20 m and increase linearly over time. The largest difference in active layer depth between the control and compacted scenarios is for the average snow cover, with thaw depths of -1.90 m and -3.20 m (1.30 m difference) below ground surface respectively. For the maximum snow cover scenario, both the control and compacted snow conditions have deeper thaw depths of -5.10 m and -4.50 m respectively. These results show that while manipulating a heavy snow fall reduces the thaw depth, the overall snow depth in the maximum scenario is sufficiently large that it still leads to an increase in thaw depth over the 20 year period. For the minimum snow fall scenario, the control and compacted snow conditions have thaw depths of -1.40 m and -1.36 m respectively. These values are stable throughout the model runtime and only slightly increase from the initial thaw depth of -1.22 m.

The average snow cover year has the largest effect on reducing the maximum thaw depth. It saw a 1.30 m difference between the control and compacted snow scenarios, as opposed to the 0.04 m difference for the minimum snow fall year and the 0.60 m difference for the maximum snow fall year. In the minimum snow cover scenario, the undisturbed snow depth has minimal insulation to begin with, such that compacting the snow to reduce its insulative properties has little effect. At the other extreme, the maximum snow cover scenario has such a large insulative effect on ground heat loss. Therefore, while compacting the snow to reduce its insulative properties has some effect, the insulation is still significant enough that there is still a notable increase in thaw depth from the initial conditions. Comparatively, compacting the average snow cover scenario changes the insulative properties sufficiently from the undisturbed snow depth that a large difference in thaw depths occurs.

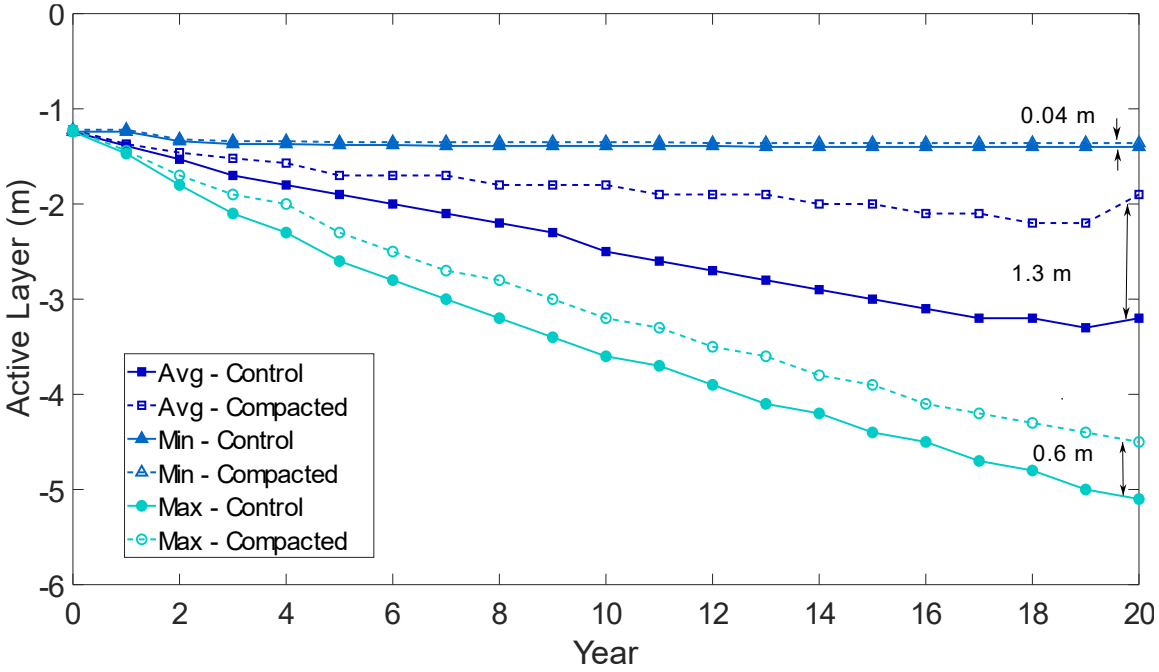

Figure 19: Active layer each year for the control and compaction snow depth scenarios with a minimum snow depth year, a maximum snow depth year, and a average snow depth year.

3.3.2 1D Models - Snow compaction annual frequency

The next step was to investigate the impact varying annual snow compaction cycles had on the active layer depth. This was done by modelling scenarios where snow compaction is applied for 1 year, 2 years, 3 years, or 4 years in a row before a year with no snow compaction. The active layer depths of these 4 scenarios, as well as the control and compacted models are plotted in Figure 20. Under the first scenario (Figure 20a) of 1 year on / 1 year off, the final thaw depth is 0.50 m less than the control and 0.80 m more than compacting every year. This indicates that there is some hold over of ground conditions from the compacted year where the thermal regime does not immediately rebound back to the same thermal conditions as the control scenario. However as seen Figure 20b-d the thermal conditions of the ground have a greater thermal memory when frequency compaction is increased. With greater frequency the active layer depth approaches the control scenario with the 4 years on / 1 year off essentially being equivalent.

Figure 21 presents the active layer depth results for the different annual snow compactions for the maximum snow fall scenario. The final depth of the active layer after 20 years for the control is -5.10 m. Similar to the average snow cover scenario results, the thermal conditions of the ground respond better when snow compaction is applied in consecutive years. However, what differs significantly is the overall difference between the maximum snow depth vs the average snow depth (shown in Figure 20). For the maximum snow depth and a 4 on / 1 off scenario, the thaw depth is

only 0.6 m shallower than the control, reaching a thaw depth of -4.50 m. This is a large increase from the initial -1.44 m active layer depth at the start of the model. Under these snow depths,

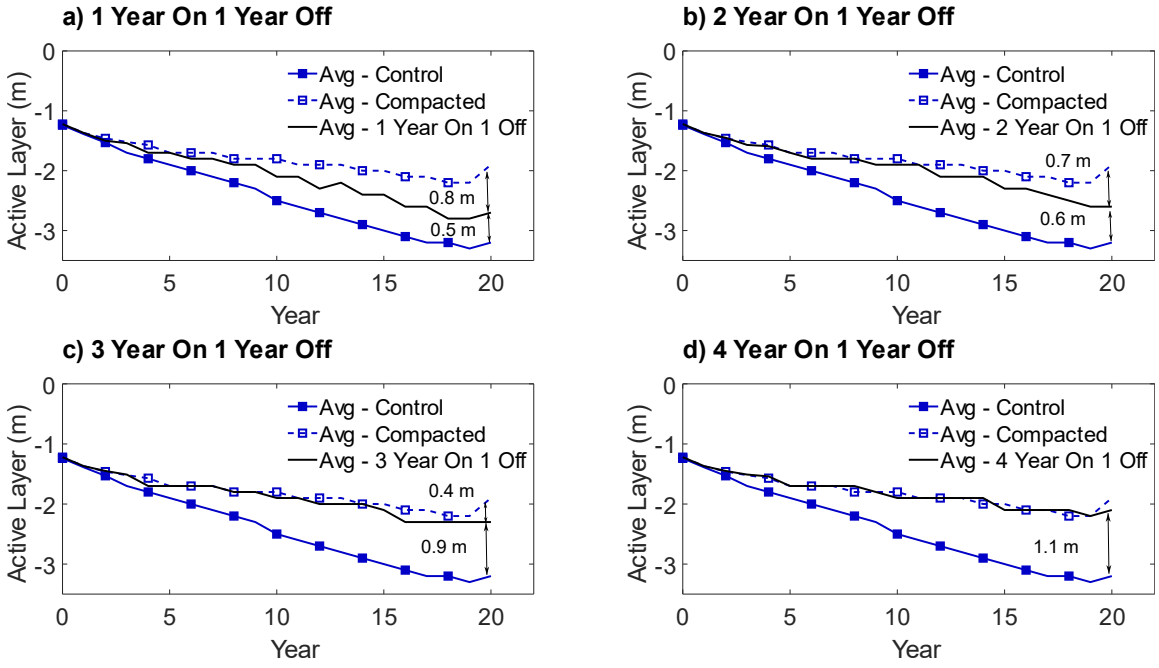

Figure 20: Active layer for average snow depth where compaction occurs a) 1year, b) 2 years, c) 3 years, & d) 4 years in row before a year occur where no snow compaction occurs. This cycle repeats for 20 years.

compaction provides limited improvement, as the snow on the ground is sufficiently deep that when compacted it still leaves a significant insulative layer. This degradation of permafrost puts overlying infrastructure, dependent on a stable active layer depths for its stability at an increased risk.

The active layer depths for the minimum snow cover scenario are shown in Figure 22, where the final depth of the active layer is -1.40 m for the control scenario. The 1, 2, 3, and 4 years in row compaction scenarios have final active layer depths of -1.37 m, -1.37 m, -1.36 m, and -1.36 m. Overall, there are no significant differences in active layer depth between the frequency scenarios. In this case, minimum snow cover depth is already providing very little insulation between the air and the ground that compacting the snow negligibly improves the ground thermal regime.

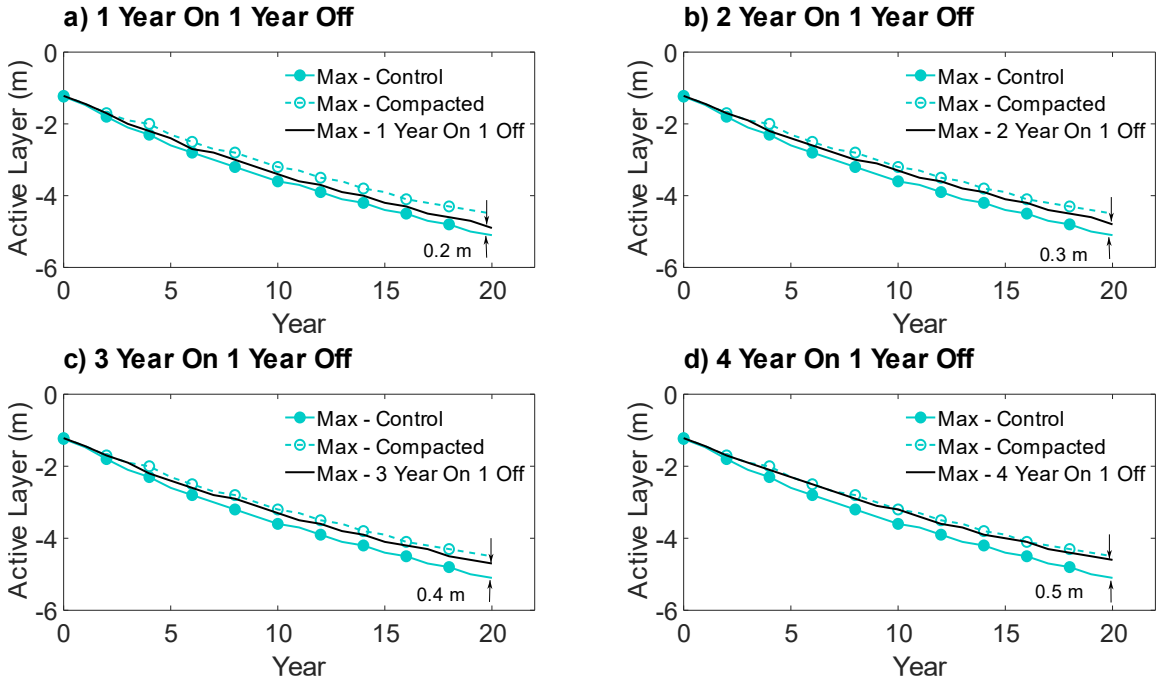

Figure 21: Active layer for maximum snow depth where compaction occurs a) 1year, b) 2 years, c) 3 years, & d) 4 years in row before a year occur where no snow compaction occurs. This cycle repeats for 20 years.

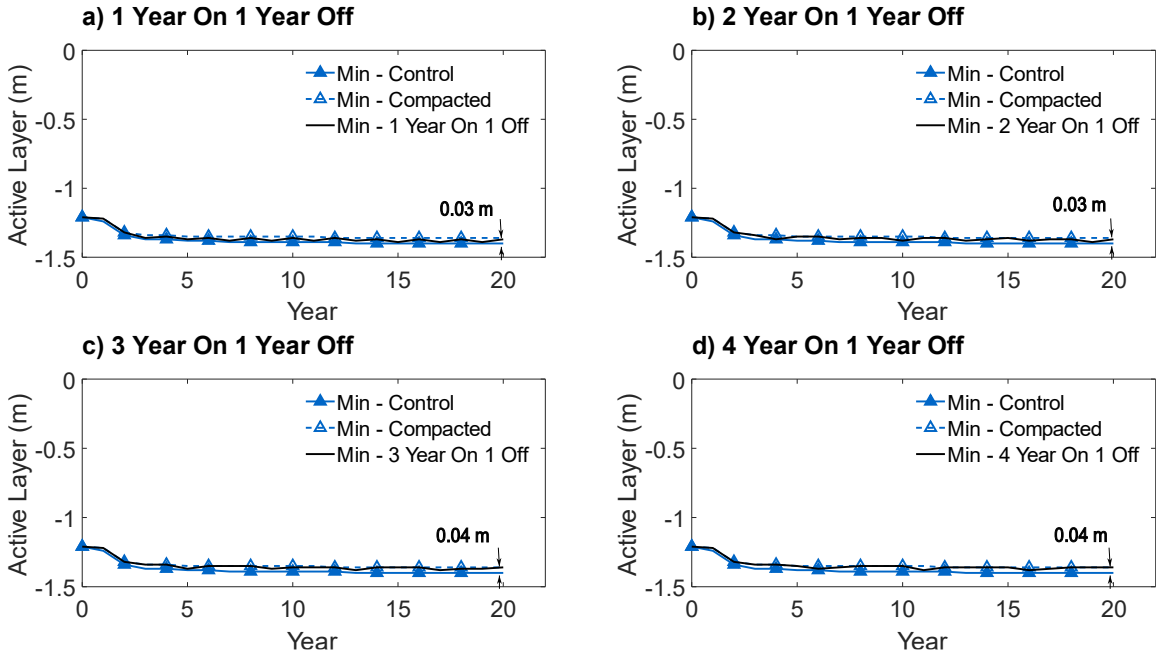

Figure 22: Active layer for minimum snow depth where compaction occurs a) 1year, b) 2 years, c) 3 years, & d) 4 years in row before a year occur where no snow compaction occurs. This cycle repeats for 20 years.

3.3.3 Snow compaction annual frequency discussion

Overall the annual snow compaction frequency has cumulative effects over the 20-year models, however, the greatest impact of snow compaction occurs in the average snow cover scenarios. The MAGT at 5 m for the 1D model for the maximum and minimum snow scenarios showed limited difference between the control and compacted snow depths. This trend was similar for the active layer depth analysis for the minimum and maximum snow depth scenarios. In comparison, there is a significant change in the active layer depth and MAGT between the control and compacted snow depths for the average snow scenario. It is apparent that there exists a range between minimum and maximum snow depths where snow compaction will result in significant cumulative effects on the ground thermal regime. This indicates that the effect of compaction on the insulative properties on snow does not follow a linear relationship, otherwise the compaction at the high and low snow scenarios would produce to change in temperature similar to the average snow scenario. This is further seen when modelling scenarios that examined annual snow compaction frequency. Once snow compaction occurs at least three or four years in a row before a year is skipped, the modeled active layer depths approach the 'every year' scenario.

3.3.4 1D Models – Snow compaction timing and frequency

The next set of scenarios investigated the impact of varying snow compaction timing and frequency within the winter season. For this analysis, models were run for 18 years, using climate and snow cover data from the ECCC Inuvik climate monitoring station (from September 1st, 2003, to August 31st, 2021). In the field, snow compaction occurred three times throughout the winter, in early December, mid-January, and mid-March (Wilson, 2021), which provides the calibration data. Using this as a framework, compaction scenarios were created where snow compaction occurred either one, two, or three times a season (using the dates December 1st, January 15th, and March 19th) in a variety of combinations. There was also a control model where no compaction occurred. A complete list of scenarios is shown in Table 3. Model scenarios included:

1. A control scenario with no snow compaction
2. 3x snow compaction in December, January, and March
3. 2x snow compaction in:
    a. December and January
    b. December and March
    c. January and March
4. 1x snow compaction in:
    a. December
    b. January
    c. March

Figure 23 shows the relative impact of compaction frequency and timing of all the model scenarios by plotting change in MAGT at a depth of 5 m versus year. The maximum difference between the control and any one compaction scenario year is less than -0.45 °C. In all the scenarios, the MAGT fluctuates depending on the weather conditions for each specific year. Looking at the final year, the scenario with the largest difference in MAGT from the control is the 3x per year compaction with a difference of -0.23 °C (Figure 23a) followed closely by the 2x compaction scenario of December+January with a- 0.21 °C difference (Figure 23b). These results show that the late season

compaction is not a significant contributor to improve ground heat loss. Comparatively the other two 2x compaction scenarios (Figure 23b) have further reduced effect on MAGT of -0.14 °C for December+March and -0.07 °C for January+March. The final MAGT for the 1x compaction scenarios (Figure 23c) are -0.12 °C for December, -0.06 °C for January, and 0.03 °C for March. The 1x compaction in December improves ground conditions more than the 2x compaction for January+March, indicating the importance of snow compaction earlier in the winter as opposed to mid- and late-winter. In fact, based on the 1x compaction of March, the late season snow compaction is shown to be detrimental to heat loss. The 1x March compaction has a positive change slightly above the control MAGT indicating the ground becomes warmer. This difference is 0.03 °C so not overly significant, but still shows the inefficacy of late winter snow compaction. By compacting in the late winter, insulation is reduced when the air starts to become warmer than the ground, leading to heat flowing from the air to the ground when less insulation exists between the two, which will result in a warmer ground. In contrast, compacting in December leads to reducing the insulation between the air and ground when the air is colder than the ground leading to an improved heat flow from the ground to the air.

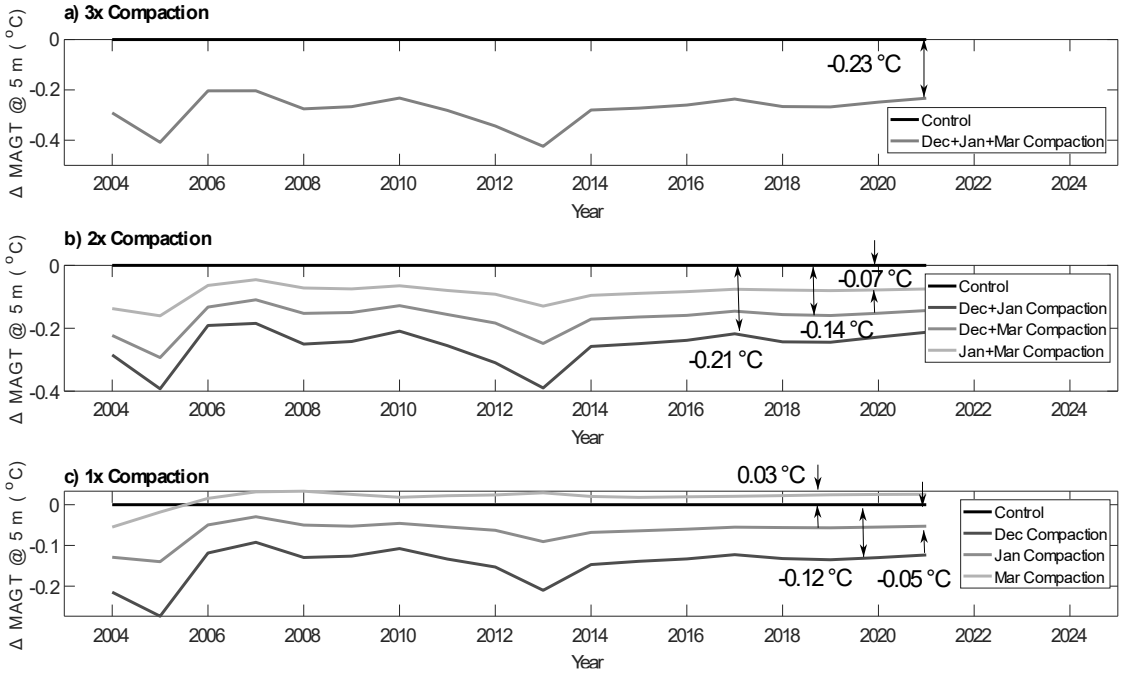

Figure 23: Change in MAGT at 5 m depth between undisturbed Inuvik snow from 2003-21 and compacted snow where compaction occurs a) 3x per winter, b) 2x per winter, c) 1x per winter.

Figure 24 shows the active layer depth per year of the different compaction scenarios from the real-world weather and snow cover data (Inuvik 2003-2021). Overall, all the thaw depths have a downward trend starting from -1.40 m thaw over the 18 modeled years. The control scenario has a final active layer depth of -1.70 m, the 3x scenario (December+January+March) has a shallower final active layer of -1.54 m, the 2x scenarios of December+January, December+March, and January+March have a range of final active layers between -1.55 m and -1.70 m. The 1x compaction scenario has final active layer depths of -1.60 m for December, -1.70 m for January, and -1.80 m for March compaction. In scenarios with December compaction, the overall increase

in thaw depth from the original thaw depth is minimized. The greatest impact on reducing active layer depth are scenarios with December+January+March and December+January compaction being essentially equivalent. This again shows the importance of early winter season snow compaction to reduce insulation between the air and ground surface. The January+March and the January compaction have the same final active layer depth as the control, showing no long-term improvement. Similar to the MAGT results, the March compaction provides a worst outcome than the control with an active layer depth that is 0.1 m deeper. This confirms previous observations that indicate late season snow compaction is detrimental to heat loss in spring.

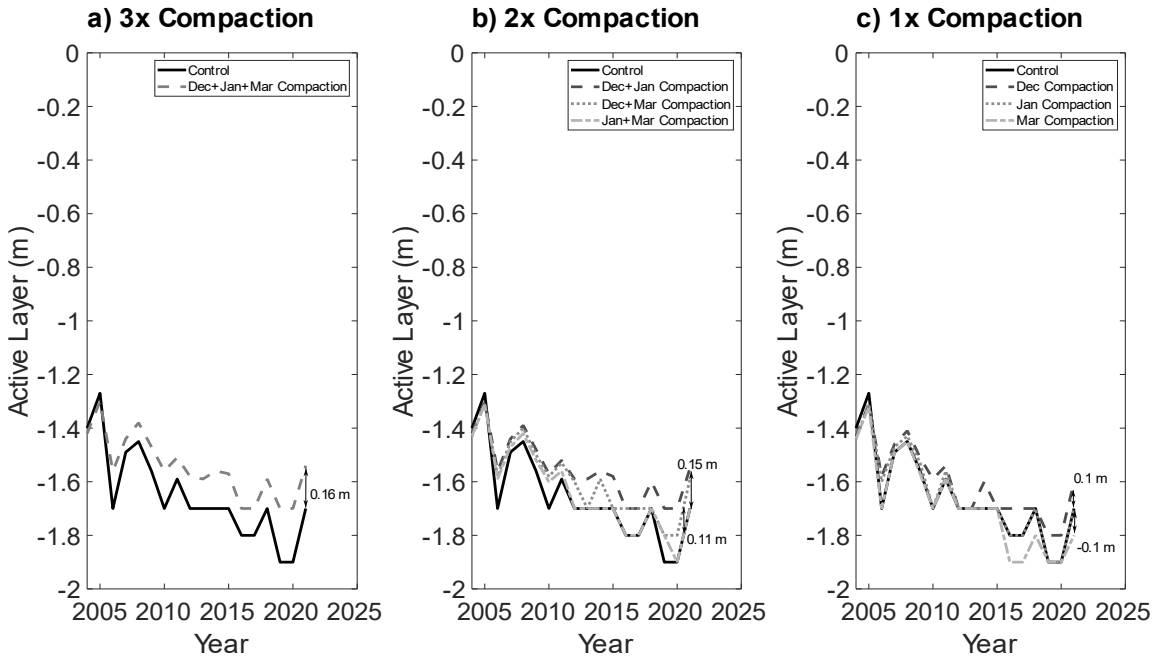

Figure 24: Thaw depth of ground under undisturbed Inuvik snow from 2003-21 and compacted snow where compaction occurs a) 3x per winter, b) 2x per winter, c) 1x per winter.

3.3.5 Snow compaction timing and frequency discussion

For the snow scenarios looking at snow compaction frequency and timing, using actual climate and snow data, there was not a significant change in the MAGT at 5 m depth between the uncompacted and compacted snow scenarios. The change in active layer depth is more significant with scenarios where December compaction occurs, having a shallower active layer depth by over 0.16 m than the control. With the variability of the 2003-21 Inuvik snow data, high snow years can undo thermal changes from compaction from other years of less snow on the ground. When modeling just maximum snow depth repeated for 20-years, compaction did not significant change the thermal profile of the ground when compared to the control as compacted high snow still has a high insulative effect. In a real-world application of snow compaction for years where there is a large amount of snow on the ground it may be better to engage in snow removal than compaction in order to remove the high insulation. It is unlikely that this would be able to be done over large areas, so specific areas would need to be selected that would most require permafrost thaw mitigation.

3.3.6 2D Models - Impact from snow compaction on lateral heat flow on 10-year repeat models

At the surface there is a clear boundary between compacted and uncompacted snow, however, subsurface lateral heat flow effects may be occurring. This section investigates subsurface lateral heat flow below this boundary and the resulting impact on the thaw depth. The two-dimensional models used in this study (Figure 16b) had 3 snow cover scenarios (minimum, average and maximum), which were repeated for a period of 10 years. The models divided the domain in half, with uncompacted snow on the left 5 m and compacted snow on the right 5 m (Figure 16b). 0 °C contour line is plotted for each snow scenario for months where ground thaw occurs in the tenth and final year starting in September.

The impact of subsurface lateral heat flow below the border of compacted and uncompacted snow is illustrated for the 10-year repeat models in Figure 25, which shows temperature contours in September as well as a graph plotting the depth of the 0 °C contour line for the three snow scenarios. The graphs use the 0 °C contour lines (rather than active layer depth) because the contour data is from months before the max thaw depth is reached and includes data from when the ground refreezes in the winter thus having two 0 °C contour lines, the original thaw depth and the freezing front.

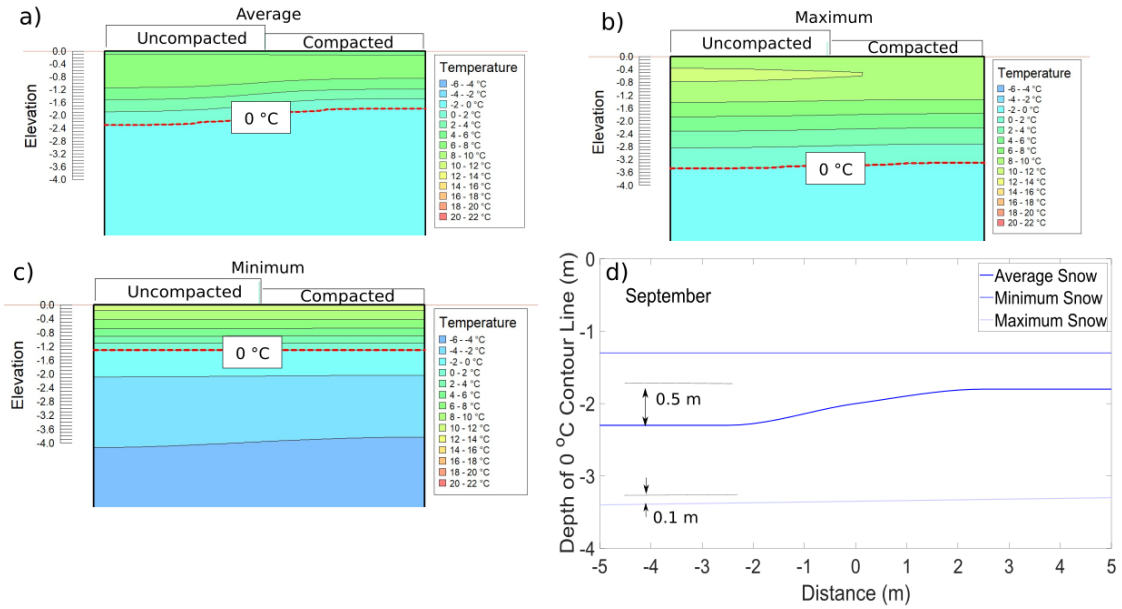

Figure 25: September temperature contours after 10 years for the three snow scenarios a) average, b) maximum c) minimum, and d) depth of the 0 °C contour line. The red dotted line in each model output indicates the 0 °C contour line.

The average snow scenario (Figure 25a) shows a 0.5 m difference in thaw depth between the uncompacted and compacted side of the domain. At the centre line where the boundary of the compacted and uncompacted snow the thaw depth is -2.00 m and increases to a maximum thaw depth of -2.30 m at 2.30 m from the boundary into the uncompacted side. From the centre line towards the compacted side the thaw depth is reduced to a depth of -1.8 m at 2.3 m away from the

snow boundary. For the maximum snow scenario (Figure 25b) there is maximum difference of 0.1 m between the uncompacted and compacted snow side. The thaw depth at the boundary of the compacted and uncompacted snow is -3.35 m and increases to -3.40 m under the uncompacted snow and decreases to -3.30 m under the compacted snow. For the minimum snow scenario (Figure 25c) there is no difference between the uncompacted and compacted snow side of the model with the thaw depth being a consistent -1. 30 m across the model domain.

Figure 26 and 27 shows the temperature contours and depth of the 0 °C contour line the final year of the model for months of October and November respectively. The overall trends are similar to those seen in September, where there is a difference in the compacted vs uncompacted sides, most predominantly in the average snow cover scenario. In November the active layer starts to refreeze, meaning there are two 0 °C contour lines for each snow scenario and with ground temperatures between the two lines being above 0 °C. For the average snow scenario (Figure 27a), the top 0 °C contour line representing the freezing front, which is at a depth of 0.40 m across the model domain. In November (Figure 27) there is a thaw down to -2.20 m at the centre line, which increases to -2.50 m at 2.50 m into the uncompacted snow side. From the centre towards the compacted snow side the thaw depth decreases to -1.80 m 4.50 m away from the centre line, indicating the 0 °C contour line is moving towards the surface, which is not the case in the uncompacted snow side when compared to the results from October. This shows that the ground with compacted snow begins to freeze earlier than the uncompacted snow side.

After November, the average and minimum snow scenario ground freezes through, with ground thawing not beginning again significantly until July. Shown in Figure 28d is the depth of the 0 °C contour line across the model domain. For the average snow scenario, the 0 °C contour line is at a depth of -1 m under the compacted snow from the centre line towards the uncompacted snow sides the 0 °C contour line increases in depth to -1.10 m, indicating a faster thaw rate as opposed to the side with compacted snow. For the minimum snow scenario there is no difference across the model domain with the 0 °C contour line being located at -0.90 m depth. For the maximum snow scenario, due to the deep snow depths applied to the model for 10 years the ground no longer fully freezes completely resulting in the 0 °C contour line existing much deeper than the other snow scenarios. Between the compacted and uncompacted snow side there is a difference of 0.3 m. The thaw depth at the boundary of the compacted and uncompacted snow is -3.10 m and increases to -3.20 m under the uncompacted snow and decreases to -2.90 m under the compacted snow. While the 0 °C contour line is already deep compared to the other snow scenarios, it is not as deep as it was before the winter. The 0 °C contour line rises slightly indicating some freezing but does not reach the freezing front from the top of the model during the winter, as opposed to the other snow scenarios of average and minimum snow.

Figure 29 shows the depth of the 0 °C contour line for the three snow scenarios during August at the end of the model runtime. The average snow scenario has a difference 0.50 m between the compacted and uncompacted snow sides. At the centre of the model the thaw depth is -1.60 m and increases down to -1.90 m into the uncompacted snow side and decreases to -1.4 m into the compacted snow side.

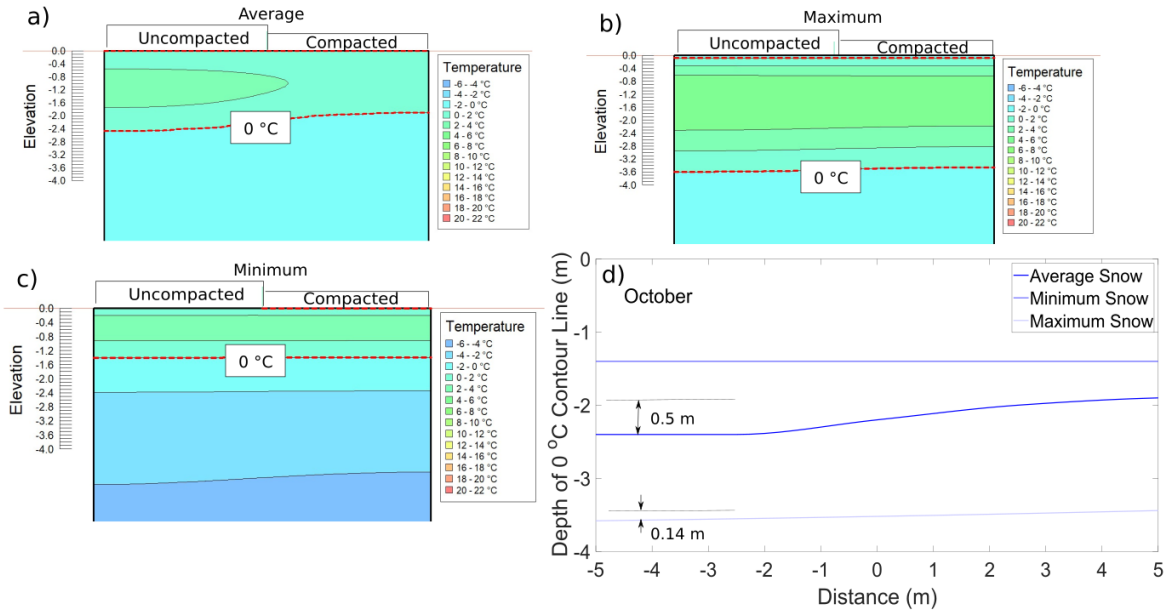

Figure 26: October temperature contours after 10 years for the three snow scenarios a) average, b) maximum c) minimum, and d) depth of the 0 °C contour line. The red dotted line in each model output indicates the 0 °C contour line.

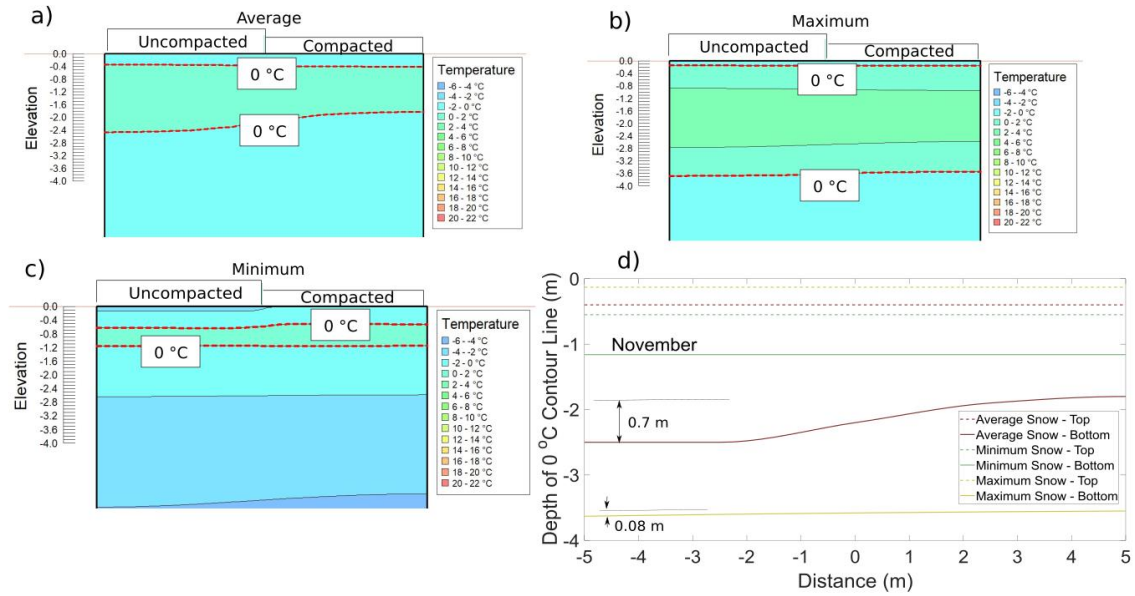

Figure 27: November temperature contours for the three snow scenarios: a) average, b) maximum, c) minimum, and d) depth of the 0 °C contour line. The active layer begins to refreeze in November, thus there are two 0 °C contour lines for each snow scenario. The red dotted line in each model output indicates the 0 °C contour line.

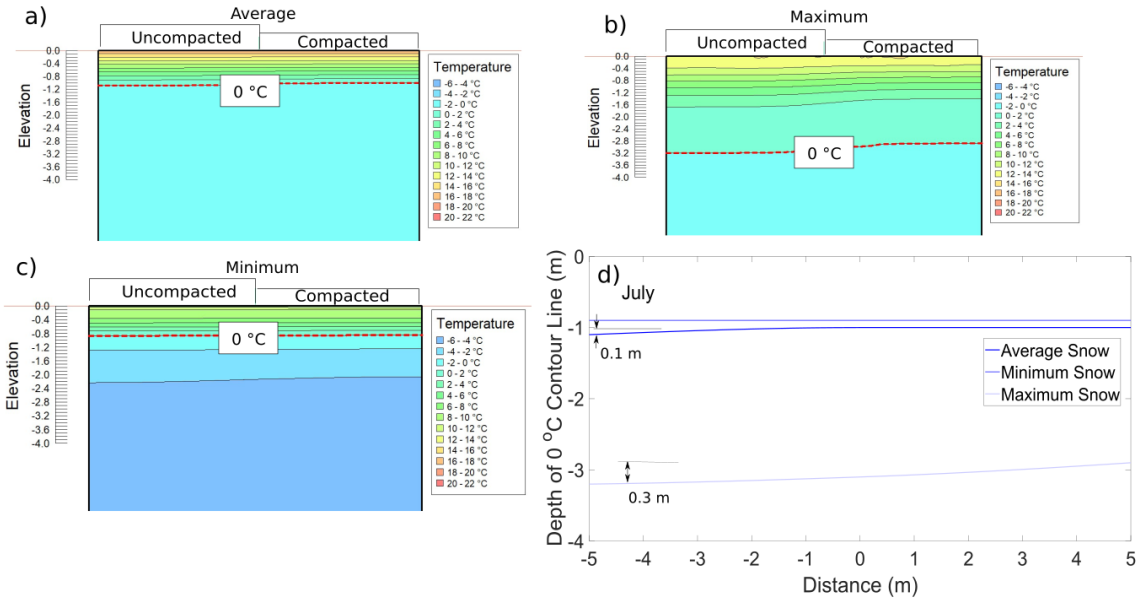

Figure 28: July temperature contours for the three snow scenarios a) average, b) maximum, c) minimum and d) the depth of the 0 °C contour line. The red dotted line in each model output indicates the 0 °C contour line.

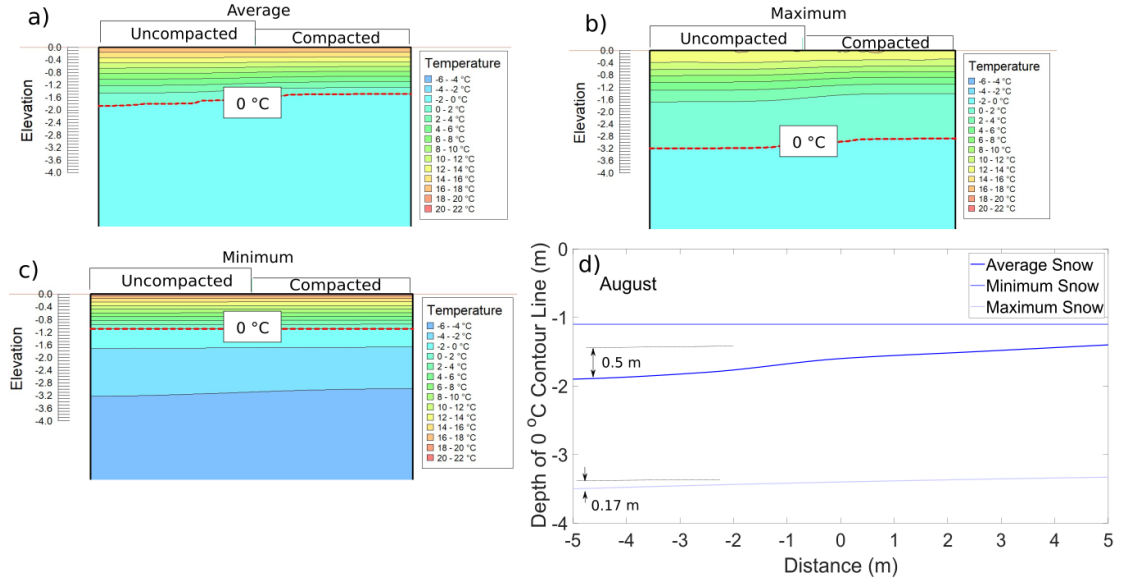

Figure 29: Temperature contours in August for the three snow scenarios: a) average, b) maximum, c) minimum, and d) depth of the 0 °C contour line. The red dotted line in each model output indicates the 0 °C contour line.

Such a difference indicates that the side with uncompacted snow thaws at a quicker rate than the ground under compacted snow for the 10 year model runtime. In the minimum snow scenario there is no difference across the model domain with the 0 °C contour line being located at -1.1 m depth,

which is a 0.20 m increase in depth from the previous month. The maximum snow scenario has a difference of 0.17 m between the compacted and uncompacted snow sides. At the boundary of the different snow at the model centre the thaw depth is -3.40 m, which increases to -3.50 m at the end of the uncompacted snow side and decreases to -3.33 m at the end of the compacted snow side.

The seasonal frequency snow scenarios (discussed in Section 3.3.4) were applied to the 2D model keeping 5 m of undisturbed snow on the left, and the right side having compacted snow. Figure 30 shows the ground surface temperatures at the beginning of each month in the final year of the model runtime at the edge of the right side of the 2D model with compacted snow depth. The snow compaction scenarios shown (December+January+March, December+January, & December) were the ones that most improved the thermal conditions, and the undisturbed snow scenario is shown as well. Differences between the scenarios occurs only in January to May with the largest difference from the normal scenario occurring in March. In March the ground surface temperatures are -16.40 °C for the December-January-March and December-January snow compaction, -14.80 °C for the December snow compaction, and -12.60 °C in the normal scenario. Graphs showing the temperatures across the model domain can be seen in Appendix D - 2D Model Temperature.

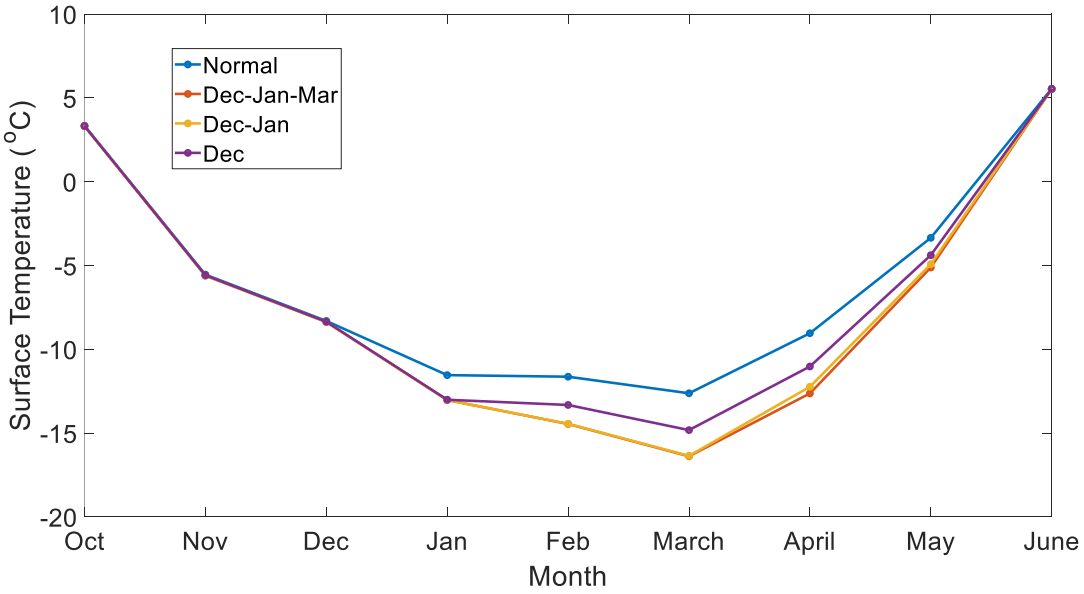

Figure 30: Ground surface temperature at the edge of the compacted area of from the 2D mode in the final year of the model runtime using Inuvik 2003-21 snow data. The model scenarios presented are normal and snow compaction occurring in December-January-March, December-January, and March.

3.3.7 Impact from snow compaction on lateral heat flow Discussion

The 2D modeling results show that the effects of snow compaction on adjacent ground through lateral heat flow extend laterally 2.3 m. This shows that over time in areas where snow compaction is applied changes in the thermal profile can occur. For example, if applying snow compaction to an embankment, the actual compaction may only need to be applied to the embankment itself and

the adjacent ground would experience benefits and reduce the thaw depth in the summer months. This could keep the area around the toe of the embankment stable and prevent lateral spreading. This only would be beneficial with average snow depths as minimum and maximum snow depths had very small thaw depth changes in ground under and adjacent to snow compaction. Shown in Figure 27, in November ground freezing occurs where in the maximum and minimum snow scenarios there is no difference between the ground under the uncompacted snow and the ground under the compacted snow. For the average snow scenario, there is a large difference of ~ 0.7 m in thaw depth at the bottom 0 °C contour line between the uncompacted and compacted snow sides. Based off the compacted average snow, the active layer freezes back earlier, which would stabilize the ground. After the winter when the ground begins to thaw and the active layer becomes present, the ground under compacted and uncompacted snow initially thaw at the same rate with similar thaw depths occurring at the same time for both sides of the model (Figure 28). Long term snow compaction does not appear to affect the initial thaw of the active layer at the near surface depths. However, once the thaw gets to a certain depth of approximately 1.5 m, the ground under uncompacted snow begins to thaw at a higher rate and reaches a lower depth overall than the compacted side. The long-term benefit for snow compaction, presents itself in later summer and fall when the active layer is significantly less deep and the ground freezes earlier and is less impactful in the spring.

3.3.8 2D Models - Snow compaction on embankments

A two-dimensional model was developed for studying the effect of snow compaction on a sloped embankment and its ability to improve the thermal conditions and subsequent stability of the road. The embankment was 3 m in height and 8 m wide, made from locally sourced fill material (Government of the Northwest Territories, 2013). Details of the model dimensions and soil property can be found in Figure 16c and Table 2. Similar to the lateral heat flow investigation, models were run that had 3 annual snow cover amounts as well as under different seasonal compaction scenarios.

The annual active layer depth results for the three snow cover scenarios are shown in Figure 31. The results were plotted for two locations, at the embankment toe (Figure 31a, b, c) and where the embankment meets the road (Figure 31d, f, g). At the toe of the embankment under the average snow cover, both the control and compacted scenarios increased the active layer depth each year, though at different rates. The control initially has an active layer depth of -1.50 m and ends with a thaw depth of -2.40 m at 10 years. In comparison, the compacted scenario has a thaw depth of -1.40 m and ends with a thaw depth of -1.80 m. For the minimum snow cover, there is negligible difference between the control and compacted active layer depths and neither change over the 10-year model runtime. For the maximum snow cover scenario there is a large increase from year 1 to year 10 for both the control and compacted scenarios. For the control scenario, the active layer depth goes from -1.60 m to -3.40 m. For the compacted, the active layer depth goes from -1.60 m to -3.20 m, producing 0.20 m difference from the control thaw depth. Overall, the average snow

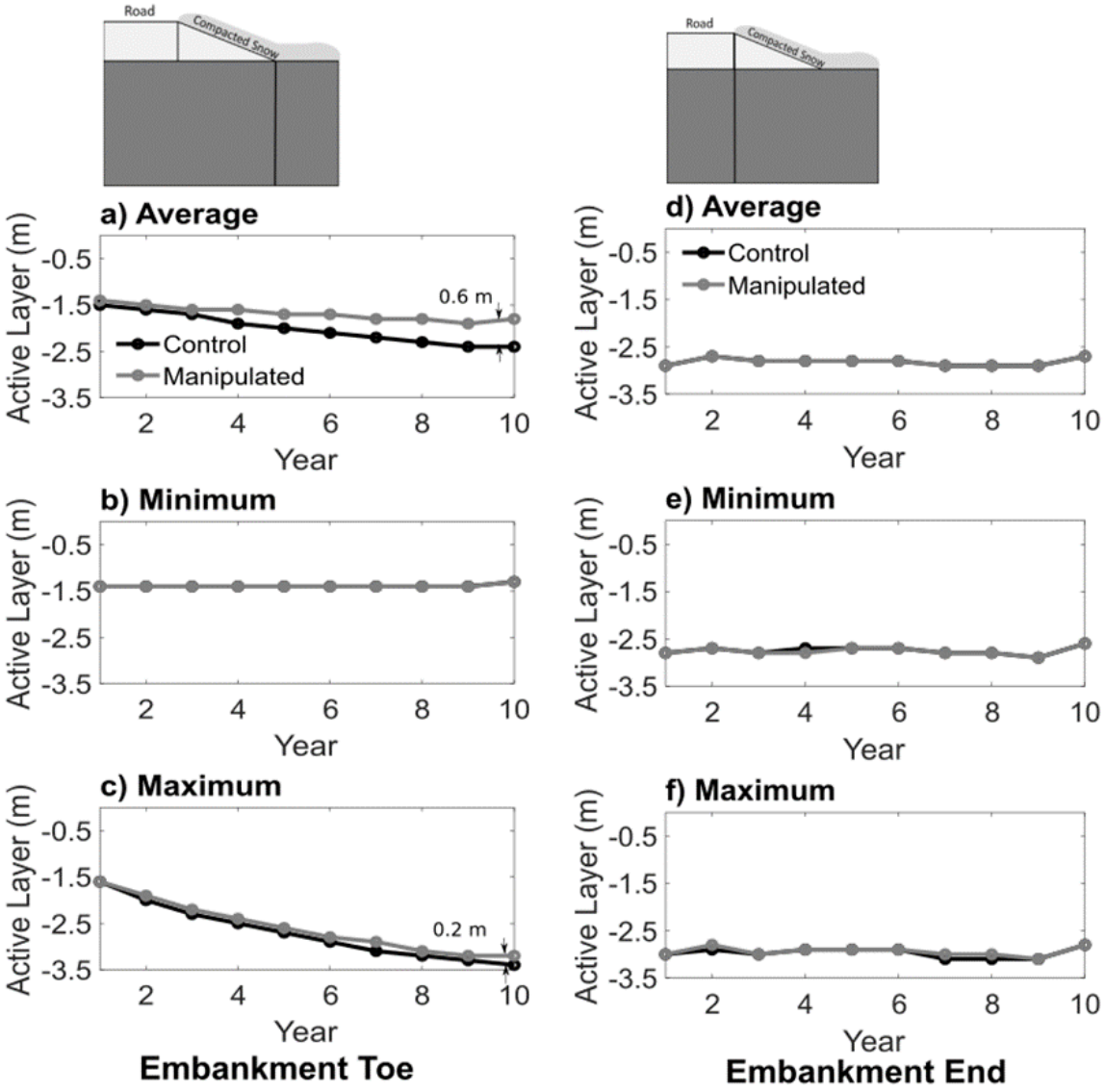

Figure 31: Yearly active layer depth at the toe and end of the embankment for snow scenarios with control and compacted snow depths of a) average snow depth, b) minimum snow depth, & c) maximum snow depth for the toe and d) average snow depth, e) minimum snow depth, & f) maximum snow depth for the end. Location of active layer measurements are shown in in the diagrams at the top graph.

cover scenario at the embankment toe has the largest response to snow compaction with a 0.6 m difference in final active layer depth between the control and compacted. These results are similar to what was found in the simplified 1D models.

Figure 31d-f plots the active layer depth at the end of the embankment for the average, minimum and maximum snow scenarios for both control and compacted snow. For all scenarios there is

negligible difference in active layer depth between control and compacted snow scenarios. At this position the snow depth along the embankment does not have a large effect on active layer depth, rather the main factor driving the active layer depth is the exposed road which allows for a large movement of heat out the road structure in the winter months. The effect on annual frequency of snow compaction on the active layer depth in the embankment can be seen in Appendix E - 2D Model w/ Embankment Within Season Frequency.

3.3.9 Snow compaction on embankments Discussion

The results from the 2D embankment model highlight that the greatest change in the thermal profile between the control and compaction snow depths occurred at the embankment toe. At the shoulder of the road there was negligible change in active layer depth between the control and compacted snow over the 10-year model runtime. In the model it was assumed that the road would be essentially cleared of snow, which would greatly affect the thermal profile at that part of the road structure. If time occurs where snow is not cleared from the road surface, or the snowpack on the road surface becomes significant then a thermal change might occur between the control and compacted snow along the shoulder. Otherwise, snow free ground will greatly affect adjacent ground like the embankment end and snow compaction will not be necessary to be applied next to the road surface.

3.4 Conclusion

Snow compaction is a mitigation technique against permafrost thaw currently being studied for its usefulness on preserving arctic infrastructure. Using numerical modeling it is possible to study snow compaction under varying conditions to ascertain its effectiveness in slowing or preventing permafrost thaw that would otherwise take years in a field study. Chapter 2 reported a calibrated ground temperature model of a site on the Inuvik-Tuktoyaktuk Highway. This chapter further examined snow compaction in 1D and 2D models under different snow compaction scenarios. The snow scenarios included snow compaction applied to historically low, high, and average snow depth and investigating the efficacy of time and frequency of when snow compaction occurs using 18 years of snow depth data (2003-21) from Inuvik.

The 1D models showed that snow compaction is most effective when applied to average snow depth in reducing annual active layer depth. The low and high snow depths were found to have either too low or too high insulation for snow compaction to change the insulation enough to result in different active layer depths. Additionally, snow compaction is most effective when applied multiple years in a row to maximize heat loss during the winter months. The investigation of the frequency and timing of snow compaction revealed that it is most effective to apply snow compaction early in the winter in December to maximize temporal effects with reduced insulative properties. Snow compaction in late winter in March was found to be counter effective to improving permafrost conditions. Generally, it was found that the more frequent snow compaction occurred, the better the permafrost conditions were.

The 2D models revealed that snow compaction during some winter months significantly lowers ground temperatures laterally from the snow compaction location. Temperature reductions of up to 1 °C were found 1 m away from the compacted-uncompacted snow border. Furthermore, snow

compaction was found to reduce the active layer depth under uncompacted snow up to 2 m away and was found to reduce the time the active layer was present by up to 37 to 45 days for average snow depth. The embankment model revealed that the active layer depth at the embankment toe was similar to the 1D results with the average thaw depth being improved while the high and low snow depths did not experience much change with snow compaction. The thermal ground condition of the embankment end was shown to not improve with snow compaction.

Overall, snow compaction could be an effective mitigation technique to reduce the thawing of permafrost under the ITH. Snow compaction was found to be most effective when applied when there was an amount of snow that is considered average by historical standards from Inuvik and when applied to the area around the embankment toe. This could help with preventing lateral spreading of the embankment and reduce repair costs. When snow depth for a given year is considered high from historical standards, snow compaction is not effective and other techniques should be applied to ground thermal profile from getting too warm.

Chapter 4
Conclusion

4.1 Summary

Northern infrastructure built on permafrost is increasingly under threat from rising temperatures attributed to climate change. Because infrastructure relies on permafrost for foundational support, any thaw that occurs risks creating structural issues leading to a lack of serviceability. For highways in the Canadian Arctic, isolated communities rely on them for reduced cost of living, and improved access to health care, education, and economic opportunities. To maintain their serviceability, mitigation techniques are being evaluated on northern highways that can slow or stop the thawing of permafrost. One such technique is snow manipulation, which compacts snow to reduce its depth and increases it density. These two consequences lower insulative properties and provide conditions for improved heat loss.

Investigating and quantifying this mitigation technique in the field require present challenges with respect to time and conditions. There is no guarantee what the depth of the snow will occur every year, and therefore field test conditions are bound to the annual snow fall that happens to occur in a given year. Using a numerical heat transfer model, the effect of snow manipulation on ground temperatures can be studied without the snow cover or time limitations of a field study. The research presented in this paper uses snow data collected at a snow manipulation testing site located along the Inuvik Tuktoyaktuk Highway to develop a ground temperature model to test the efficacy of snow manipulation under a variety of conditions and scenarios.

Chapter 2 of this thesis presents the model calibration to a site along the Inuvik to Tuktoyaktuk Highway and demonstrates how to develop a model with limited information about soil properties. Using snow depth and density measurements from two sites, one undisturbed and one compacted, a calibrated model was developed. Utilizing ground temperature records obtained from thermistor strings installed at the two sites, the model was developed by iterating soil properties so model temperature outputs reasonably matched record temperatures. Because of the two sites with two different snow covers it was possible to calibrate the site to two different snow conditions. The model results show that the temperatures agree with measured data from September 1st, 2019, to August 31st, 2020. Using the minimum, maximum, and average annual ground temperatures from the thermistor recordings to gauge accuracy, all control recordings were within 1 °C of the final model outputs, whereas compacted recordings had all but one recording within 1 °C. This shows the viability of using an iterative approach to the development of ground temperature models when information on soil properties is absent.

Using the calibrated soil properties of the ITH site, Chapter 3 presents the results of 1D and 2D models under different snow manipulation scenarios. The snow scenarios included snow manipulation applied to historically low, high, and average snow depth and an investigation into the efficacy of the time and frequency of when snow manipulation occurs using 18 years of snow depth data (2003-21) from Inuvik. In the 1D model and 2D model with embankment it was found that snow manipulation works best with a historically average snow depth and had little effect on when applied to maximum or minimum snow depths. Snow manipulation also works best when

applied multiple years in a row, as changes in ground temperatures will eventually revert to non-compacted conditions when snow is left undisturbed. When investigating lateral heat flow with the 2D model during winter months ground temperatures can be reduced up to 1°C approximately 1 m away from the area where snow manipulation occurred. Furthermore, changes in thaw depths can be seen up to 2 m into an area of uncompacted snow from and area with that has undergone snow compaction. The 2D model also revealed long term snow compaction can greatly reduce the time the active layer is present, with a 37-to-45-day reduction after 10 years of snow compaction. The investigation into the time at which snow manipulation is applied in a winter revealed that it is most effective to apply snow manipulation early in the winter in December for a single compaction occasion. Results were improved in the ground thermal conditions when further compaction times occurred in January and March. Only having snow compaction in late winter in March were found to produce worse ground thermal conditions than the control.

4.2 Study Limitations

It is important to note that for the different snow scenarios, only the minimum control and compacted snow data was from field data. For the average and maximum snow scenarios, the compacted snow was obtained by applying a factor to data taken from Inuvik snow records, that would change the snow depth at the same magnitude that occurred to the minimum snow data in the field. This was necessary because the two years of field data from the ITH site happened to be years of snow depth that was on the historically low range of snow depth for the area. The snow compaction study along the ITH is ongoing, so in the coming years different snow depths will occur that can be used to identify the true magnitude that average and high snow depths will change when subjected to snow compaction on site.

Furthermore, it was assumed that snow density was uniform throughout the snowpack. Snow can be heterogenous with density, especially between more compacted snow near the ground and freshly fallen snow near the top. The decision to keep a uniform density was done due to the limitations of the modeling software, which only allows for a single density value by way of thermal conductivity to be inputted.

Finally, limitations existed with the runtimes of the models, which require significant computational power to run. Runtimes for the models were selected on what could be completed in a reasonable period of time (e.g., within 24 hours). As such, long term effects of snow compaction on ground thermal conditions were not modelled past a 20 year time period. With either more time or greater computational power, greater runtimes could be conducted to project the effect of snow compaction further into the future than what was accomplished in this study.

4.3 Further Research

While the results of this research have improved the understanding on snow compaction as a mitigation technique for permafrost thaw, a number of additional questions arose which would further develop this mitigation technique. First, research should be conducted at other sites along the ITH and across other linear transportation infrastructure in the Arctic. This would provide results under different ground conditions and could determine how important soil type and initial thermal regime is on snow manipulation results. The snow manipulation study used as the basis for this research is being conducted at 5 other sites, leaving multiple different ground conditions

for research readily available. Additionally, future models could incorporate climate projections to evaluate the viability of snow manipulation in much longer terms under the expected rise in air temperatures.

Secondly, all the models used in the study used a constant geothermal flux, which represented the flow of heat from the earth's core towards the surface. Future modelling could apply a geothermal heat function, which would reduce the of the depth of the model that is required for the results to be accurate. Shorting the model by 10s of meters would greatly reduce the calculation time required for running models. This would allow for longer model runtime to further study the more long-term effects of snow compaction without having to deal with increasingly long runtimes, which otherwise limit the length of runtimes that can be reasonably done.

Based on the results from the 2D model it was shown that the ground under compacted and uncompacted snow initially thawed at the same time in the spring. The difference in active layer thaw depths do not appear between the two sides until later in the summer. Further work could be done to quantify the rate of thaw between the two sides of the model and to identify exactly when and the depth at which the difference between the two rates occurs. This could allow for predictions of the ground thermal conditions when snow is compacted to predict the maximum depth an active layer can be expected to reach year after year and for when the active layer will experience freeze back. This could help in knowing when conditions for northern roads with snow compaction will be expected to be more stable due to earlier freezing of the ground.

References

Andersland, O. B. & Ladanyi, B. (2004). *Frozen Ground Engineering 2nd Ed.*. Wiley & Sons, Hoboken.

Bell, T. and Brown, T. (2018). *From Science to policy in the Eastern Canadian Arctic: An Integrated Regional Impact Study (IRIS) of Climate Change and Modernization,* ArcticNet, Quebec City, QC, Canada.

Blackwell, D.D. and Richards, M. (2004). *Geothermal Map of North America, AAPG Map, scale 1:6,500,000, Product Code 423*.

Bowling, E., (2020). Great Slave MLA Katrina Nokleby calls for acceleration of Inuvik-Tuktoyaktuk Highway repairs, <https://www.nnsl.com/inuvikdrum/great-slave-mla-katrina-nokleby-calls-for-acceleration-of-inuvik-tuktoyaktuk-highway-repairs/>

Brown, R. J. (1973). *Permafrost in Canada: Its influence on Northern Devlopment.* University of Toronto Press, Toronto.

Côté, J. and Konrad, J.-M. (2005). "A generalized thermal conductivity model for soils and construction materials." *Canadian Geotechnical Journal*, 42(2), 443–458.

Dore, G., Niu, F. & Brooks, H. (2016). "Adaption Methods for Transportation Infrastructure Built on Degrading Permafrost". *Permafrost and Periglacial Processes*, 27, 352-364.

Ednie, M. and Smith, S.L. (2011). "Establishment of community-based permafrost monitoring sites and initial ground thermal data, Baffin region, Nunavut." *GEO2010*, Calgary, AB, Canada, 1205-1211.

Environment and Climate Change Canada. (2019). Changes in temperature. <https://www.canada.ca/en/environment-climate-change/services/climate-change/canadian-centre-climate-services/basics/trends-projections/changes-temperature.html> (Marchch.10, 2021).

Flynn, D. et al. (2016). "Forecasting Ground Temperatures under a Highway Embankment on Degrading Permafrost". *Journal of Cold Regions Engineering*, 3(4).

Fortier, R., LeBlanc, A.-M. & Yu, W. (2011). "Impacts of permafrost degradation on a road embankment at Umiujaq in Nunavik (Quebec), Canada". *Canadian Geotechnical Journal*, 48, 720-740.

GEO-SLOPE International Ltd. (2014). Thermal Modelling with TEMP/W, <http://downloads.geo-slope.com/geostudioresources/books/8/15/temp%20modeling.pdf> (Marchch.10, 2021).

Government of the Northwest Territories. (2013). Design Brief – Inuvik to Tuktoyaktuk Highway, < https://www.inuvwb.ca/sites/default/files/130131_ith_land_type_and_desin_brief_-_ground_thermal_analysis.pdf>

Government of the Northwest Territories. (2019). Inuvik Tuktoyaktuk Highway Project, <https://www.inf.gov.nt.ca/en/ITH >

Harlon, R. & Nixon, J. (1978). Ground thermal regime. In *Geotechnical Engineering for Cold Regions* (pp. 103-168). McGraw-Hill, New York, NY, USA.

ITH Winter 2017 Geotechnical Drilling Program. (2017). "Inuvik-Tuktoyaktuk Borehole Data". *Unpublished Data*

Kong, X., Dore, G. & Calmels (2019). "Thermal modeling of heat balance through embankments in permafrost regions". *Cold Regions Science and Technology,* 158, 117-127.

Lepage, J.-M., Dore, G. & Fortier, D. (2012). "Thermal effectiveness of the mitigation techniques tested at Beaver*". 15th International Conference on Cold Regions Engineering,* Quebec City, QC, Canada 19-22.

Ling, F., and Zhang, T. (2004). "A numerical model for surface energy balance and thermal regime of the active layer and permafrost containing unfrozen water." *Cold Regions Science and Technology*, 38(1), 1–15.

Mittaz, C., Hoelzle, M. & Haeberli, W. (2000). "First results and interpretation of energy flux measurments of Alpine permafrost". *Annals of Glaciology,* 31(1), 275-280.

National Snow & Ice Data Center. (2020). "Thermodynamics: Albedo" *www.nsidc.org, <https://nsidc.org/cryosphere/seaice/processes/albedo.html> (Marchch.23, 2021).*

O'Neill, H. & Burn, C. R. (2017). "Impacts of Variations in snow cover on permafrost stability including simulated snow management, Dempster Highway, Peel Plateau, Northwest Territories". *Arctic Science,* 3, 150-178.

O'Neill, H B; Wolfe, S A; Duchesne, C. (2022). *Ground Ice Map of Canada, Geological Survey of Canada, Open File 8713, (ed. version 1).*

Parent, M. et al. (2019). "Preliminary investigation for mechanical degradation of permafrost embankment: Inuvik Tuktoyaktuk Highway case study". *Cold Regions Engineering,* 186-194.

Riseborough, D. Shiklomanov, N. Etzelmüller, B. Gruber, S. and Marchenko, S. 2008. “Recent advances in permafrost modelling.” *Permafrost and Periglacial Processes*, 19(2), 137–156.

Ross, C., Siemens, G. & Beddoe, R. (2019). “Challenges stabilizing a ground-temperature model at a permafrost site”. *Proceedings of the XVII ECSMGE-2019*, Reykjavik, Iceland.

Ross, C., Siemens, G. & Beddoe, R. (2021). “Initialization of thermal models in cold and warm permafrost”. *Arctic Science*, 8, 362–394.

Ross, C., Beddoe, R., and Siemens, G. (2022). “Novel bottom boundary condition for shallow, cold permafrost models”. In Review, *ASCE Journal of Cold Regions Engineering* (July 2022, #CRENG-692).

Rudy, A., Kokelj, S., Wilson, A., Ensom, T., Morse, P., and Klengenberg, C. (2020). Developing a collaborative permafrost research program: The Dempster - Inuvik to Tuktoyaktuk highway research corridor, Northwest Territories, Canada, EGU General Assembly 2020, Online, 4–8 May 2020, EGU2020-12610, https://doi.org/10.5194/egusphere-egu2020-12610,

Vincent, W., Lemay, M. & Allard, M. (2017). “Arctic permafrost landscapes in transition: towards an integrated Earth system approach”. *Arctic Science*, 3(2), 39-64.

Wilson, A. (2021). “Inuvik-Tuktoyaktuk Snow Compaction Study”. Northwest Territories Geological Survey. Open Source Dataset (*currently Unpublished)*

Yen, Y. 1981. *Review of thermal properties of snow, ice and sea ice,* United States Army Corps of Engineers, Hanover, New Hampshire, USA.

Zhang, Y., Chen, W. & Cihlar, J. (2003). “A process-based model for quantifying the impact of climate change on permafrost thermal regimes”. *Journal of geophysical Research*, 108(D22).

Appendix A - Kingston Case Study

To deal with the problem of a site with no snow information this chapter presents a case study developed in Kingston, ON, to evaluate the accuracy of ground temperature models with snow data sourced away from the site. Furthermore, the selected sites only had unfrozen thermal conductivity measured, so this paper also shows model development with only partial knowledge of soil properties. This paper originally conceived for submission to the GeoNiagara 2021 conference and is presented here as supplementary material for the development of the ground temperature model presented in Chapter 2.

To conduct the study, two climate monitoring stations were established at different locations situated 20 km apart in Kingston, ON, Canada. At each site ground temperatures were modelled using the inputs from the two weather stations. The model results were compared to ground temperatures recordings from multibeaded thermistor strings to evaluate their accuracy. The numerical models developed generated from the GeoStudio TEMP/W (version 11.1.1.22085) module developed by GEOSLOPE INC.

The results of the study showed differences in the recorded temperature data and modelled temperature data. The measurement of one soil property left many unknowns into the soil profile and no known borehole log was located near the sites to give indications into the soil composition. This highlights the importance of thorough ground investigations in the development of ground temperature models where less estimations are required to fill in gaps of the soil properties. Furthermore, the lack of onsite snow measurements required using snow data measured kilometers away from the sites. Based on observations of the conditions at both sites it was determined that the snow cover conditions were greater than what was recorded at the airport. Future studies should install weather stations equipped with snow depth sensors on site, because snow conditions can be quite variable in short distances and snow cover greatly impacts ground temperatures.

Site Background

Two weather stations (station 1 and station 2) were set up at two sites (site 1 and site 2) in the Kingston, ON area to collect weather data (air temperature, wind speed, and relative humidity). Figure 32 shows the locations of the sites in the Kingston region along with the local ECCC climate monitoring station that provided snow depth data.

Figure 32: Location of sites and weather stations in the Kingston area. Site 1 is located nearer to Kingston and site is north of Howe Island. The ECCC climate monitoring station is located at the red Marchker.

At each site, along with the climate monitoring stations, multibeaded ground thermistor strings were installed to retrieve ground temperature data at five depths to a depth of 1.06 m (i.e., 0.30 m, 0.51 m, 0.70 m, 0.87 m, and 1.06 m). Measurements from two nodes (0.3 m and 1.06 m) are shown in Figure 33. Also, at each site the unfrozen thermal conductivity of the soil was measured using a KD2 Pro meter. Figure 34 shows a schematic diagram of the weather station setup at each site.

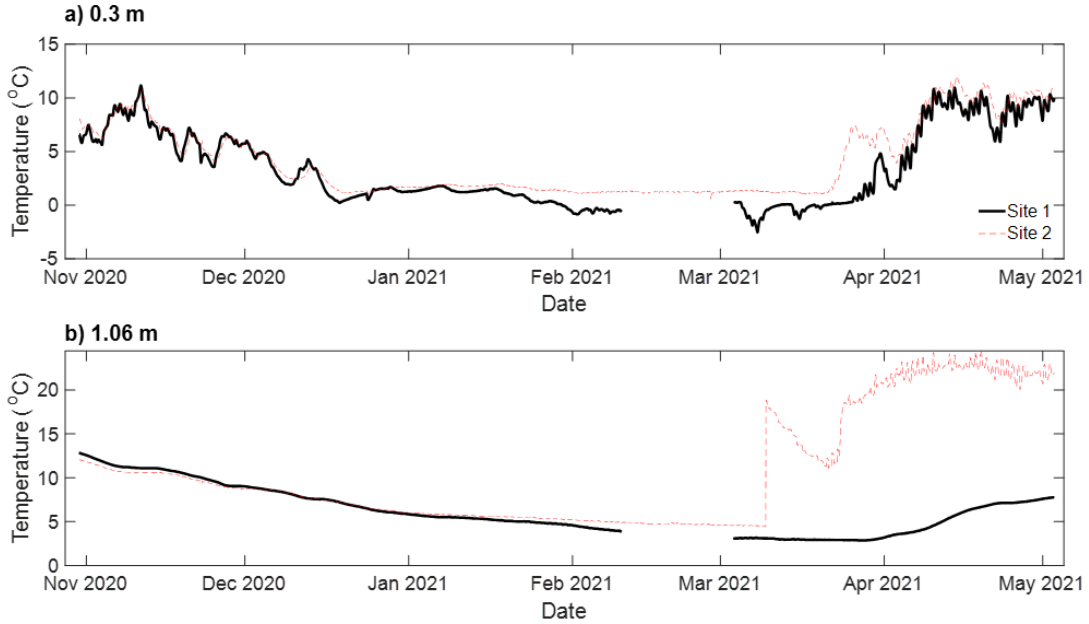

Figure 33: Ground temperature data recorded at each Kingston site at depths of a) 0.3 m, and b) 1.06 m. Temperatures were recorded from October 30th, 2020, to May 3rd, 2021. Site 1 has a break in recordings from February 10th, 2021, to March 4th, 2021, due to weather

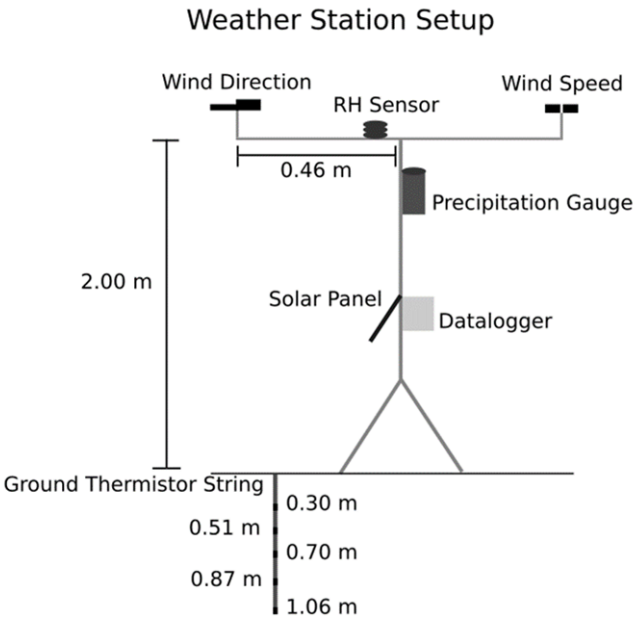

Figure 34: Schematic of weather station setup at sites 1 and 2 in Kingston, ON.

The temperature data recorded at each site is shown in Figure 35. Station 1 at site 1 recorded weather data from October 31st, 2020, to February 10th, 2021, and again from March 4th, 2021, to May 3rd, 2021 with the break in recording due to station maintenance. Station 2 at site 2 recorded data from October 31st, 2020, to May 3rd, 2021. Both weather stations recorded weather data every 10 minutes. The differences in the wind speed and relative humidity measurements between the two sites are shown in Figure 36. A weather station from Environment Canada (Kingston Climate) located at the Kingston airport (44°13'24.000" N, 76°35'58.000" W) provided daily snow measurements for the model run times.

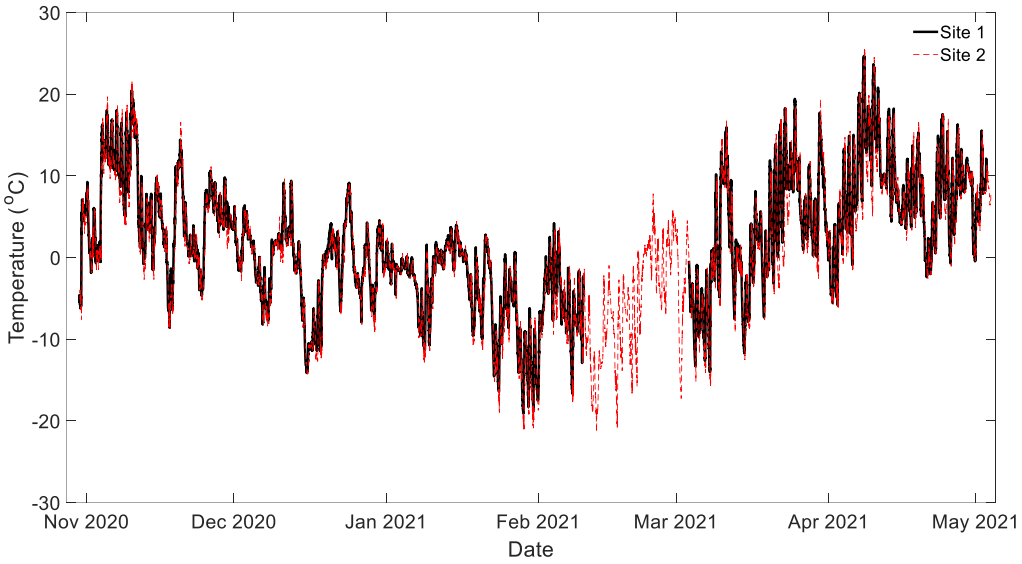

Figure 35: Weather data retrieved from climate monitoring stations at sites 1 and 2.

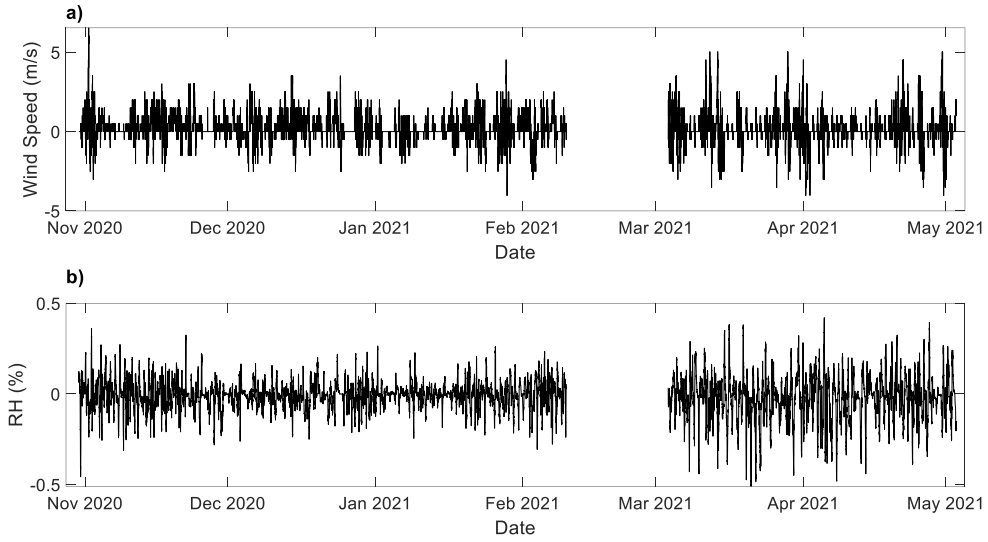

Figure 36: Differences in recording of a) wind speed, and b) relative humidity between the two weather stations recording data in the Kingston, ON area.

Model Development

The ground temperature models for calibration at each site were generated as 1D models. The program used to develop the model was the Geostudio TEMP/W (version 11.1.1.22085) module developed by GEOSLOPE INC.

For the model, the mesh size was finer (0.01 m) in the upper layer and larger in size at the lower layer (0.1 m). The finer mesh size closer to the surface allow for more accurate modeling of temperature changes, where lower depths do not vary in temperatures significantly over the year and do not require as many calculations. The time step length was established as 0.00694 (10 minutes) day-lengths. The upper boundary condition was set as a land-climate interaction boundary using air temperature, wind speed, and relative humidity from the onsite weather stations and snow depth data from the Kingston ECCC climate monitoring station. Furthermore, solar radiation was estimated using a built-in function in Geostudio with the latitude of Kingston (44.23°). Albedo was designated a value of 0.2 when there was no snow and 0.8 when there was snow on the ground (National Snow and Ice Data Center, 2020). Snow was established as having a thermal conductivity initially of 15 kJ/d/m/ °C and was set to 5 kJ/d/m/ °C for the final version of the model (Yen, 1981). The lower boundary condition was designated as a heat flux boundary with a constant value of 4.32 kJ/d m^2, which represents heat flow from the earths core (Blackwell & Richards, 2004).

At both sites, the models were established to have a soil layer 0-3 m in depth and a bedrock layer 3-15 m in depth (Figure 37). Unfrozen thermal conductivity measurements were taken at both sites and were found to be 0.878 M/m/k at site 1 and 0.946 W/m/k at site 2. This was used to inform on the development if the ground profile. The ground profile for each site was estimated using the Johansen 1975 method (GEO-SLOPE, 2014; Andersland & Ladanyi, 2004), while having an unfrozen thermal conductivity close to the measured values. The unfrozen & frozen volumetric heat capacity and the frozen thermal conductivity were calculated from the soil porosity and degree of saturation. Initial porosity was selected from the theoretical range of porosity for silty sands, then was selected for theoretical values for clays. In the end, the same ground profile was used for site 1 and 2 and the properties are shown in Table 4.

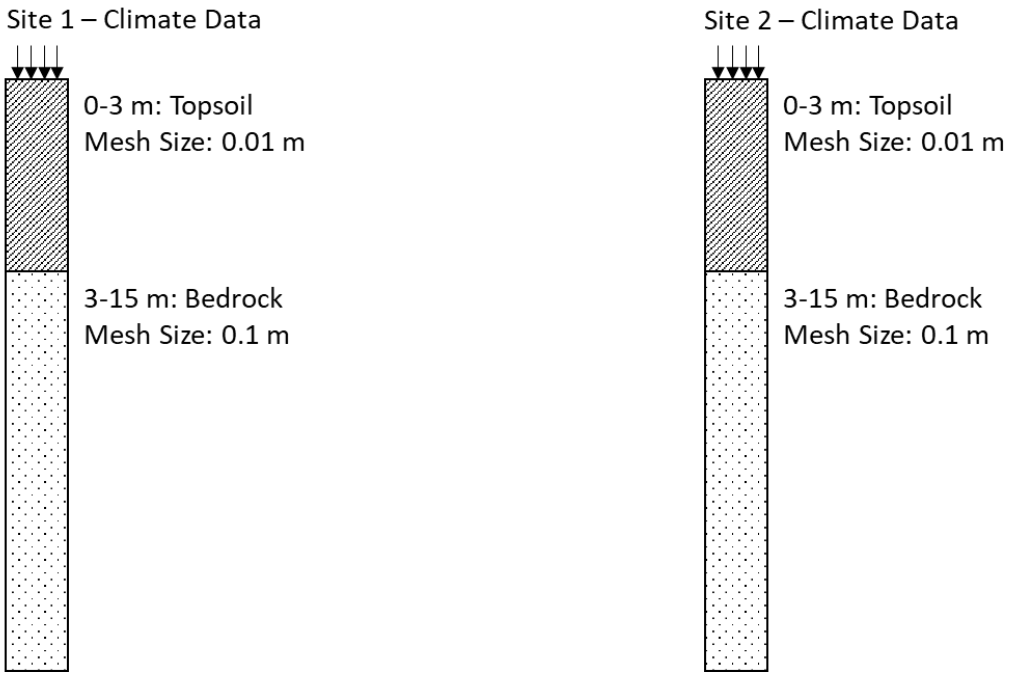

Figure 37: Ground profile of sites 1 and 2 in the Kingston, ON area.

Table 4: Final material properties used in Kingston ground temperature model.

Material	Unfrozen thermal conductivity (KJ/d m °C)	Frozen thermal conductivity (KJ/d m °C)	Unfrozen volumetric heat capacity (KJ/m^3 °C)	Frozen heat capacity (KJ/m^3 °C)	Water Content (%)
Top Soil	104	181	2,616	1,778	40
Bedrock	260	260	2,100	2,100	0

The initial ground temperatures were established through a spin-up function. The top boundary condition was established using weather data from Environment Canada from the Kingston Airport between October 30, 2019, and October 30, 2020. The initial ground temperature throughout the model was set to 5°C. The model was set-up to run for 50 years repeating the weather data from the site over the 50 years. The ground temperature profile was deemed to reach equilibrium when the ground temperatures after each cycle were the same values.

The accuracy of the models was assessed by comparing the ground temperature model outputs from 0.30 m, 0.51 m, 0.70 m, 0.87 m, and 1.06 m ground depths against the same values from the multibeaded thermistor string recording temperatures at the same depths.

Results

The ground temperature models were iteratively changed until model outputs more accurately represented the recorded ground temperature data. The final model outputs are shown in Figure 38 for site 1 and Figure 39 for site 2. As seen in both figures, the model outputs for site 1 and site 2 from meteorological input data from both station 1 and station 2 are very similar.

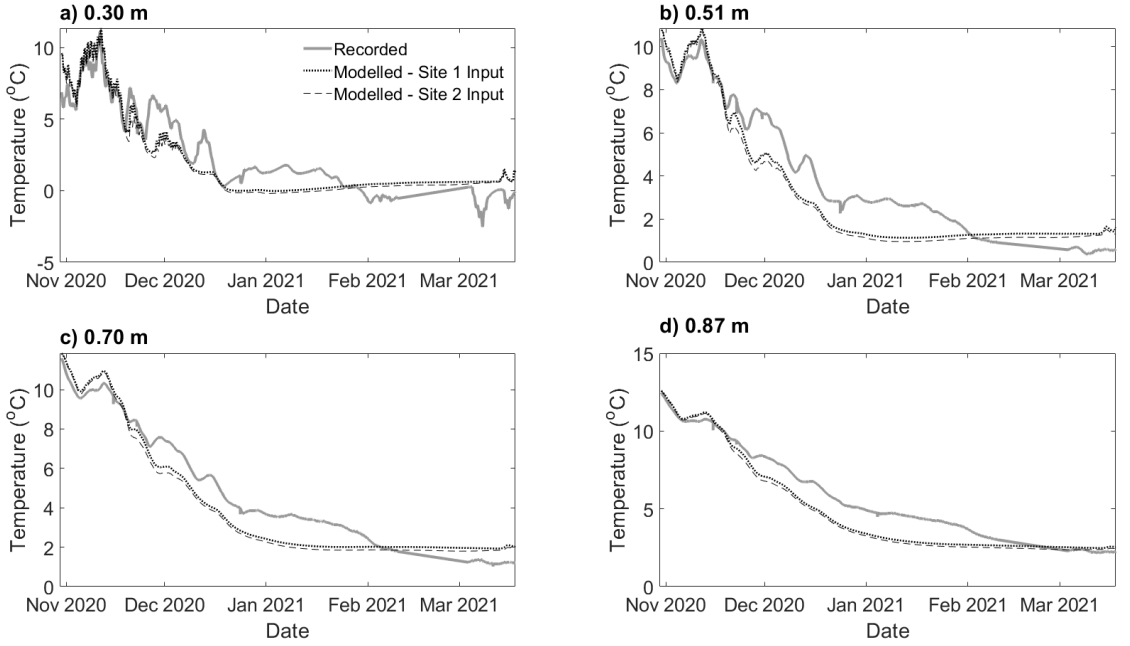

Figure 38: Modelled ground temperatures for site 1 with weather data from station 1 (close) and station 2 (far) compared to thermistor data at depths 0.3 m, 0.51 m, 0.70 m, and 0.87 m.

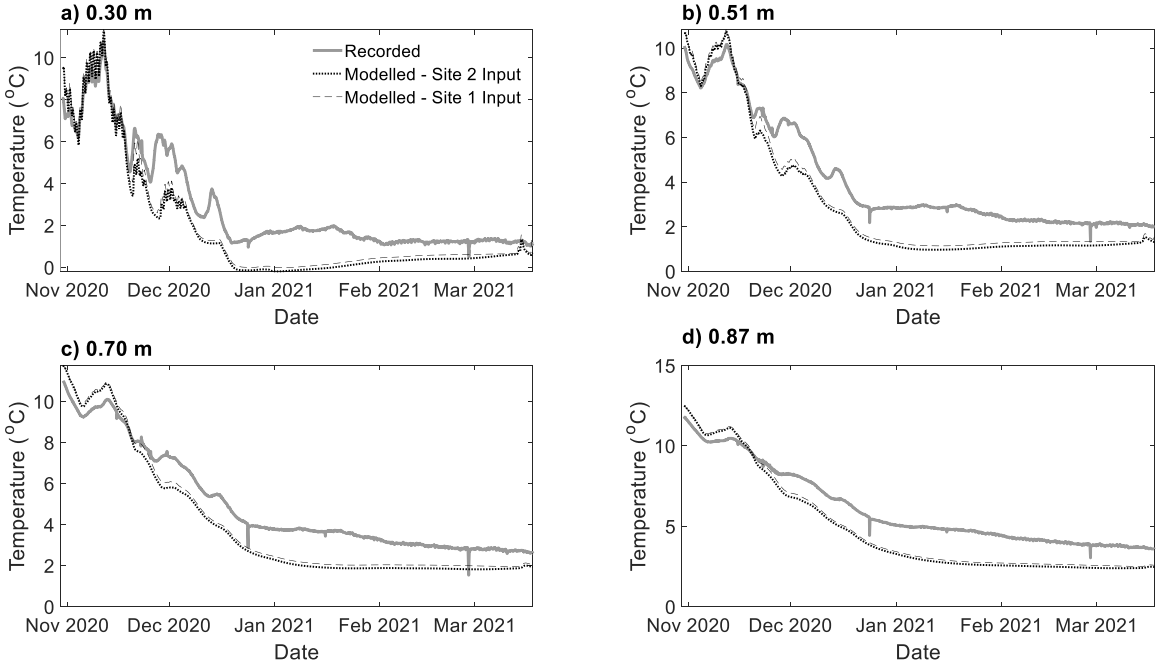

Figure 39: Modelled ground temperatures for site 2 with weather data from station 2 (close) and station 1 (far) compared to thermistor at depths 0.3 m, 0.51 m, 0.70 m, and 0.87 m.

As seen in the graphs in Figure 38 for site 1 there is no major difference between the model results from the model develop from the onsite weather data and the weather data from site 2. Between the modelled ground temperatures and the recorded ground temperatures, the temperatures do show differences that are greater than 2 °C at certain time periods. The differences in temperature decreases with depth where the lower depth model outputs are more accurate than the model outputs nearer to the surface when compared to the recorded ground temperatures. Initially, the modelled ground temperatures do not show a major difference until approximately November 24th, 2020, when the recorded ground temperatures experience a spike in temperature, whereas the spike in the modelled temperatures are less pronounced and occurs later on the 25th. As seen in the graphs in Figure 39 similar to site 1, there is not a major difference between the model outputs from the two input sources, with the results being indistinguishable for most of the model run time. Similar to site 1, there is no major difference between modelled and recorded ground temperatures in the initial part of the model runtime until November 24th, 2020. At this date at site 2 there is again a spike in ground temperature at a larger magnitude and an earlier date than this temperature spike in the modelled temperatures. Some of the differences may be attributable to snow depth measurements, which were taken from the Kingston airport and may not represent the conditions at site 1 and 2. However, a lasting snow cover did not occur until January 2nd, 2021, and cannot account for major differences in recorded and modelled ground temperatures before then. Another issue that could be contributing to the differences in recorded and modelled ground temperatures is the development of the ground profile. No borehole data was available from near the sites, and it was not clear what the ground prolife was except near the surface. Information from a ground survey could have provided a better idea of soil layers at the sites, which could provide better model results. This goes to show the difficulty in modelling ground temperature of specific sites, as one could have most of the input data originating from the site and still have some significant differences in recorded and modelled ground temperatures.

Discussion

A major challenge in the development of ground temperatures models is getting accurate soil property data. As shown in the results from the two sites modelling ground temperatures from the two weather stations, ground temperature modelling can still be a challenge when the land climate interaction boundary data is located directly at the site of interest. In this study only soil property known was unfrozen thermal conductivity. This was used to inform the material properties for the soils, however differences in the recorded temperature data and modelled temperature data still existed. Furthermore, only a sample from near the surface was used to measure thermal conductivity. It was also assumed that the soil properties from surface to bedrock were uniform. It is possible that the soil properties are more variable than what was represented in the model, leading to variations in recorded and modelled ground temperatures. While the sites modelled in this study had a soil thermal property measured, for some sites all that is known is a description of the soil type, which could be from a borehole log kilometers away. This highlights the importance of thorough ground investigations in the development of ground temperature models where less estimations are required to fill in gaps of the soil properties.

While most weather conditions were measured on both sites, snow depth was not. The snow depth values inputted into the model from daily weather data are from the Kingston Airport, which itself is of a distance from site 1 and 2. Based on observations of the conditions at both sites it was determined that the snow cover conditions were greater than what was recorded at the airport. It is

recommended that weather stations be equipped with snow depth sensors, because snow conditions can be quite variable in short distances and snow cover greatly impacts ground temperatures. To better simulate ground temperatures snow data in close proximity to the site should be used.

When looking at how well the model simulates the recorded ground temperatures at the set depths at the two different sites, in both cases the deeper depths in the model show more accuracy. Near surface ground temperatures are more greatly impacted by the surface conditions. In the future it may be more beneficial to have thermistor stings with sensors more concentrated near the surface to better calibrate ground temperature models.

With regards to the differences in model outputs at both sites 1 and 2 using input data from stations 1 and 2, there was no significant difference. The weather stations being located 20 km apart indicates that it is possible to use input data not sourced directly at a site of interest for ground temperature modelling. In this study the weather stations were 20 km apart in a temperate climate region. However, while this can inform on using weather data in the development of ground temperature models, there could be variables between areas that were not apparent between the two sites used. For example, there could be more significant differences in coastal areas and neighboring inland areas than what was between the two sites used in this study. Furthermore, while this study indicates 20 km is a distance for weather data that is acceptable, there still is the question of an upper limit to distance from a site of interest. Future studies could be conducted where sites chosen for weather stations are at greater distance to better give an indication of how far a weather station needs to be from a site of interest when it significantly impacts the ground temperature model outputs.

Appendix B - 2D Model Mesh Structure

The mesh structure of the 2D models were automatically generated as an unstructured mesh of quads and triangles by the TEMP/W software. The automatic meshing ensures compatibility across different regions in the model domain (GEO-SLOPE, 2014). Figure *40* below shows the meshing for the 2D model and 2D model with an embankment.

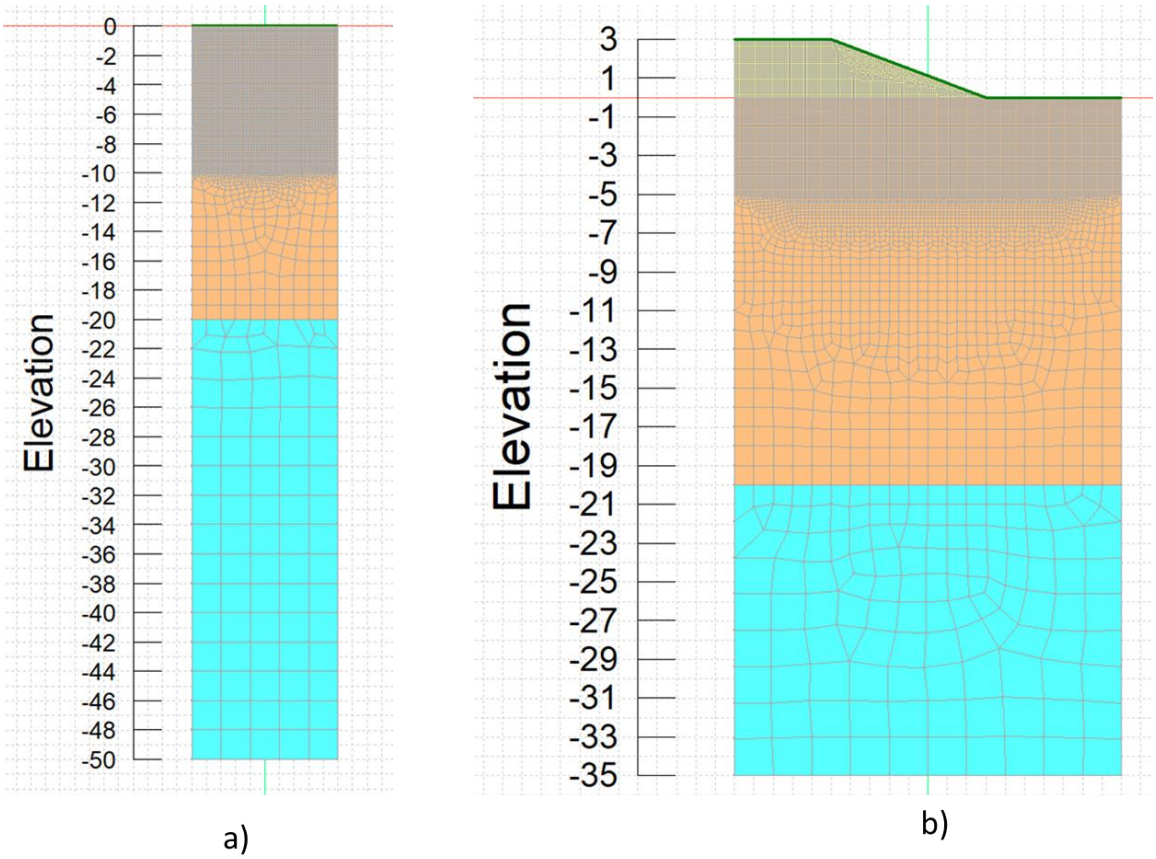

Figure 40: a) Meshing for the 2D model, b) meshing for the 2D model with an embankment. Both models were meshed with quads and triangles automatically generated by TEMP/W.

Appendix C - Compacted Snow Data

The compacted snow scenarios for the high, low, and average cumulative snow covers applied in the various model scenarios are shown below in Figure 41. The cumulative snow cover scenarios were based off of historical data from the Inuvik climate monitoring station and the measurements from the study site located on the ITH. The minimum snow year was taken from the 2019-2020 depths recorded at ITH snow compaction site. The maximum snow cover year was taken from September 1st, 2005, to August 31st, 2006, and came for the ECCC Inuvik climate monitoring station. The average snow cover scenario was not a specific year, but rather was built by averaging the daily snow from the data set. Snow compaction for each scenario occurs on December 1st, January 15th, and March 19th.

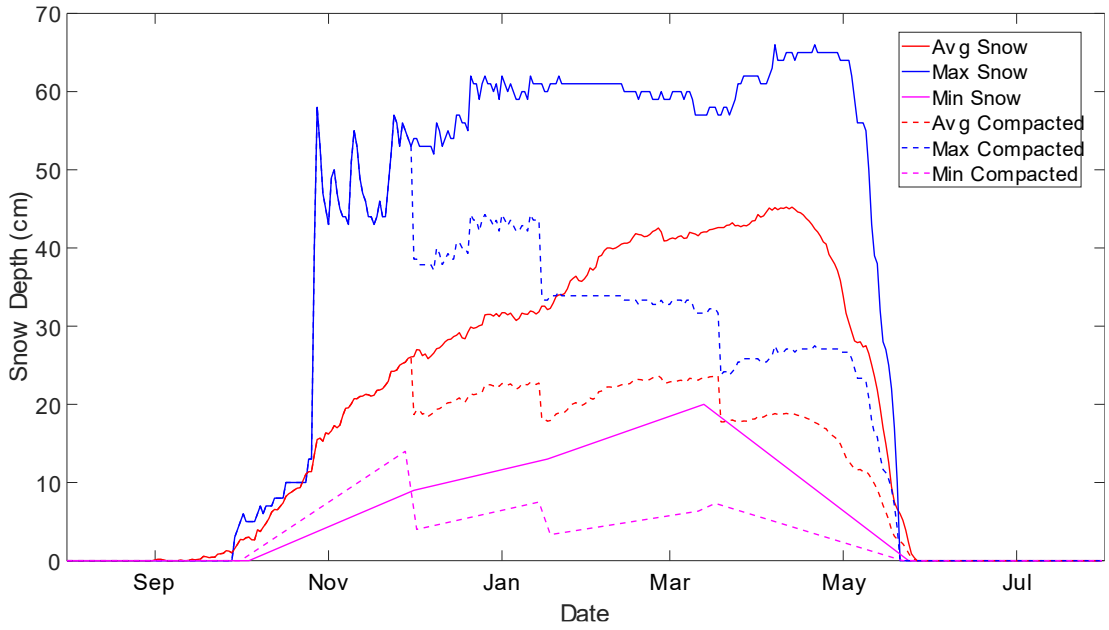

Figure 41: Snow depth measurements showing uncompacted and compacted maximum, avg., and minimum snow depths used in the model scenarios.

The compacted snow scenarios for the within season cumulative snow covers using the the ECCC Inuvik climate monitoring station daily snow depth data (from September 1st, 2003, to August 31st, 2021) applied in the various model scenarios are shown below in Figure 42. Compaction scenarios were created where snow compaction occurred either one, two, or three, times a season, in a variety of combinations, using the dates December 1st, January 15th, and March 19th. There was also a control model where no compactions occurred. Model scenarios included a control with no snow compaction, a model where snow compaction occurred at all three dates, three scenarios were snow compaction occurred two times in a winter (December and January, December and March, or January and March), and three scenarios where snow compaction occurred once a year (December, January, or March).

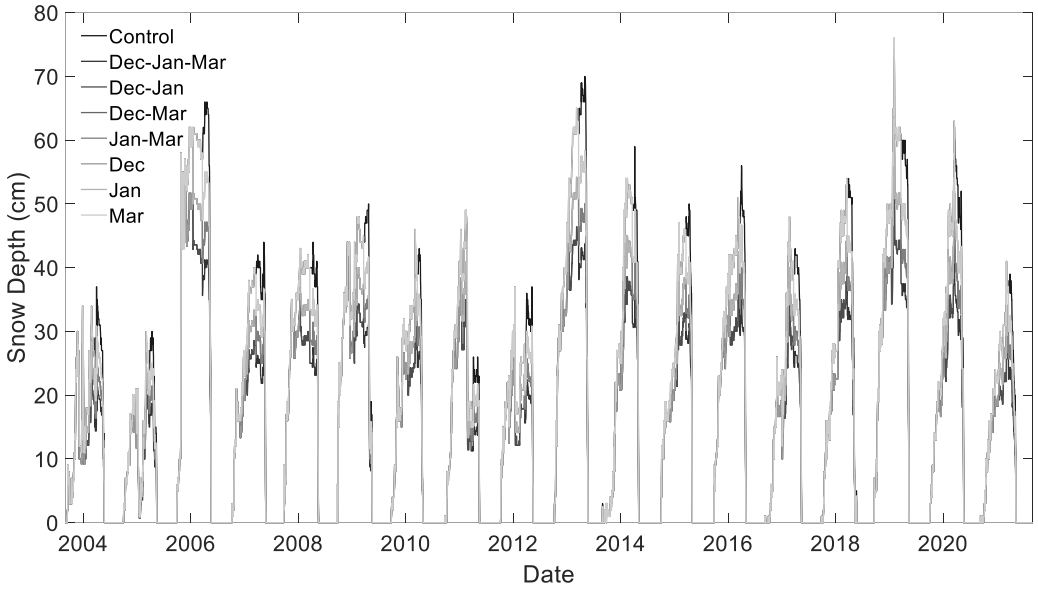

Figure 42: Snow depth measurements showing eight snow scenarios used for the within season frequency analysis.

Appendix D - 2D Model Temperature

When snow compaction occurs in the field it leaves a boundary line between compacted and uncompacted snow. This section investigates the lateral heat flow that occurs at this boundary and the resulting impact on the ground temperatures. The two-dimensional models used in this study (Figure 16b) had 3 snow cover scenarios (minimum, average and maximum) and were run for a period of 10 years. The first group of models applied these snow conditions across the model domain (10 m). The second group of models divided the domain in half, with uncompacted snow on the left 5 m and compacted snow on the right 5 m. In Figure 43, the difference in temperature between the control model and the half-compacted models are plotted, with the contours representing the monthly ground surface temperatures in the tenth and final year.

Figure 43a shows the results for the average snow cover year. Differences between the compacted and control models begin to appear during November and continue through February where there is a max -1.75 °C difference. Following, February the difference between the control and compacted decreases until May where from June to October there is no difference. The effect of the compacted snow on the ground temperature under the control area is not significant. In months where there is a difference between, the control and compacted snow, the temperature gradient between the two sides is steep. The months with the greatest extent of lateral heat flow are February, March, and April where there is a -0.25 °C difference at 1 m and a -0.1 °C difference at 2 m when compared to the control model.

Figure 43b shows the results from the minimum snow cover year. Significant change in temperature begins to occur in November, however this is a positive change from the compacted snow. This is due to the minimum snow data being taken from field data and the compacted snow depth before the first compaction, happens to be slightly higher in depth. In December the compacted side starts to show a negative difference with -0.8 °C near the boundary of the control and compacted side and -0.35 °C at the edge of the compacted side. The difference increase to a max in February of -5.7 °C, where the difference decreases until May with a big jump between March and April. The most significant months for lateral heat flow are February and March where there is a -1 °C 1 m into the control side at 1 m and a -0.54 °C different at 2 m.

For the maximum snow cover results in Figure 43c, there are fewer months where significant changes occur when compared to the average and minimum snow fall. Overall, there is not a large difference in temperature between the control and compacted snow. The temperature difference first appears in December with -0.16 °C and the difference increases until February -0.74 °C. In March the difference decreases down to -0.69 °C and then increases in April to a max difference of -0.91 °C. This decrease and increase come form the high surface temperature resulting from the high snow layer over the ground. In March the actual surface temperature under compacted snow is -2.7 °C, so the air will still be colder than the ground and unlike in average and minimum snow depth, heat will still go from the ground to the air in late winter. In March when the third compaction occurs, the insulation from the snow is reduced, which results in a cooling effect from the greater extent of heat flow from the ground to the air, resulting in the increase in temperature difference in April. The lateral heat flow is minimal where only a -0.06 °C occur at 1 m into the control side.

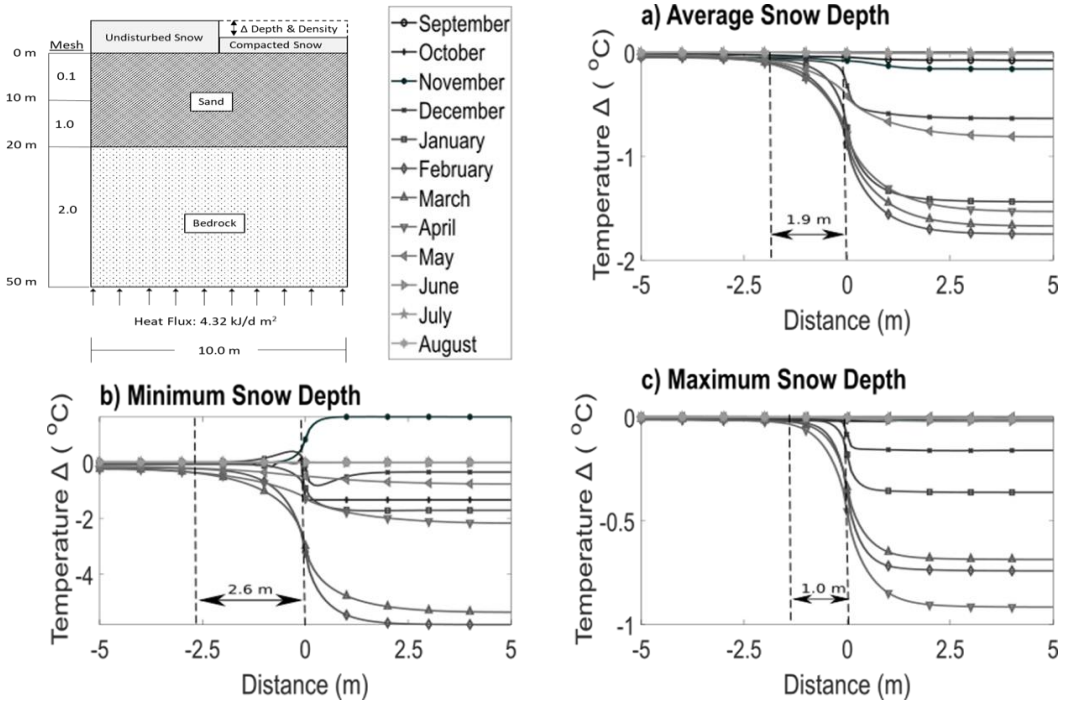

Figure 43: Difference between temperatures across the 2D model at 0 m depth between a model with control snow applied across the whole ground surface and a model where the right 5 m had compacted now applied. This was done for a) average, b) minimum, & c) maximum snow depth.

Figure 44 shows the temperatures in the 2D model for the different scenarios at 0.5 m depth. In Figure 20a, for the average snow cover, there is significant change each month. The largest change in temperature occurs in March with a difference of -1.26 °C. This temperature difference then decreases until June with the lowest difference of 0.11 °C, where the difference increases again back to March. The month with the greatest extent on lateral heat flow is September with a -0.4 °C 1 m into the control side and a -0.26 °C at 2 m. While March has the largest temperature difference, the temperature gradient between the control and compacted side is much steeper than what occurs in September. This is unlike what was observed at 0 m depth where the coldest month had the greatest response with lateral heat flow.

For the minimum snow cover, seen in Figure 44b, the largest difference occurs in March with a temperature difference of -4.3 °C. The difference decreases up to June, July, August, and September which all have a temperature difference just around -0.1 °C. There is no change in October and November, and a slight positive change in December from reasons previously explained for the minimum snow year. The temperature difference than increases back to March. Lateral heat flow is most significant in March where at 1 m into the control side there is a 1 °C difference and at 2 m there is a 0.63 °C difference.

In Figure 44c, the largest difference in temperature for maximum snow fall occurs in July with a difference of -1 °C. This difference then decreases to October where there is a difference of -0.13 °C. November through February there is no significant difference in temperature between the control and compacted snow depths. March to May, show increases in difference in temperature to -0.5 °C. There is no significant difference in June, which then is followed by a large increase to the

biggest difference in July. Like the temperatures observed at 0 m, very little lateral heat flow occurs, with a max difference of -0.2 °C observed a 1 m into the control side in July.

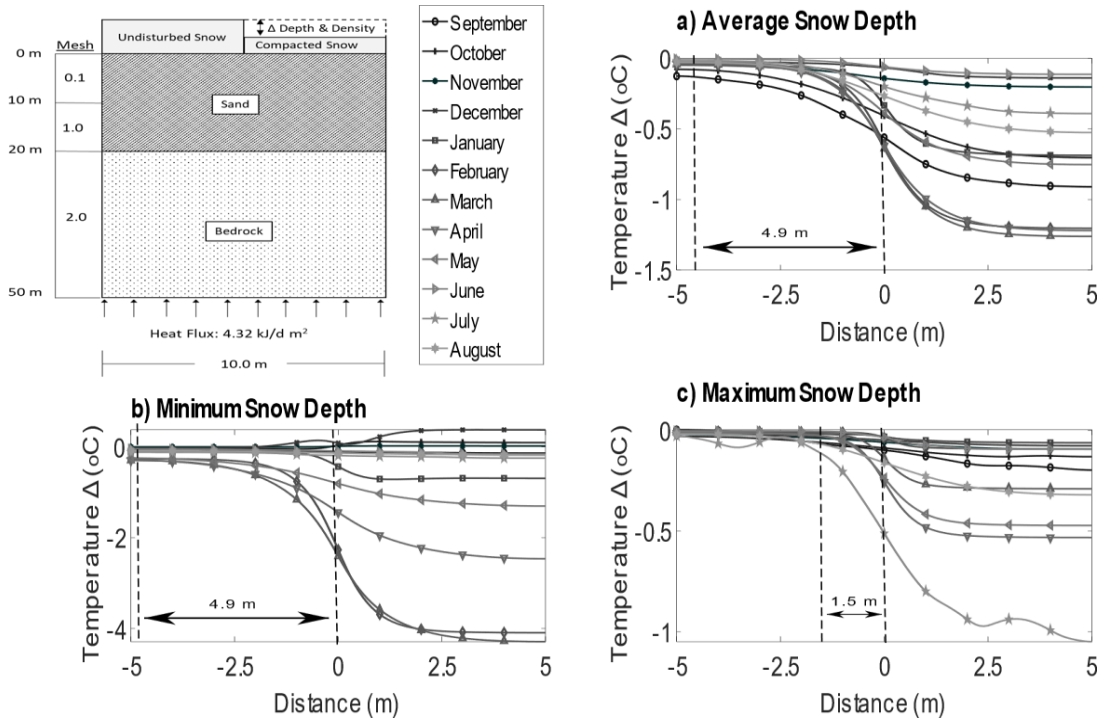

Figure 44: Difference between temperatures across the 2D model at 0.5 m depth between a model with control snow applied across the whole ground surface and a model where the right 5 m had compacted now applied. This was done for a) average, b) minimum, & c) maximum

Figure 45 shows the temperatures in the 2D model for the different scenarios at 1.0 m depth. In Figure 45a, the temperature difference for average snow depth is shown where the largest difference occurs in September with -1.7 °C. In the following months the temperature difference decreases until December where there is a -0.11 °C difference followed by no difference in January. In February there is a difference of 0.2 °C, which increases to April at -0.85 °C, which then decreases to June with -0.34 °C, then increases to the max in September. For lateral heat flow the largest difference occurs in September, where there is a -0.67 °C difference 1 m into the control side and a -0.42 °C at 2 m in.

For the minimum snow cover, seen in Figure 45b, the largest difference occurs in March with a temperature difference of -3.5 °C, which decreases over the months to September with a difference of -0.15 °C. From October to December no significant difference in temperature occurs. A difference of -0.4 °C occurs in January, which increases in difference to the maximum difference in March. For lateral heat flow the largest difference occurs in March, where there is a -1.15 °C difference 1 m into the control side and a -0.68 °C at 2 m in. In Figure 45c, the largest difference in temperature for maximum snow fall occurs in July with a difference of -1 °C, which decreases to the temperature difference in February of -0.1 °C. From March to June no significant temperature difference between the control and compacted snow. For lateral heat flow the largest difference

occurs in July, where there is a -0.3 °C difference 1 m into the control side and a -0.12 °C at 2 m in.

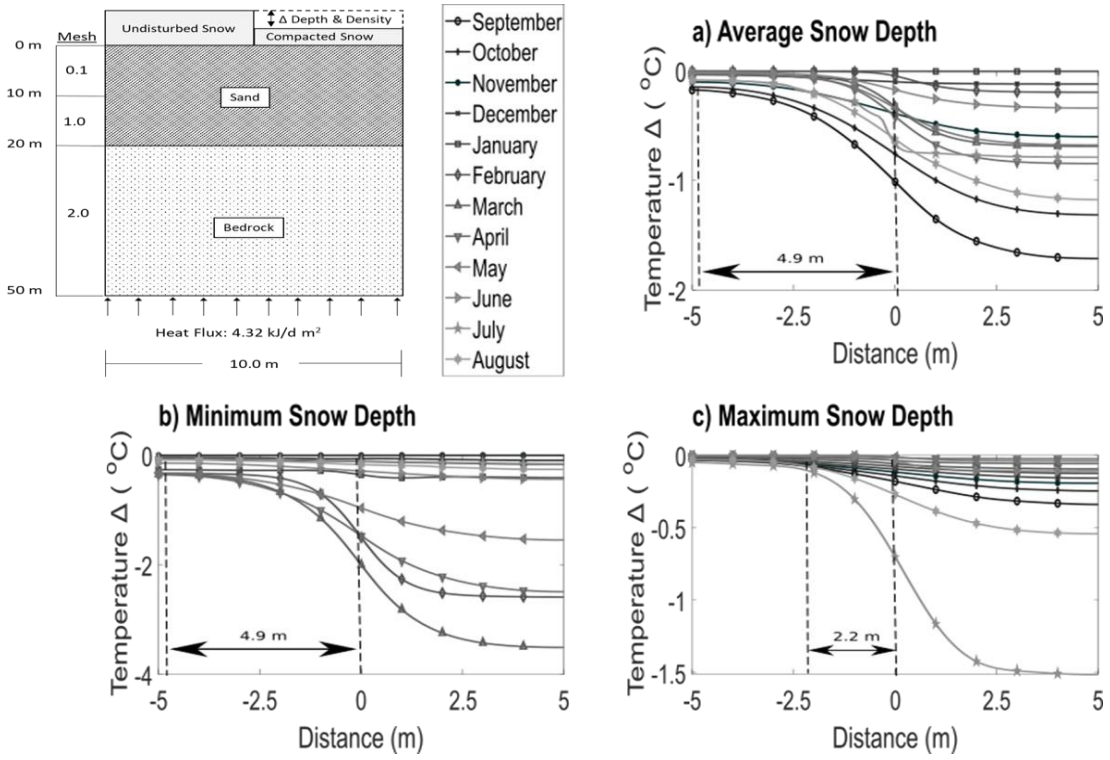

Figure 45: Difference between temperatures across the 2D model at 1.0 m depth between a model with control snow applied across the whole ground surface and a model where the right 5 m had compacted now applied. This was done for a) average, b) minimum, & c) maximum

Figure 46 shows the temperatures in the 2D model for the different scenarios at 2.0 m depth. In Figure 46a, the temperature difference for average snow depth is shown where the largest difference occurs in September with -1.9 °C. This temperature change between the control and compacted changes decreases up to January where there is a difference of -0.13 °C. From January to June the temperature between the control and compacted is similar with an increase to -0.27 °C difference, followed by a large increase back to the max temperature difference in September. For lateral heat flow the largest difference occurs in September, where there is a -1.1 °C difference 1 m into the control side and a -0.6 °C at 2 m in.

For the minimum snow cover, seen in Figure 46b, the largest difference occurs in March with a temperature difference of -2.2 °C, which decreases over the months to January with a difference of -0.1 °C. The temperature difference then increases over February to March. For lateral heat flow the largest difference occurs in March, where there is a -0.95 °C difference 1 m into the control side and a -0.65 °C at 2 m in. In Figure 46c, the largest difference in temperature for maximum snow fall occurs in July with a difference of -0.8 °C, which decreases to the temperature difference in March of -0.1 °C. From April to June no significant temperature difference between the control and compacted snow occurs. For lateral heat flow the largest difference occurs in July, where there is a -0.18 °C difference 1 m into the control side.

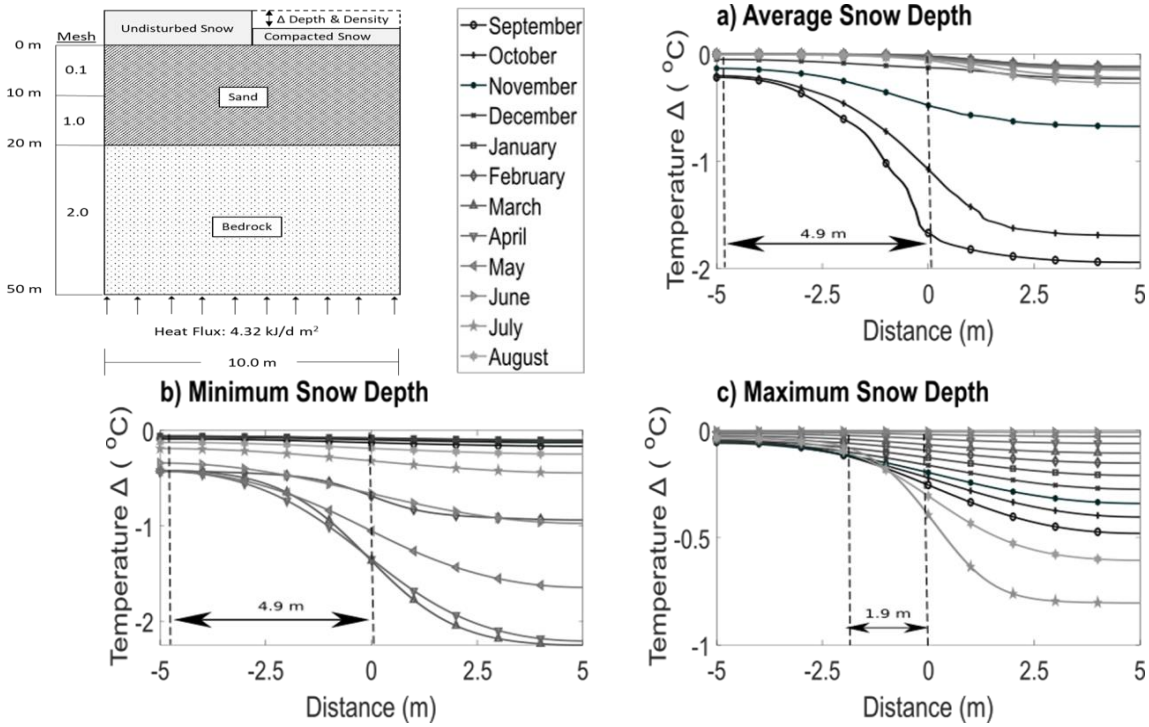

Figure 46: Difference between temperatures across the 2D model at 2.0 m depth between a model with control snow applied across the whole ground surface and a model where the right 5 m had compacted now applied. This was done for a) average, b) minimum, & c) maximum

When looking at the temperature changes at lower depths shifts occur in the average and high snow scenarios where the months of largest temperature differences between control and compacted snow go from late winter/early spring (February to April) down to late summer (August to September). Through compaction by changing the thaw depth areas at the same depth can then become significantly different if one area has gone through a phase change from frozen to unfrozen or not. It is important to understand that such results are determined by the thermal properties of the soil. For the ITH site the frozen volumetric heat capacity is 2806 kJ/m^3/ °C and the unfrozen volumetric heat capacity is 1883 kJ/m^3/ °C. Different thermal properties would require different heat levels to change temperatures, which would result in phase changes at different times depending on if the frozen volumetric heat capacity was higher or lower. Thus, it is important to note that these results are specific to the soil of the site and snow compaction as a mitigation technique may fair better or worse to change a thermal profile at other sites.

Further modeling was done on the 2D model to illustrate the effect of when and how frequently snow compaction was applied. Figure 47 shows the ground temperature across the model ground surface at the beginning of each month at the end of the 18 years runtime for the Inuvik 2003-21 snow depth data. In the model undisturbed snow was applied to the left 5 m of the model and the compacted snow was applied to the right 5 m of the model. Only the months of January, February, March, April, and May are shown, while other months do not have a difference between the undisturbed and compacted side are not shown. Similar to the results seen in the 1D model, the best scenarios for cooling the ground are those that compaction occur in December.

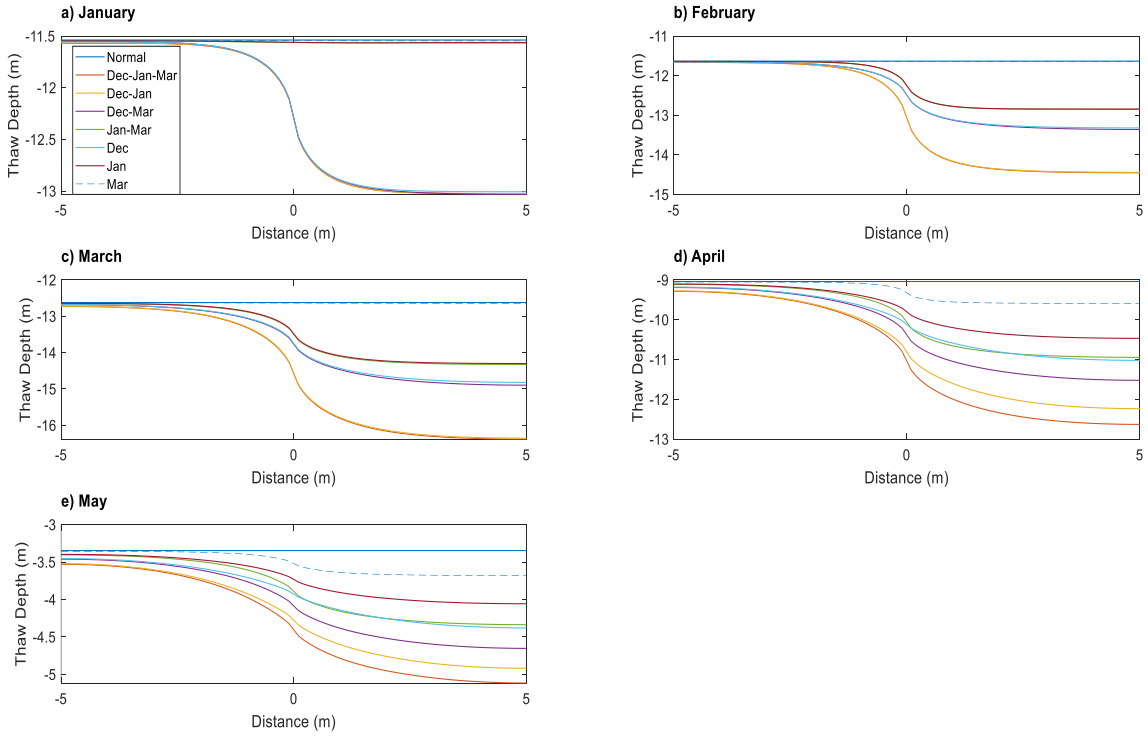

Figure 47: Ground surface temperatures resulting from snow compaction applied to the right 5 m of the model under different scenarios using Inuvik 2003-21 snow depth data. Months were taken from the final year of the model runtime, months where no difference occurs between undisturbed and compacted snow are not shown.

Appendix E - 2D Model w/ Embankment Within Season Frequency

For the 2D embankment model further modelling was done to show the effect of snow compaction time and frequency on the thaw depth of the embankment toe and end using the 2003-21 Inuvik snow depth. Figure 48 shows the maximum thaw depth at the toe for each year where similar to the 1D results modelling the same scenarios the shallowest thaw depth occurs when snow compaction occurs in December. The final thaw depths are for undisturbed snow is -1.9 m, for the December-January-March compaction the thaw depth is -1.6 m, the December-January thaw depth is 01.6 m, the December-March thaw depth is -1.7 m, the January-March thaw depth is -1.8 m, the December thaw depth is -1.7 m, the January depth is -1.8 m, and the March thaw depth is -1.9 m. Figure 49 shows the maximum thaw depth at the embankment end for each year. Similar to the 1D results there is no major difference in thaw depths between the different scenarios. The final thaw depth for each scenario is -2.9 m.

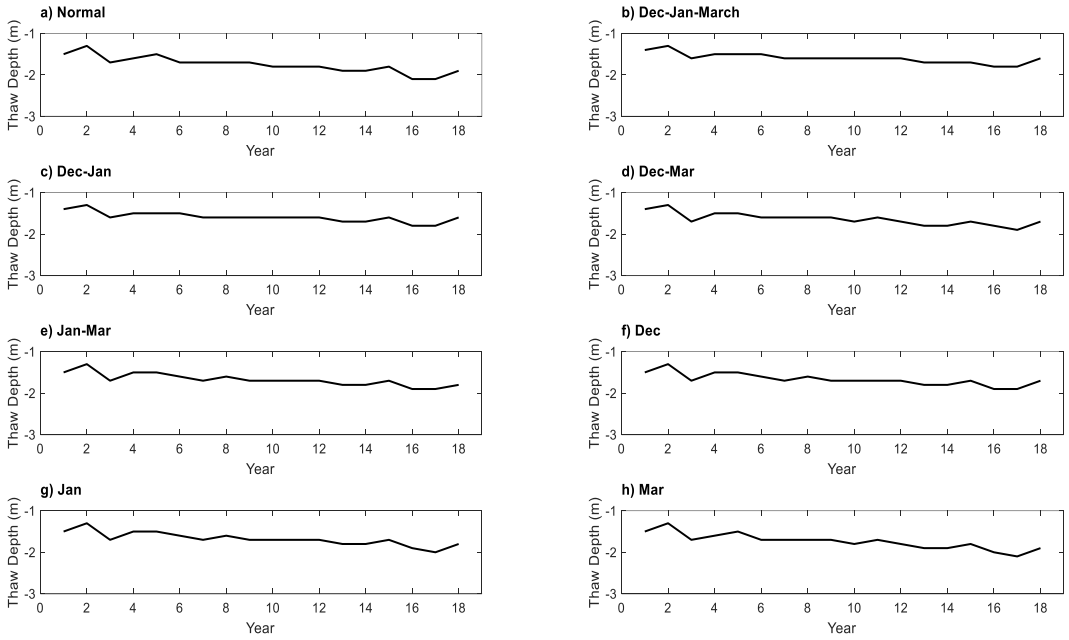

Figure 48: Maximum thaw depths at the embankment toe for each year using the Inuvik 2003-21 snow depth data.

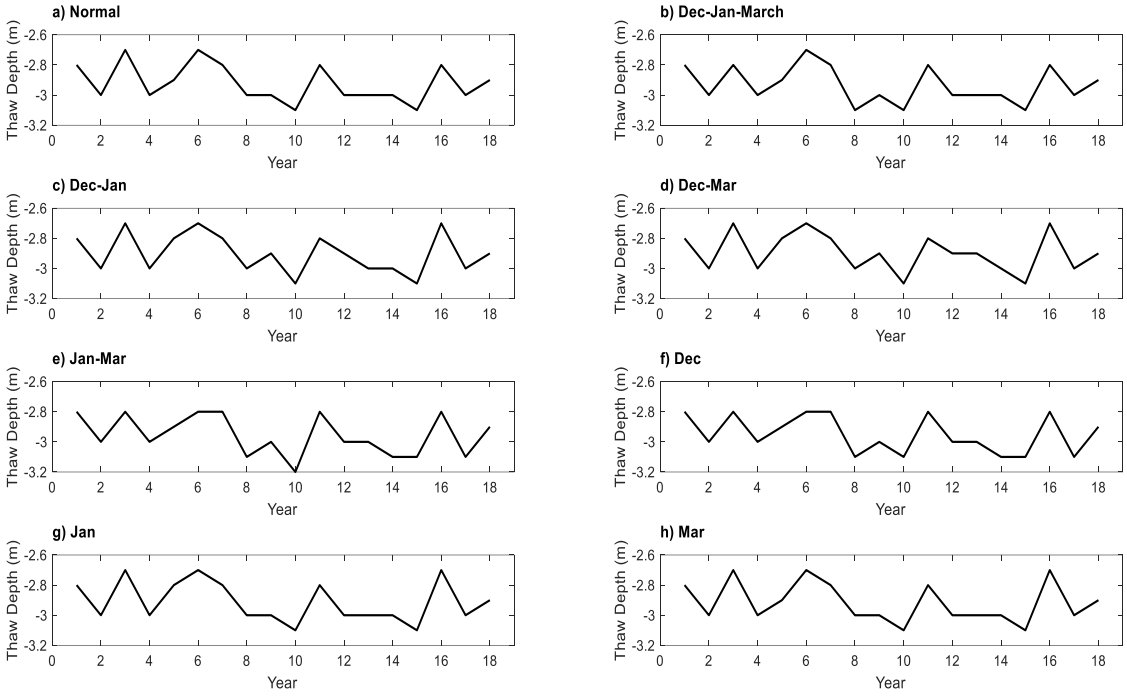

Figure 49: Maximum thaw depths at the embankment end for each year using the Inuvik 2003-21 snow depth.